INFORMATION TO USERS

This manuscript has been reproduced from the microfilm master. UMI films the text directly from the original or copy submitted. Thus, some thesis and dissertation copies are in typewriter face, while others may be from any type of computer printer.

The quality of this reproduction is dependent upon the quality of the copy submitted. Broken or indistinct print, colored or poor quality illustrations and photographs, print bleedthrough, substandard margins, and improper alignment can adversely affect reproduction.

In the unlikely event that the author did not send UMI a complete manuscript and there are missing pages, these will be noted. Also, if unauthorized copyright material had to be removed, a note will indicate the deletion.

Oversize materials (e.g., maps, drawings, charts) are reproduced by sectioning the original, beginning at the upper left-hand corner and continuing from left to right in equal sections with small overlaps.

Photographs included in the original manuscript have been reproduced xerographically in this copy. Higher quality 6" x 9" black and white photographic prints are available for any photographs or illustrations appearing in this copy for an additional charge. Contact UMI directly to order.

ProQuest Information and Learning
300 North Zeeb Road, Ann Arbor, MI 48106-1346 USA
800-521-0600

UNIVERSITY OF OKLAHOMA

GRADUATE COLLEGE

Mechanism of Ferric Enterobactin Transport Through *Escherichia coli* FepA: The Evolution of a Bacterial Venus Flytrap

A Dissertation

SUBMITTED TO THE GRADUATE FACULTY

in partial fulfillment of the requirements for the

degree of

Doctor of Philosophy

By

Daniel C. Scott

Norman, Oklahoma

2001

UMI Number: 3034886

UMI Microform 3034886

ProQuest Information and Learning Company
300 North Zeeb Road
P.O. Box 1346
Ann Arbor, MI 48106-1346

Mechanism of Ferric Enterobactin Transport Through *Escherichia coli* FepA: The Evolution of a Bacterial Venus Flytrap

A Dissertation APPROVED FOR THE DEPARTMENT OF CHEMISTRY AND BIOCHEMISTRY

BY

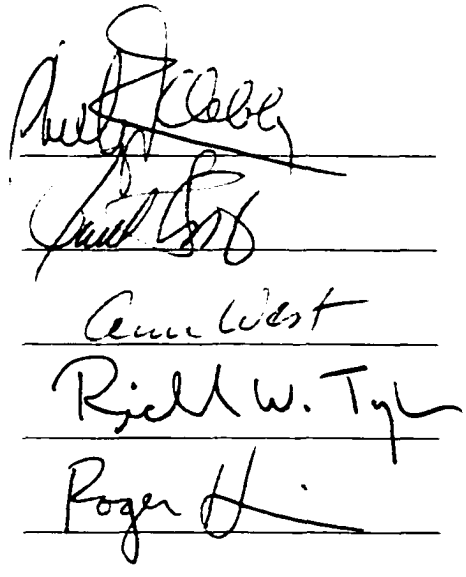

ACKNOWLEDGEMENTS

I would first like to thank my advisor, Dr. Phillip Klebba, for giving me the opportunity to join his laboratory. I truly appreciate his guidance and willingness to share his plethora of knowledge of outer membrane biochemistry. His passion for science and undying will for success served as a powerful inspiration in developing my career goals. I am also very grateful for having the opportunity to work with Dr. Sally Newton whose advice, training, and discussions were critical to the completion of my doctoral degree.

I would also like to thank the members of my doctoral committee, Drs. Paul Cook, Roger Harrison, Richard Taylor, and Ann West, for their advice and support throughout my graduate studies.

I would like to extend my gratitude to the many members of the Klebba lab who have, over the years, become colleagues and confidants; They are, Zhenghua Cao, John Igo, Matt Bauler, Paul Warfel, Wallace Kaserer, Bo Jin, Raju Annamalai, Marj Montague and Cathy Sprencel. I thoroughly enjoyed working with you and I am grateful for your suggestions and the discussions we had. Special thanks to Zengbiao Qi...it's definitely time for a brrrrreak.

Last but not least, I would like to thank my dad, my mom, my grandmother, my sister, and my brother in law for their support, encouragement, and eternal love.

In dedication to my late grandpaw Scott, who I know is intently watching over me with great pride and a big smile.

Table of Contents

List of Tables

List of Illustrations:

ABSTRACT

The TonB-dependent, energy dependent ferric siderophore transporters of the gram-negative bacterial outer membrane possess a unique architecture: Their N-termini fold into a globular domain that lodges within, and physically obstructs, a transmembrane porin β-barrel formed by their C-termini. I exchanged and deleted the N-domains of two such receptors, FepA and FhuA, which recognize and transport ferric enterobactin and ferrichrome, respectively. The resultant chimeric and β-barrel proteins avidly bound appropriate ligands, including iron-complexes, protein toxins, and bacteriophages. Thus, the ability of these receptors to discriminate these molecules fully originates in the transmembrane β-barrel domain. Both the chimeric and deletion constructs transported the siderophore they bound. The FepA constructs showed less activity than the wild type receptor protein, but constructs of FhuA functioned with turnover numbers equivalent to wild type. The mutant proteins displayed the full range of functionality indicating the globular domain within the pore is dispensable to the internalization reaction, and when present, acts without specificity during solute uptake. These and other data suggest siderophore receptors undergo multiple conformational states that ultimately expel the N-terminus from the channel concomitant with internalization.

Chapter 1

Introduction

Gram-negative bacteria differ from Gram-positive bacteria by the production of an additional cell wall external to the underlying peptidoglycan layer, the outer membrane. This additional lipid bilayer serves as an effective permeability barrier, protecting the bacterium from the detergent action of bile salts and degradation by degradative enzymes they encounter within the intestinal tract of animals. It also provides the bacterium with an increased resistance towards numerous antibiotics that are effective against gram-positive bacteria (Macrolides, novobiocin, rifamycins, see Nikaido and Nake 1979). The restrictive

permeability properties of the outer membrane of Gram-negative bacteria are attributed to both the structural components of the membrane and the proteins that reside therein.

The outer membrane of Gram-negative bacteria is an asymmetric bilayer, consisting of an inner leaflet composed of typical phospholipids, and an outer leaflet composed of lipopolysaccharide (LPS). Classical phospholipid bilayers are permeable to hydrophobic molecules, whereas the asymmetric outer membrane of enteric bacteria is virtually resistant, allowing the diffusion of hydrophilic molecules smaller than 600 Da (Nikaido and Vaara 1985). The permeable resistance to hydrophobic molecules is credited to the LPS component of the membrane. Composed of a polysaccharide linked lipid A anchor, the hydrophilic polysaccharide unit effectively increases the hydrophilicity of the membrane surface, thereby restricting the diffusion of hydrophobic molecules to the membrane. Mutant strains of *E. coli* K-12 that possess lesions within the biosynthetic pathway of LPS prove these suppositions. The lesions result in the production of so called "rough" or "deep rough" mutants that display an enhanced permeability to hydrophobic dyes and antibiotics (Makela and Stocker 1976). The structure of LPS from *Salmonella typhimurium* and *E. coli* were determined (for reviews see Galanos et al. 1977; Luderitz et al. 1982; Nikaido 1973), and in contrast to typical phospholipids, the LPS molecule contains six to seven fatty acids linked to a glucoseamine disaccharide backbone. In addition, the fatty acids

of LPS are saturated and, in some cases, are 3′ hydroxy fatty acids. An additional fatty acid residue is typically linked to this 3′ hydroxyl group in LPS producing the characteristic 3-acyl-oxy-acyl structure.

Since the crystallographic depiction of the first membrane protein (Photosynthetic Reaction Center; Deisenhofer et. al. 1984), substantial advances were made in understanding the structure-function relationships of this family of proteins. Initial spectroscopic studies of outer membrane proteins indicated there were substantial differences in their secondary structure as compared to inner membrane proteins. Unlike inner membrane proteins, whose transmembrane spanning segments are predicted as all alpha-helical, circular dichrosim spectra of purified outer membrane proteins indicated they consisted primarily of beta-structure with little or no alpha content (Nakamura and Mizushima 1976). These observations were explained with the subsequent solution of the crystal structures of numerous outer membrane proteins (OmpA, Pautsch et. al. 1998; OmpF, Cowan et al. 1992; LamB, Schirmer et al. 1995; ScrY, Forst et al. 1991; FhuA, Ferguson et al. 1998; FhuA, Locher et al. 1998; FepA, Buchanan et al. 1998; TolC, Koronakis et. al. 2000; OmpT, Vandeputte-Rutten et. al. 2001). Outer membrane proteins fold within the membrane as beta-barrels, and the size of the pore formed by the barrel depends, in part, on the number of beta-strands that make up the barrel. The size-imposed exclusion limits of the outer membrane (<600da) are directly attributed to these β-barrel porins located within the outer membrane. Accordingly, they are

classified into one of four groups depending on the number of beta-strands they possess, and their function.

8-stranded non-porin OM proteins

One of the most abundantly expressed proteins of the *E. coli* outer membrane, OmpA provides structural integrity to the bacterial cell surface. It is composed of a N-terminal membrane spanning segment of 170 amino acids and a C-terminal domain that extends into the periplasmic space. The crystal structure of the N-terminal membrane domain of OmpA has been solved (Pautsch and Schulz 1998). The size of the pore formed by the membrane embedded domain indicates that OmpA does not function as a non-specific diffusion channel, since the diameter of the pore is smaller than the diameter of a small molecule like water. The C-terminal periplasmic exposed domain is hypothesized to specifically interact with the underlying peptidoglycan layer providing a link between the outer membrane and peptidoglycan. This idea is supported by the observation that mutations to OmpA and lipoprotein, a separate outer membrane protein known to interact with peptidoglycan, result in the formation of spherical cells that can grow only under strictly regulated osmotic conditions (Sonntag et. al. 1978).

16-stranded general porins

The general porins provide the framework for the permeability of hydrophilic molecules (<600da), without possessing specificity towards substrate

molecules. However, they generally show a cation-selective preference for the passage of small charged molecules. Schulz and co-workers were the first to solve the structure of a bacterial porin, from *Rhodobacter capsalatus* (Weiss et. al. 1991). Crystal structures of other porins belonging to this family were also determined, most notably, OmpF, a osmo-regulated porin that displays a preference for the passage of cationic molecules (Cowan et al. 1992), and PhoE, a phospho-regulated porin showing anion-selectivity (Cowan et al. 1992). The general architecture of these porins is virtually identical to the membrane embedded domain of OmpA with a few notable exceptions. First, a uniquely oriented cell surface loop (L3) folds inward, projecting into the pore formed by the transmembrane beta-barrel. The disposition of this loop within the channel restricts the size of the pore and limits the size of molecules that may freely diffuse across it. Secondly, the general porins associate to form trimeric complexes in the outer membrane, that were originally observed in SDS-PAGE electrophoresis as heat-modifiable trimers (Nakamura and Mizushima 1976). The crystallization and structural determination of these proteins in their trimeric state further support the physiological relevance of these oligomeric complexes.

18-stranded specific porins

In addition to the general porins, which allow the diffusion of molecules based on size and charge, the outer membrane also contains channels that possess

an affinity for binding of a specific diffusable substrate. Maltoporin (LamB) of E. coli is the prototypical example of this class of porins. LamB is a sugar transporter in the bacterial outer membrane, recognizing and transporting maltose and malto-type saccharides up to maltoheptose (Szmelcman and Hofnung 1975; Benz et. al. 1992; Klebba and Newton 1998). Binding studies with radio-labeled sugars, and crystallographic structures of LamB complexed with maltose and malto-saccharide derivatives explained the molecular basis for substrate selectivity for this class of porins (Schirmer et al. 1995; Forst et al. 1998; Charbit et. al. 1998; Andersen et. al. 1999). Analogous to the general porins, substrate-specific porins form functional trimeric complexes in the outer membrane (Schirmer et al. 1995; Forst et al. 1998). The addition of specific periplasmic and inner membrane-imbedded proteins for transport of the ligand to its final destination in the cytoplasm is one notable difference between general and substrate-specific transport. Upon transport of the substrate across the outer membrane, a periplasmic binding protein captures the ligand and delivers it to a inner membrane embedded ABC-type permease complex. (Koster and Braun 1990a; Rohrbach et. al. 1995a; Klebba et al. 1997; Rohrbach et al. 1995b; Szmelcman and Hofnung 1975; Szmelcman et al. 1976; Sprencel et al. 2000). Transport of the ligand into the cytoplasm across the inner membrane complex is energy-dependent and requires ATP hydrolysis (Koster and Braun 1990b).

22-stranded energy dependent LGP

In contrast to the general and substrate-specific porins are the TonB-dependent, energy-dependent ligand-gated porins (LGP). Examples of this class of porins include FepA and FhuA, transport proteins for the ferric-siderophores enterobactin and ferrichrome, respectively (McIntosh et. al. 1979; Wayne et. al.1976). The overall structural organization of the membrane embedded component of these porins reiterates the structures of general and substrate-specific proteins. However, this class of porins participates in active transport across the outer membrane, requiring the input of energy for transport of the ligand. No direct energy source in the outer membrane exists, and as a result active transport by LGP proceeds *via* energy input from cytoplasmic membrane derived proton motive force (PMF; Pugsley and Reeves 1977; Bradbeer 1993). Transport of ligand across the outer membrane also requires the participation of an inner membrane localized complex, composed of TonB, ExbB, and ExbD. In contrast to the general and substrate-specific porins, there is little evidence to support the existence of oligomeric complexes of LGP (Locher and Rosenbusch 1997). The multimeric organization of these receptors remains an unresolved question regarding their structure, although the monomeric crystal structures of the receptors may suggest that they do not function as an oligomeric complex within the outer membrane (Ferguson et al. 1998; Locher et al. 1998; Buchanan et al. 1998).

Upon close inspection of the crystal structures of outer membrane proteins, several common structural characteristics appear (Buchanan et. al. 1999; Koebnik et. al. 2000). First, β-sheets forming the core of the barrel are arranged in an anti-parallel orientation and wrap to form the beta-barrel conformation within the membrane. The anti-parallel β-sheets are tilted at an angle of approximately 45 degrees with respect to the lipid bilayer, and are connected by short turns on the periplasmic face and large loops on the extracellular surface. In addition, the size and complexity of surface exposed loops increases in accordance with the function of the protein. For example, extracellular loops of OmpA and OmpF are much smaller than the cell surface loops of LGP like FepA and FhuA. Secondly, the β-sheets of outer membrane proteins are amphipathic, with hydrophobic amino acid residues facing the lipid bilayer and hydrophilic ones protruding towards the aqueous channel they form. Typically, aromatic residues of the transmembrane β-sheets are found at the interface of the membrane bilayer, generating what is commonly referred to as the "aromatic girdle." This placement of aromatic amino acids is believed to be an important structural feature in anchoring the protein within the membrane (Jelokhani-Niaraki et. al. 1998). Indeed, these commonly shared characteristics were employed, in conjunction with immunological and biophysical data, to construct fairly accurate folding models of numerous outer membrane proteins (Schenkman et. al. 1984; Murphy and Klebba 1989; Murphy et.

al. 1990; Armstrong et. al. 1990; Murphy et. al. 1990; Hufton et. al. 1995; Armstrong and McIntosh 1995; Klug et. al. 1997).

1.1 Importance of Iron Uptake for Bacterial Growth

Due to its presence in numerous biological and metabolic processes, iron is an essential nutrient for bacterial growth (Guerinot 1994; Neilands 1995). The dependence on iron in metabolic processes is due primarily to the chemistry of the iron atom itself. It is well suited for electron transfer reactions because, depending on its liganded state and environment, the oxidation-reduction potential of ferros/ferric iron spans +300mV to -500mV. For example, typical oxidation-reduction potentials of a-type cytochromes in the electron transport chain are +300mV, whereas certain iron-sulfur proteins may possess potentials as low as -490mV. The importance of this broad oxidation-reduction potential is exemplified in cellular reactions of the oxidative phosphorylation chain. Cytochromes, iron containing heme proteins, and iron-sulfur proteins are critical for the transfer of electrons from donors in oxidative phosphorylation, ultimately resulting in the production of cellular energy. In addition, acconitase, an iron-sulfur enzyme, is responsible for the conversion of citrate to isocitrate in the second step of the citric acid cycle. Finally, a specific iron containing non-iron sulfur protein, ribotide reductase, is responsible for the catalytic reduction of ribotide precursors, a necessary step preceding DNA synthesis. These metabolic needs compel bacteria

to acquire this metal in sufficient amounts to support growth within the particular niche in which they reside. Although under acidic and anaerobic conditions sufficient amounts of iron in the ferrous form are available to support growth, upon exposure to oxygen ferrous iron is easily oxidized to the ferric form. Anaerobically growing or acid tolerant bacteria may obtain sufficient quantities of ferrous iron to support growth under these conditions by simple diffusion across the outer membrane, bypassing the need for a specific iron transport system. However, for aerobically growing bacteria, the amount of freely available iron is on the order of 10^{-18}M (Neilands et. al. 1987). The decrease in iron availability is attributed to the poor solubility of ferric iron under physiological conditions, forming large insoluble iron-hydroxide polymers with water. To sustain growth, bacteria require a minimal iron concentration of 10^{-8} M, and thus under physiological conditions the amount of free iron readily accessible to bacteria falls far below their requirement for growth. For bacterial species colonizing an animal host, the problem is further complicated by the presence of host iron-binding proteins such as transferrin and lactoferrin. In order to acquire sufficient amounts of iron to support growth, bacteria have developed highly specific and specialized transport systems for obtaining this precious metal ion.

1.2 Iron Acquisition and Bacterial Virulence

In mammals, iron is bound to eukaryotic proteins (transferrin, lactoferrin, hemoglobin, ferritin) which maintain a low level of iron availability for invading microorganisms (Griffiths and Williams 1999). In response to bacterial infection, the amount of freely available iron is further reduced by shifting iron from transferrin to lactoferrin in the liver, a process called induced hypoferrima. Successful infection and the ability of a bacterial pathogen to cause disease depends directly on the ability of these pathogens to acquire sufficient amounts of iron. Relationships between iron-acquisition and bacterial pathogenesis are well established for a number of gram-negative pathogens. including *Escherichia, Salmonella*, *Neisseria*, *Vibro*, *Yersinia*, *Pasteurella* and *Haemophilus* (Wooldridge and Williams 1993; Fernandez-Beros et. al. 1989; Furman et. al. 1994; Cornelissen and Sparling 1998; Zhu et. al. 2000; Bearden and Perry 1999; Occhino et. al. 1998; Cope et. al. 2000; Carniel E. 2001; Lo 2001). Virulence mechanisms are linked to both iron uptake systems and iron-regulated expression of virulence genes, including toxins (Takase et. al. 2000; Reeves et. al. 2000).

1.3 Bacterial solutions to the iron supply problem

Bacteria employ numerous strategies in order to overcome the environmental limitations of iron. Iron acquisition is opportunistic, in that, depending on the particular niche that the microorganism resides in, one of many

transport systems may be utilized either predominately or exclusively. The evolution of numerous transport systems, each of which transport different iron containing ligands, serves to ensure that sufficient levels of iron may be obtained in the differing environments they may encounter.

The synthesis and secretion of organic iron-chelating molecules called siderophores (Greek for iron bearer; for reviews see Neilands et. al. 1987;Neilands 1995) is a common strategy for obtaining iron. These iron scavenging molecules are recognized at the cell surface by specific receptor proteins and are transported into the cell *via* a specific network of transport proteins. Gram-negative iron acquisition systems typically contain three components: (i.) a specific outer membrane receptor capable of binding the iron-ligand complex with high affinity, (ii.) a cognate periplasmic binding protein for delivery of the ligand from the outer membrane to the inner membrane, (iii.) an ABC-type inner membrane permease complex for transport of the ferric-ligand into the cytoplasm. The synthesis and secretion of siderophores is not the only mechanism by which bacteria obtain iron. They may also possess specific transport systems for utilization of host iron binding proteins such as lactoferrin or transferrin (Heesemann et. al. 1993; Cornelissen and Sparling 1994; Jarosik et. al. 1995; Gray-Owen and Schryvers 1996; Cornelissen et. al. 1998; Schryvers et. al. 1998; Schryvers and Stojilikovic, 1999). Finally, bacteria may utilize iron loaded heme upon hemeloysis of erythrocytes (Jarosik et. al. 1995; Zhu et. al. 2000; Torres and Payne, 1997; Torres et. al. 2001).

1.4 Siderophores

Siderophores form high spin, kinetically labile complexes with ferric iron that possess an exceptional thermodynamic stability. Siderophores are commonly classified by their chemical composition and generally fall within three major classes; hydroxymate-type siderophores, catechol-type siderophores, or mixed. Complexation of ferric iron by these molecules occurs through the participation of three bidentate ligands resulting in a hexa-coordinate octahedral complex between the metal and ligand. The affinity of siderophores for gallium is also quite high, but the attraction for aluminum and other divalent cations is substantially lower. Thus, siderophores can be viewed as specific for ferric iron. The preferential affinity of siderophores for higher oxidation states of iron discriminate them from other iron complexing molecules such as heme, which shows similar affinities for both ferrous and ferric iron. In addition, the weaker affinity for ferrous iron provides for an efficient means of release within the cell, *via* reduction. However, it appears that the reduced oxidation-reduction potential imposed by the differing affinities exceeds the reducing power of natural reducing agents. For instance, release of ferric iron from ferric enterobactin requires the action of a cytoplasmic esterase Fes (Brickman and McIntosh 1992). Mutations to *fes* result in the accumulation of ferric enterobactin within the cytoplasm, with cells remaining iron-starved. Fes participates in iron release by catalytically degrading the macrocyclic ester ring of enterobactin (Brickman and McIntosh 1992). This degradation results

in a substantial reduction of the dissociation constant of the iron complex facilitating release.

Enterobactin is the native siderophore of *E. coli* (Figure 1.1; Hantke, 1990). Its synthesis is directed within the cell by the action of seven synthetic enzymes (*ent*A-G). Enterobactin possesses a remarkable affinity for ferric iron (10^{52}; Neilands et. al. 1998). This extraordinary affinity for ferric iron is attributed to both the chemical properties of the siderophore and the characteristics of the metal ligand. Ferric iron's size, electronegativity, charge, and electron configuration typically allow it to form stable high spin complexes with hard base atoms such as oxygen. For enterobactin, the hard base atoms are donated *via* three catechol groups. Enterobactin is composed of three dihydroxybenzoylserine groups that are esterified to form a cyclic backbone. The three catechol rings wrap around ferric iron in the chelated complex creating the hexa-coordinate octahedral complex that carries a net charge of minus three. Due to the chirality of enterobactin two optical isomers exist for the iron complex. The first (Λ-conformation) results in the production of a left-handed propeller conformation, while the second (Δ-conformation) produces a right-handed propeller. Although both isomers are possible, the Δ-conformation is the predominant form observed in nature. The cell surface receptor responsible for transporting ferric-enterobactin recognizes either isomer, but only the Δ-isomer promotes bacterial growth under conditions of iron-

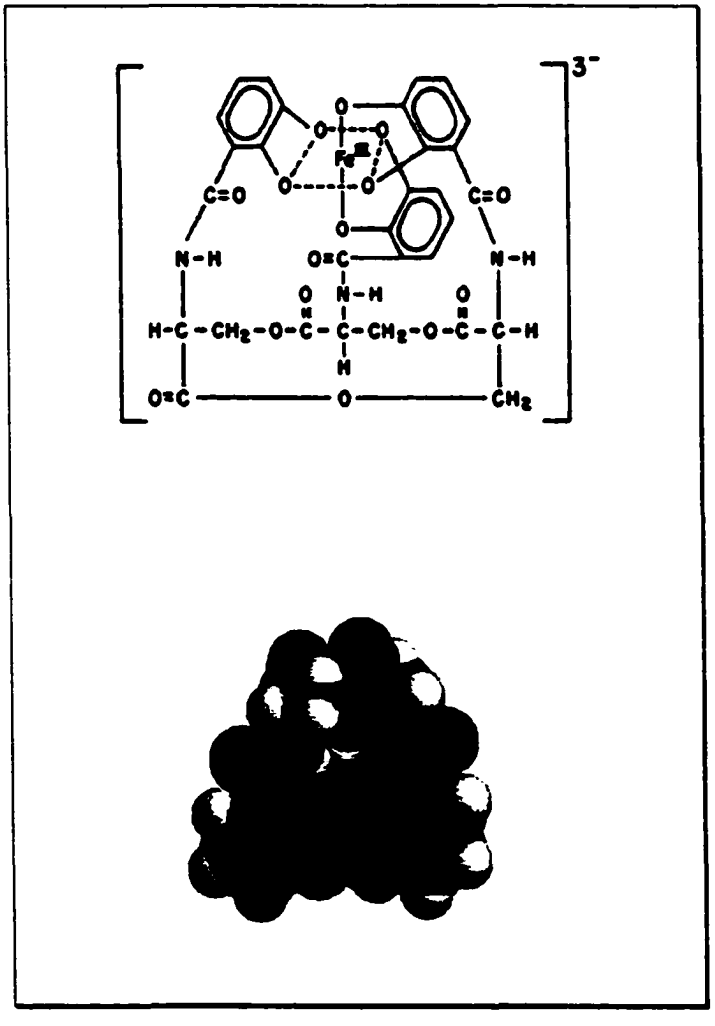

Figure 1.1 Structure of Ferric Enterobactin: Diagram representation (top), and the crystal structure of the vanadium:enterobactin complex.

starvation, indicating the preference for chirality resides in a subsequent step following recognition at the cell surface (Neilands et. al. 1981; Thulasiraman et. al. 1998).

E. coli, although never reported to wear an eye patch, appears to have mastered the art of piracy, in that it possesses genes for expressing siderophore receptors that recognize and transport other fungal or bacterial produced siderophores. One such example is the *E. coli* transport system for uptake of the hydroxamate-type siderophore ferrichrome. Synthesized and secreted by the fungus *Ustilago sp*, ferrichrome is utilized by *E. coli via* the production of a specific outer membrane receptor that recognizes and transports it, FhuA. Hydroxamate-type siderophores consist of a peptide derived backbone containing hydroxamic acid side chains that contain the six liganding oxygens.

1.5 The outer membrane receptor for ferric enterobactin, FepA

In the quest for the evolution of a binding agent for ferric iron with characteristics such as high affinity and stability, bacteria exceeded the permeability properties of the outer membrane. Ferric enterobactin, with a molecular weight of 714 daltons (Da), is too large to penetrate the water filled channels of the outer membrane that allow free diffusion of molecules smaller than 600 Da (Nikaido and Vaara 1985). As such, the production of specific outer membrane receptors for the iron-complexes was required.

Synthesized as a 746 amino acid pre-protein in the cytoplasm, Ferric Enterobactin Permease A (FepA) is directed to the outer membrane by virtue of its amino terminal signal sequence. Homologues of FepA occur throughout the gram-negative world (Lundrigan and Kadner, 1986; Baumler et. al. 1998; Rutz et. al. 1991; Dean et. al. 1993; Beall and Sanden, 1995; Richardson and Park, 1995; Carson et. al. 1999). The synthesis of FepA is iron regulated by a specific repressor protein Fur (Hantke 1984; Pettis et. al. 1988). Under iron replete conditions, iron containing Fur binds to the promoter regions of iron regulated proteins, referred to as the "Fur box," preventing mRNA transcription (Pettis et. al. 1988; Hunt et. al. 1994). Upon encountering iron deficient environments Fur dissociates from the "Fur box" to allow expression of iron regulated proteins.

FepA is organized into two domains; a C-terminal 22-stranded anti-parallel beta-barrel domain, and a N-terminal "plug" domain that folds within the barrel physically obstructing the pore (Figure 1.2; Buchanan et al. 1998). The plug and barrel organization is unique among bacterial outer membrane proteins. Binding of ferric enterobactin by FepA is saturable and specific, displaying subnanamolar affinity of the receptor:iron-siderophore complex (Newton et. al. 1999; Cao et. al. 2000). In fact, the affinity for ferric enterobactin is so high that mutational alterations resulting in 1000 fold increases in K_d still permit ferric enterobactin-dependent bacterial growth under conditions of iron starvation (Newton et. al. 1999). The recognition of ferric enterobactin by FepA occurs through the iron-

center and not the cyclic triseryl backbone; Ferric Mecam (1,3,5-N,N',N''-tris-(2,3-dihydroxybenzyol) triamnomethylbenzene; FeMECAM), a synthetic derivative of enterobactin in which the triseryl backbone is replaced with a phenyl group efficiently competes for binding with ferric enterobactin (Heidinger et. al. 1983; Ecker et. al. 1986), suggesting that the receptor recognizes the iron center and catechol chelating groups of the iron complex. Additional studies employing synthetic derivatives of enterobactin altering either the catechol chelating groups or triseryl backbone corroborate this conclusion (Thulasiraman et. al. 1998). Basic and aromatic amino acids of FepA were proposed to participate in siderophore recognition since the ferric-siderophore complex possess an overall net charge of minus three and iron chelating groups of aromatic nature. In support of this view, numerous basic and aromatic residues were found to participate in ligand recognition thorough mutational studies (Newton et. al. 1997; Cao et. al. 2000; Barnard et. al. 2001). Kinetically, the binding process is biphasic; fluorescent spectroscopic techniques employing site-directed labeled fluorescein derivatives of FepA showed an initial rapid adsorption of the siderophore followed by a slower step to the presumed transport competent complex (Payne et. al. 1997; Cao et. al. 2000). The crystal structure of liganded FepA presumably defined these two sites (B1 and B2), although not definitively (Buchanan et al. 1998). Two weak iron peaks that localized within the cell surface loops were observed in the liganded structure. The peaks were sufficiently close to each other to rule out the presence

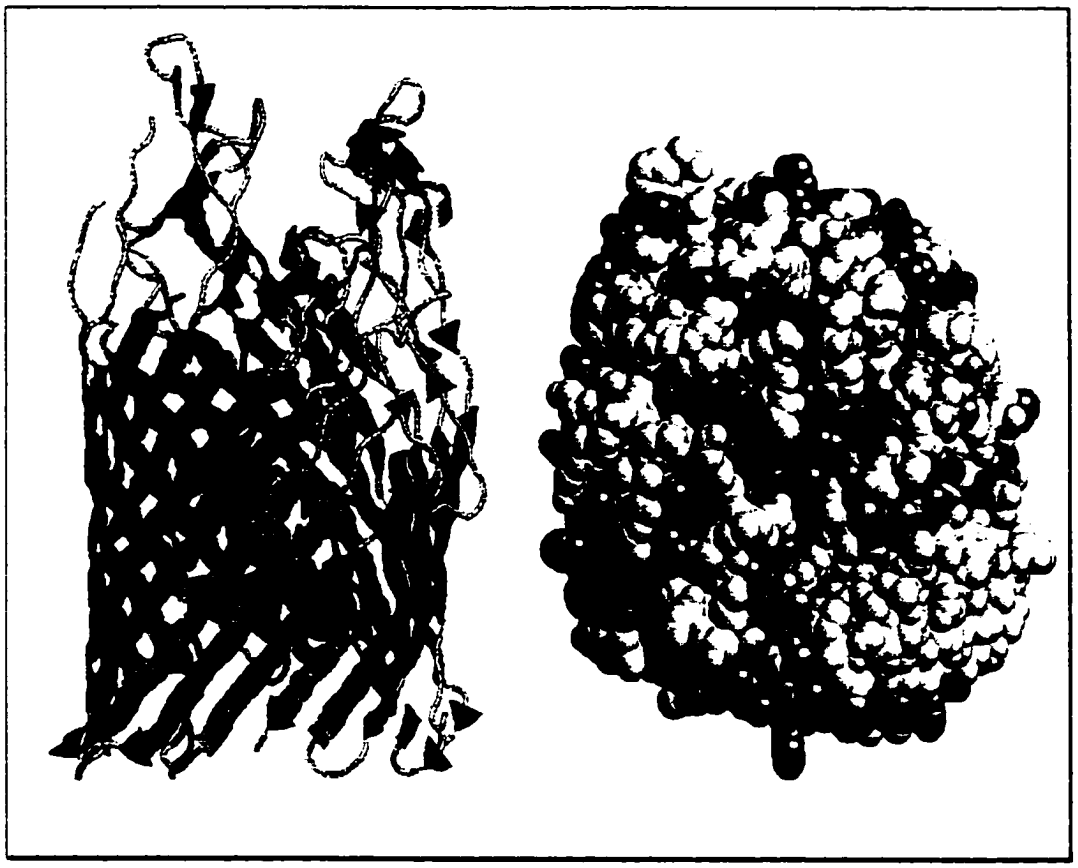

Figure 1.2 Crystal Structure of FepA: Left, Ribbon diagram with β-strands green and α-helices orange the N-terminal plug domain is colored red; Right, spacefilling representation viewed looking down onto the extracellular loops, the color scheme remains the same.

of two ferric enterobactin molecules, suggesting partial occupancy of multiple binding sites. An analysis of the biphasic kinetics of FepA mutants deficient in siderophore binding revealed residues that effect either the rapid or slow adsorption step (Cao et. al. 2000), further supporting the existence of two successive binding sites for ferric enterobactin (Buchanan et al. 1998; Payne et. al. 1999).

1.6 Structure and function of FhuA

FhuA, the *E. coli* cell surface receptor for the fungal siderophore ferrichrome, possesses an identical architecture to that of the receptor for ferric enterobactin, FepA. A 22-stranded anti-parallel beta-barrel possessing a N-terminal "plug" domain is reminiscent of the FepA structure (Ferguson et al. 1998; Locher et al. 1998; Figure 1.3). FhuA binds Ferrichrome with a similar affinity as that observed for the FeEnt:FepA interaction (K_d = 0.2nM; Scott et. al. 2001). Lack of studies on mutational derivatives of FhuA deficient in ferrichrome binding prohibit an analysis of determinants responsible for ligand recognition. However, mutational deletion of cell surface loop four (L4) of FhuA impairs ferrichrome uptake suggesting the importance of this cell surface loop in ferrichrome binding. The crystal structure of FhuA liganded with ferrichrome permitted the identification of residues involved in siderophore binding (Ferguson et al. 1998;

Locher et al. 1998 ;Figure 1.3). Residues participating in binding are provided from both the barrel (Y244 and Y315) and the N-terminal "plug" domain (R81, Y166, G99; Ferguson et al. 1998; Locher et al. 1998).

1.7 Protein toxins and Bacteriophages that utilize siderophore receptors

In order to gain a selective growth advantage in the environment, many strains of *E. coli* produce protein toxins known as colicins (Greek for coli killer). Colicins have evolved to exploit the bacterial necessity of iron uptake systems as they are recognized and transported across the outer membrane by specific interaction with TonB-dependent LGP. In search of iron-bearing siderophores, LGP are tricked into transporting a toxin that, upon entry, exerts its lethal effect. The killing mechanisms are varied and depend upon the particular colicin; they include inner-membrane pore formation (Colicins A, B, E_1, K, N, Ia, I_b, 10, and 5; Schramm et. al. 1987; Wiener et. al. 1997; Gouaux 1997; Lazdunski 1998), inhibition of peptidoglycan bio-synthesis (Colicin M; Kock et. al. 1987), and ribonuclease activities (Colicins D, and E_2-E_9). FepA serves as the cell surface receptor for two *E. coli* produced toxins, Colicin B and D, while FhuA recognizes and transports Colicin M. Residues that are important for siderophore recognition in most cases were shown to alter the binding of colicin B by FepA (Newton et. al. 1987; Newton et. al. 1999; Cao et. al. 2000; Barnhard et. al. 2001). In support of these findings is the observation that colicin B and ferric-enterobactin compete for

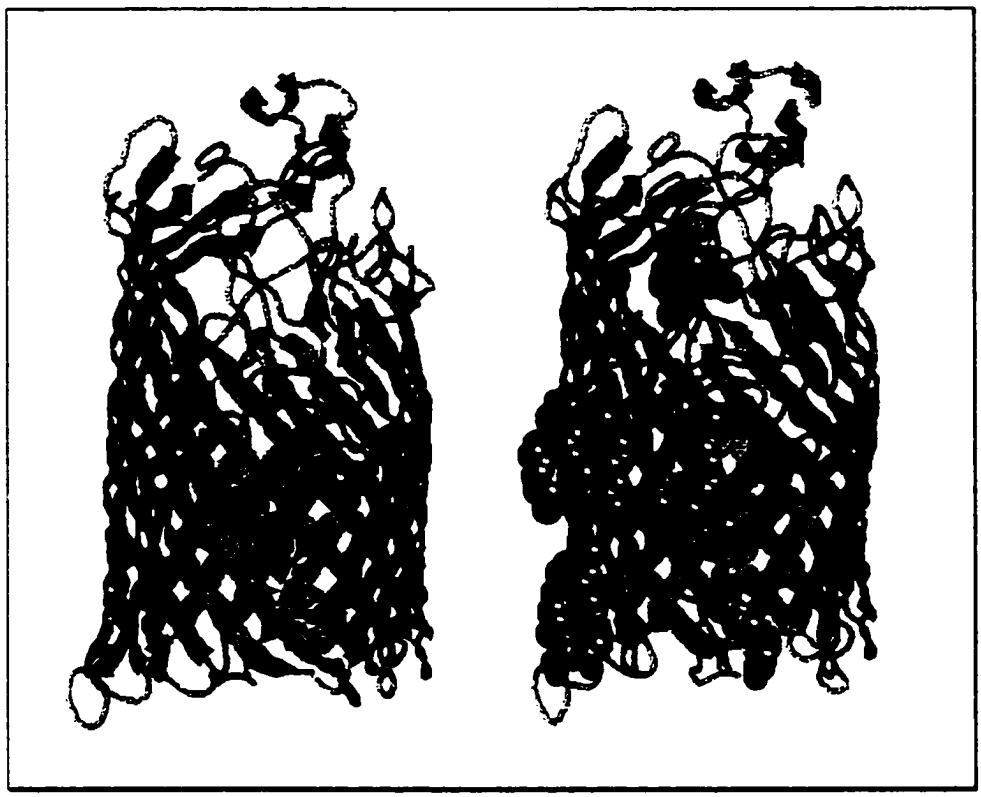

Figure 1.3 Ribbon representation of the crystal structures of FhuA (left) and FhuA with bound Ferrichrome and LPS. β-strands are colored green and α-helices orange. The bound ligands Ferrichrome and LPS are colored red and are in spacefilling representation.

binding, suggesting their binding sites overlap (Wayne et. al. 1976). However, the binding site for colicins is believed to be more complex and involve multiple residues since, colicins are large protein molecules (colicin B MW: 55Kd). In addition to recognition of colicin M, FhuA also serves as the receptor for bacteriophage T5, phi-80, and the antibiotic albomyicin (Coulton et. al. 1983; Braun et. al. 1999). To date, no bacteriophage has been discovered that utilizes FepA for reception. Analogous to siderophore transport, LGP dependent bacteriophage infection and colicin penetration across the outer membrane also show dependency for energy and participation of TonB.

1.8 TonB Dependence of Transport

Since the discovery of the dependency of TonB in the siderophore transport process, its mechanistic action has remained obscure and controversial. Numerous theories have arisen during this time in an attempt to describe the function of TonB, yet its exact function clearly remains the "black box" of siderophore transport (Evans et al. 1996; Klebba et al. 1993; Postle, 1990; Moeck and Coulton, 1998). TonB is a 239 amino acid protein that contains three distinct domains: (i.) a N-terminal alpha-helical transmembrane domain that anchors it to the inner membrane (Skare et al. 1989; Postle and Skare, 1988), (ii.) a central region containing Glu-Pro and Lys-Pro repeats that forms a rigid and extended structure, capable of spanning approximately 100 angstroms and commonly referred to as the

"rigid rod" (Evans et al. 1996; Larsen et al. 1993; Brewer et al. 1990), (iii.) a C-terminal domain of mixed secondary structure. Through its single transmembrane domain TonB associates with two additional inner membrane proteins, ExbB and ExbD, forming a functional complex (Karrlson et. al. 1993b; Ahmer et. al. 1995). The nature of association and function of this complex remains a topic for debate, but appears to occur through a SLHS motif that is exposed on one face of the transmembrane helix (Braun et. al. 1996; Higgs et. al. 1998; Kampfenkel and Braun, 1993; Larsen et. al. 1994; Larsen et. al. 2001).

1.9 Domains of TonB and their Function

TonB's N-terminal transmembrane domain appears to be essential for function and productive interaction with ExbB and ExbD (Higgs et al. 1998; Larsen et al. 1999). Replacement of this domain with the transmembrane segment of TolA, a similar inner membrane protein, abolishes TonB function (Karlsson et al. 1999).

The central "rigid rod" domain of TonB is apparently dispensable to TonB function, as deletions of it do not hinder TonB function (Larsen et. al. 1993). Rather, it seems this domain is crucial for allowing the protein to span the periplasmic space, placing the C-terminal domain within the outer membrane, or in the vicinity of OM receptors. Under high osmolarity, conditions in which the periplasm expands, deletion of the central region of TonB adversely affects

function (Larsen et. al. 1993). However, under low osmolarity the deletion mutant functions normally, supporting the idea that this domain serves as a link, or bridge, between the inner and outer membranes.

It remains unclear what function the C-terminal domain of TonB plays in the transport process, although its importance was observed in mutations that deleted portions of it (Anton and Heller 1991; Letain and Postle 1997; Larsen et. al. 1997). The overwhelming view by most is that this domain is involved in protein-protein contacts with the outer membrane receptors (Postle, 1990; Postle 1993, Koebnik et. al. 1993; Tuckman and Osburne, 1992).

1.9.1 Physical Interactions between TonB and TonB-dependent OM receptors

TonB-dependent siderophore receptors, like FepA and FhuA, possess a region of sequence homology at their N-termini known simply as the TonB box. It was proposed that TonB functions by direct interaction with this region of sequence homology, and this interaction would promote conformational changes in the receptors that allow them to transport bound ligand. Experimental evidence for this conclusion is three fold: (i.) genetic suppressors in TonB that result in a partial restoration of transport to mutations within the TonB-box (Heller et. al. 1988; Schoffler and Braun 1989; Bell et al. 1990; Kadner, 1990; Bradbeer, 1991; Braun et al. 1991), (ii) *in vivo* formaldehyde cross-linking studies suggest the formation of TonB-FhuA and TonB-FepA complexes (Skare et al. 1993; Larsen et al. 1997;

Moeck et al. 1997), (iii.) *in vivo* disulfide bridges were observed between cysteine mutations within the TonB-box of BtuB, the receptor for cobalimin, and cysteine mutations within the C-domain of TonB (Cadieux and Kadner 1999; Cadieux et al. 2000). These data, although suggestive, must be taken with caution since each example lacks crucial controls which undermine the mechanistic interpretation. I will briefly point out some of these objections.

i.) The existence of genetic suppressors is weak evidence for direct interaction between TonB and the siderophore receptors. First, the isolated genetic suppressors only weakly restore receptor function (Bell et al. 1990; Kadner, 1990; Bradbeer. 1991; Braun et al. 1991). In addition. the isolation of genetic suppressors at sites other than the TonB-box seriously undermine the interpretation of interaction between TonB and the TonB-box (Bell et al. 1990). Secondly, as pointed out elsewhere (Klebba et al. 1993), there exist examples in which the isolation of classical genetic suppressors were ultimately shown not to correspond to direct interaction between the two mutant proteins. For instance, mutations to the periplasmic binding protein (HisJ) and the inner membrane permease (HisP) of the *Salmonella typhimurium* histidine transport system were initially viewed as supportive evidence for interaction between these two components (Ames and Spudich 1976). However, later experiments clearly demonstrated that the mutations did not affect interaction between the two, but rather mutations in HisP increased the rate of ATP hydrolysis by this protein (Speiser and Ames 1991;

Petronilli and Ames 1991). Finally, the TonB-box appears to be relatively resistant to mutation, with only proline insertions resulting in abolished function (Gudmundsdottir et. al. 1989; Sauer et. al. 1990; Braun et. al. 1991; Bradbeer 1991; Larsen et. al. 1997; Cadieux et. al. 2000). These proline substitutions may alter function by abolishing the native secondary structure, and the structural alterations they could induce remains to be addressed. Finally, from a conceptual standpoint, it is difficult to rationalize how a single amino acid substitution in TonB can correct for this deficiency, and no direct explanations have surfaced.

ii and iii.) Experiments designed for displaying interaction between TonB and TonB-dependent receptors fail to include appropriate controls, most notably, the search for the appearance of complexes between TonB and non-TonB-dependent outer membrane porins. In addition, formaldehyde cross-linked complexes contain a very small amount (<1%) of cellular TonB. Another baffling observation is how limited amounts of TonB (3000 copies/cell; Skare and Postle 1991) are able to recognize and interact with as many as eight TonB-dependent receptors (Fiu, FepA, FecA, FhuE, FhuA, Cir, IutA, BtuB) which are each expressed at levels of 10,000-80,000 copies/cell under iron starvation.

By a combination of these three experimental observations, TonB is commonly referred to as an energy transducer and the complex formed with ExbB and ExbD known as the energy transduction complex. However, as pointed out above, when closely inspecting and critiquing these experiments it becomes

apparent that this distinction is unsubstantiated. Rather, it appears that the distinction of being an energy transducer is formed by deduction: Both TonB and energy input are required for transport, and both reside in the inner membrane, therefore TonB must transduce energy to the outer membrane receptors.

1.9.2 Crystal structure and function of the TonB C-terminal Domain

The importance of the C-terminal domain of TonB in the transport process was first recognized in two deletion mutants (Anton and Heller 1991). Deletion of the C-terminal eight amino acids of TonB had no deleterious effect on TonB function whereas deletion of the C-terminal fifteen amino acids resulted in a non-functional protein (Anton and Heller 1991). Studies aimed at discovering the cellular localization of TonB suggest this domain may reside within, or associate with, the outer membrane (Letain and Postle 1997). TonB was observed to partition between inner (60%) and outer membranes (40%) when cell envelopes are separated *via* sucrose density gradient fractionation. Truncations to the C-terminal domain of TonB resulted in a cognate loss of this partitioning pattern with the outer membrane fraction (Letain and Postle 1997).

Recently the crystal structure of the C-terminal domain of TonB was solved at 1.55 Å (Chang et al. 2001; Figure 1.4). It exhibits a novel fold, lacking homology to any other known structure, and the crystal structure provides the first evidence that TonB exists as an interwound dimer. Each monomer contains a

three-stranded β-sheet and one alpha helix, with the six beta strands forming one anti-parallel β-sheet within the dimeric structure (Figure 1.4). The authors suggested two models for TonB function based, in part, upon the dimeric structure. In both models, inner membrane derived PMF promotes torsional movement of either ExbB-ExbD that is transduced to the C- terminal domain of TonB mediating its transient interaction with OM receptors (Chang et al. 2001). The two models differ primarily in the number of ExbB:ExbD complexes with which dimeric TonB interacted, one per dimer or alternatively two per dimer. The PMF-promoted torsional movement of ExbB-ExbD is assumed to be similar to that observed for rotational movement of the flagellar motor or ATPase. Superficially supporting this idea is the observation of weak sequence homology between ExbB and MotA (mobility protein of the flagellar motor), and similar membrane topologies of ExbB and MotA (Chang et. al. 2001).

1.10 Siderophore transport mechanisms; Unresolved questions

The crystal structures of FepA (Figure 1.2) and FhuA (Figure 1.3) defined the overall architecture of siderophore receptors but failed to answer several pertinent questions regarding their biochemical function. Ligand recognition and their internalization, for instance, were only vaguely defined. The siderophore receptors of *E. coli* discriminate between numerous ferric siderophore complexes, which, despite their similar size (600-1000 da) and chelation geometry (hexa-

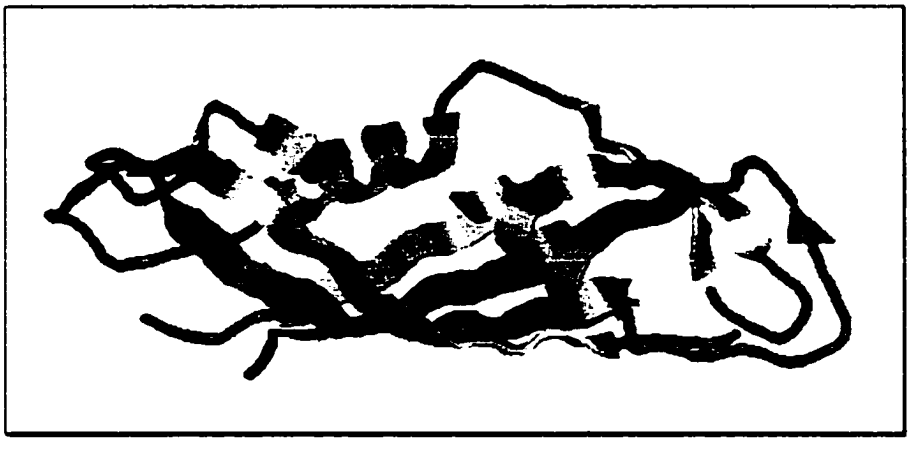

Figure 1.4 Dimeric crystal Structure of the C-terminal Domain of TonB. The C-terminal fifteen amino acids have been colored red and green respectively for each monomer.

coordinate) differ in their net charge and chemical composition (Neilands, 1982; Neilands, 1995). Does specificity arise from residues within cell surface loops, residues within the N-domain, or a combination of the two? Although liganded structures of FhuA superficially defined the FhuA ligand binding pocket for ferrichrome, poor resolution of the ferric-siderophore in ligand-bound structures of FepA prevented the determination of similar residues within FepA.

Despite numerous biophysical studies implicating conformational change within cell surface loops as an inescapable phenomenon of the siderophore transport process (Liu et al. 1994; Klug et al. 1998b; Payne et al. 1997; Jiang et. al. 1997; Bos et. al. 1998; Cao et al. 2000), virtually no difference in the conformation of cell surface loops were identified between free and liganded receptors, casting a shadow of doubt as to what role conformational change plays in the siderophore binding and transport process (Ferguson et al. 1998; Locher et al. 1998; Buchanan et al. 1998).

Undoubtedly, the most intriguing question arising from the crystal structures was what the function and ultimate disposition of the N-domain was relative to the transport process. Passage of ferric-siderophores through outer membrane receptors requires a minimum diameter of approximately 15 Å, which does not exist in either the FepA or FhuA structure. Two likely alternatives exist: (i.) the N-domain alters its conformation within the channel forming a substrate-customized pathway for the ferric-siderophore to pass into the periplasm (ii.) the

entire N-domain is removed from the channel producing a open pore through which the ferric-siderophore may pass. The latter faces, among others, a large energetic barrier to overcome since the crystal structure defined some fifty hydrogen bond and ionic interactions between the N-domain and the barrel wall (Ferguson et al. 1998; Locher et al. 1998; Buchanan et al. 1998). However, this could, in part, explain the energy dependency of the transport process (Bradbeer, 1993). The former, appears to be more plausible, but transient channels of such size have not been observed in membrane proteins. Siderophore receptors also transport synthetic siderophore-antibiotics, called "Trojan-horse antibiotics," that often double the size of the iron complex without affecting its recognition or transport (Mckee et al. 1991; Dolence et al. 1990; Miller et al. 1991). In addition, although it remains unclear how protein toxins like colicin B transverse the membrane, the complete removal of the N-domain must precede transport if the protein toxins are transported through the barrels of outer membrane receptors.

1.11 Fluorescence Spectroscopy

Molecules adsorbing light may either return to the ground state by a non-radiative transition or by the emission of light at a longer wavelength. The probability of occurrence of the latter, called fluorescence, is defined by the molecules quantum yield (Q), that is, the ratio of the number emitted to absorbed photons. Proteins contain three amino acids which may contribute to fluorescence:

tyrosine (tyr), tryptophan (trp), and phenylalanine (phe). Protein fluorescence is normally excited at an absorption maximum near 280nm, or longer wavelengths. Consequently, phenyalanine (λ max = 260nm) is not excited under these conditions. Furthermore, the quantum yield of phenyalanine in proteins is quite low, so that emission from it is rarely observed. At wavelengths longer than 295nm, the adsorption is due primarily to tryptophan. The emission properties of tryptophan are highly sensitive to solvent polarity. As a result, the emission spectra of tryptophan residues reflect the polarity of their surrounding environment. Tryptophan fluorescence is, in many cases, sensitive to the binding of substrates, association of complexes, and to denaturation. As such, the fluorescence of this residue has been exploited to study the folding/unfolding of proteins, in measurements of affinity between protein and ligands, and assembly of macromolecular complexes. The ability of the indole nucleus of tryptophan to donate electrons within the excited state provides for a unique sensitivity to fluorescence quenching by a variety of substances. Referred to as any process that decreases the intensity of fluorescence, quenching includes excited state reactions, energy transfer, complex formation (static), and collisional (dynamic) quenching. Collisional quenching requires a molecular contact between the fluorophore and quencher, in that the quenching agent must diffuse to the fluorophore during the lifetime of the excited state. Collisional quenching of fluorescence is described mathematically by the Stern-Volmer equation:

Equation 1.1 The Stern-Volmer Equation: $F_o/F = K_D[Q] + 1$

In this equation, F_o and F are the relative intensities in the absence and presence of quencher respectively, [Q] is the concentration of quencher, K_D is the Stern-Volmer quenching constant, and can be further reduced to $K_D = k_q\tau_o$: k_q is the bimolecular quenching constant, and τ_o is the lifetime of the fluorophore in the absence of quencher. The Stern-Volmer constant K_D, is obtained graphically through Stern-Volmer plots, F_o/F vs. [Q] where the y intercept is equal to one, and the slope is equal to the Stern-Volmer constant. Typically three quenchers of tryptophan fluorescence are employed to investigate the environment of the fluorescing residue: acrylamide (hydrophobic, uncharged), iodide (hydrophilic, negatively charged), and cesium (hydrophilic, positively charged). Stern-Volmer plots for a particular quencher in the presence and absence of a protein denaturing agent, such as guanidine, allow for an estimation of the local environment in which the tryptophan residue resides in the folded protein structure.

1.12 Cross-linking of cell membrane proteins.

Chemical crosslinking of proteins is widely used in biochemical research to identify the subunit organization of multimeric proteins (Nicolson and Singer 1971; Frye and Edidin 1970), as a tool for determining protein-DNA and protein-RNA

interactions (Wang et. al. 1997), and for studying the interaction of proteins (Mikkelsen and Wallach 1976; Trommer et. al. 1975). In chemical cross-linking, proteins are treated with a crosslinking reagent (usually bifunctional) producing a covalent linkage between two components. Resulting complexes are then separated by SDS-PAGE, and if cleaveable reagents are employed, the components of the cross-linked species are regenerated by cleavage and subsequent identification on a second SDS-PAGE gel.

Cross-linking of membrane proteins is a straight forward procedure, since it is usually achieved by simply mixing a crosslinking reagent with cell membranes or live cells. However, due to the extensive variety of reagents available, the first decision to be made is the selection of an appropriate reagent for the membrane system. A separate and different concern when cross-linking membrane proteins is the possibility that random collision-dependent crosslinking could occur at a high frequency as a consequence of the fluidity of lipid bilayers. For crosslinking studies of Gram-negative bacterial outer membrane proteins, this concern is limited by the nature of the membrane. The outer membrane is not a typical fluid mosaic model of lipid-bilayers, rather diffusion in the asymmetric outer membrane is quite low when compared to a prototypical lipid bilayer. Important considerations for reagent choice of cross-linking studies include: (i.) cleavability, (ii.) homo- versus heterobifunctionality, (iii.) specificity, and (iv.) molecular dimensions of the reagent. There are three major divisions of reactive crosslinking

groups, the imidates, N-Hydroxysuccinimide (NHS) esters, and azides. Each has its distinct advantages and disadvantages for use in crosslinking experiments. Both imidates and NHS esters react specifically with amino groups, while azides react more non-selectively with a large variety of chemical groups. In addition, the half-life of a NHS ester at pH = 8.6 is approximately 10 min., yet 4-5 hr. at pH = 7. This trend is reversed for imidates, and while the reactivity of both are optimal at a pH = 9.0, as the pH drops towards neutrality the reactivity of NHS esters is about one-half of that at pH = 9.0, whereas that of imidates is considerably lower. Furthermore, the reactivity of NHS esters at lower temperatures is less affected than that of imidates or azides, allowing them to react efficiently at temperatures of 0-4 °C. These considerations suggest that NHS esters are the reagent of choice if reactions are to be performed at physiological pH. The homo-bifunctional NHS ester Sulfo-EGS [Ethyleneglycolbis (sulfosuccinimidylsuccinate)] was employed for cross-linking studies of FepA. Sulfo-EGS was chosen as the candidate cross-linking reagent for numerous reasons: (i.) it is water soluble and membrane impermeant. (ii.) the size of Sulfo-EGS (664 Da) prevents its diffusion across the water-filled channels of the outer membrane and thus restricts its action to targets on the surface of the outer membrane. (iii.) the reactive homo-bifunctional cross-linking groups of Sulfo-EGS react specifically towards defined chemical targets (primary amines: Lysine). (iv.) a defined spacer length (16.1 Å) between the two

reactive groups permits the knowledge of relative distances between the components of the cross-linked species.

Chapter 2

Materials and Methods

2.1 Bacterial strains and plasmids

All bacterial strains used in these studies are derivatives of *E. coli* K-12, listed in Table 2.1 with their genotype and reference. AN102 was used for the purification of enterobactin, UT5600 and ER2507 were used for purification of outer membrane and TonB-fusions respectively. KDF541 and KDF571 were used for phenotypic characterization of FepA, FhuA, and derivatives whereas BN1071 and KDO23 were employed for characterization of TonB fusion protein derivatives,

Strain	*Relevant genetic loci*	*Reference*
JS54	*leu, thyA,* ϕ80immLAM,	Bejar and Bouche 1985
AN102		Cox et. al. 1970
UT5600	*pro, leu, trp, thi lac, entA, ompT*	McIntosh et. al. 1979
BN1071	F⁻, *thi, entA, pro, trp, rpsL*	Klebba et. al. 1982
KDF541	BN1071, *recA, fepA, fhuA, cir*	Rutz et. al. 1992
KDF571	KDF541, *tonB*	Rutz et. al. 1992
AN193	F⁻, *pro, leu, trp, thi, fhuA, lac, rpsL, entA*	Klebba et. al. 1982
ER2507	*Δ(malB), zjb::Tn5, rpsL, supE44, fhuA*	New England Biolabs
KDO23	BN1071, *tonB*	This study
AN718	F⁻, *uncA401, argH, pyrE, entA*	Gibson et. al. 1977
ANC718	F⁻, *uncA401, argH, pyrE, entA, fepA*	This study

Table 2.1. Bacterial strains utilized: their genotype and reference.

Plasmid Name	*Genotype*	*Reference*
pRZ540	*tonB*	Postle and Good 1983
pMF19	*wbbL* (rhanmosyltransferase)	Feldman et. al. 1999
pMalp2		New England Bio-labs
pHSG575		Hashimoto-Gotoh et. al. 1981
pITS449	*fepA*$^+$ on pUC18(-35 region missing)	Rutz et. al. 1992
pITS23*	*fepA*$^+$ on pHSG575(Full promoter)	This study
pFepβ*	*fepA*Δ17-150	This study
pFepβ2*	*fepA*Δ3-150	This study
pFepNFhuβ*	*fepA*1-152::fhuA160-723	This study
pITS11*	*fhuA*$^+$ on pHSG575	This study
pFhuβ*	*fhuA*Δ5-160	This study
pFhuNFepβ1*	*fhuA*1-155::*fepA*149-724	This study
pFhuNFepβ2*	*fhuA*1-160::*fepA*153-724	This study
pSTON	pMalp2 *malE::tonB* 170-239	This study
pSTON104	pMalp2 *malE::tonB* 104-239	This study
pSTONRig	pMalp2 *malE::tonB* 69-239	This study
pSTONFull	pMalp2 *malE::tonB* 1-239	This study
pTon23	*tonB*$^+$ on pHSG575	This study
pTon23Flag	*tonB*1-239::α-FLAG epitope	This study

Table 2.2: Listing of names and genotypes of plasmid constructions. Plasmid names denoted with an * indicate they are also cloned on the high copy vector pUC18.

in the wild-type and *tonB* backgrounds respectively. Plasmids used in the studies are listed in Table 2.2 along with their genotype.

2.2 Growth Media

Table 2.3 lists the growth media used to culture bacterial strains for these studies. DNA manipulations were performed with strains grown in the rich Luria-Bertani Broth (LB); expression of iron-regulated genes was stimulated by growth in minimal media that is deficient in iron (MOPS or T-media). Siderophore Nutrition assays were performed in Nutrient Broth, and bacterial lawns for either colicin killing or antibiotic susceptibility were prepared with tryptone top agar.

Media	Reference
Luria-Bertani Broth	Miller, 1972
T-media	Klebba et. al. 1982
MOPS media	Neidhardt et. al. 1974

Table 2.3. Media and References

2.3 Polymerase Chain Reaction (PCR)

The constructs generated in this study were cloned by PCR amplification of either existing plasmids or genomic DNA containing the gene of interest, and noted accordingly in each individual description. In general, the following PCR procedure was used for amplification. 100μl reactions contained 10ng or 60ng of template DNA for plasmid or genomic targets respectively, 10μM dNTP mixture, 200ng each of the two primers designed for amplification, 1X pfu buffer (Stratagene), and 2.5units of pfu polymerase (Stratagene). The following PCR cycling parameters were used as a standard, and modified accordingly corresponding to the length of template to be amplified: 1 cycle of denaturation at 98 °C; 30 cycles of denaturation for 30 sec. at 98 °C, primer annealing at 55 °C for 30sec or 1 min. for plasmid and genomic templates respectively, and X min. of extension at 72 °C where X is equal to 2 min. times the length in kilobases of the target to be amplified; 1 cycle of extension for X min at 72 °C to ensure complete DNA strand synthesis; 1 cycle at 4 °C for infinity to chill the reaction until manipulations would be performed. Agarose load buffer (0.04% bromophenol blue, 5% glycerol in water) was added to the reactions and electrophoresed on agarose gels (0.8 to 1.2 % depending on the size of product). Products were visualized by UV illumination, incorporating ethidium bromide in the gel matirx at a concentration of approximately 0.5 μg/ml. The size of the product was estimated by running a control lane containing standard molecular weight markers (λ1kb;

Gibco BRL). The amplification product was excised from the gel with a razor blade and isolated by use of GENECLEAN™ (Bio 101, Vista, CA, USA). Genecleaned DNA was then digested in 40 µl reactions containing 10 units each of the two restriction enzymes whose sites were incorporated at the terminal end of the PCR primers, and 1X React buffer (Gibco BRL) chosen to be compatible for 100% activity for the two enzymes. The digestions were electrophoresed on agarose gels and DNA recovered by GENECLEAN. The DNA was then ligated into its appropriate vector at 16 °C for 12 to 18 hours in 15 µl reactions containing 1 unit of T_4 DNA Ligase (Gibco BRL), 1X T_4 ligase buffer, and a 10 fold molar excess of insert to vector. The vector used in the ligation was previously digested and purified with the appropriate enzymes, essentially as described for the digestion of PCR products. The ligation reaction was ethanol precipitated to remove salts, and resuspended in 20µl of distilled H_2O. Two microliters of the resuspended ligation reaction was transformed into competent cells with an *E. coli* pulser (Bio-Rad), 600 µl of SOC media was added and the mixture shaken at 37 °C for 1 hour. The cells were then plated on LB-agar plates containing either ampicillin (100µg/ml) or chloramphenicol (20µg/ml) for pUC18 and pHSG575 derivatives respectively. Clones were selected and grown overnight in LB broth, and plasmid DNA isolated with the CONCERT™ rapid plasmid purificitation system (Gibco BRL). Clones were screened by restriction digest and/or di-deoxysequencing.

2.4 *malE::tonB* fusions

All MalE-TonB fusions were constructed in the recipetent vector pMalp2 (New England Biolabs). It contains a P_{tac} promoter that regulates transcription of a MalE-LacZ′ fusion. The multiple cloning site of this vector allows replacement of the *lacZ′* moeity with another gene of interest. The expression level of the resulting fusion protein may be regulated by variation of the IPTG concentration in culture media, and the hybrid protein itself may be affinity purified by chromatography on an amylose resin. After purification, the MalE portion may be removed by enzymatic digestion of a Factor X_a site in the linker region between MalE and LacZ′. Four TonB fusions were generated between MalE and TonB, each TonB portion of the fusion was PCR amplified from pRZ540 (*tonB*; Table 2.2). Table 2.3 lists the primers utilized, the restriction sites incorporated, and the annealing location of each primer in the TonB sequence.

2.5 pITS23: *fepA* on pHSG575

The pUC derived plasmid pITS449, contains *fepA* cloned *via* PstI and Sac I restriction sites (Rutz et. al. 1992). *fepA* in pITS449 possesses the -10 promoter region of the wild type gene, but lacks the -35 region (Rutz et. al. 1992). To construct a full promoter containing *fepA* plasmid, BN1071 genomic DNA was PCR amplified with the forward primer 5′-

AC**CTGCAG**TCTCACTTCCTACTTTTAACG-3', which anneals 60 nucleotides 5' of the -35 promoter region and incorporates a PstI site for cloning. The reverse primer, 5'-**GTTGAT**ATCCCACGCGTCA-3', anneals at amino acid residue 206 of the mature FepA sequence at an internal MluI site within FepA. The 900 base pair product was then ligated into PstI:MluI digested pITS449, creating pITSP23 on the high copy pUC18 vector.

Host strains (KDF541, KDF571, AN193, etc..) containing the full promoter clone in the high copy pUC vector were toxic to cell growth when grown in minimal media (MOPS and T-media; data not shown). Therefore, the full promoter containing FepA gene was transferred onto the low copy vector pHSG575 (Hashimoto-Gotoh et. al. 1981). The gene was exchanged using two mutual restriction sites within the multiple cloning sites of pUC18 and pHSG575, EcoRI and HindIII. To accomplish this in the presence of the natural EcoRI site, at position 170 of the FepA mature sequence, pITSP23 DNA was partially digested with EcoRI; 5ug of pITS23 DNA, 5ul React II (Gibco-BRL), 1ul of EcoRI at 2.5u/ul in a 50 ul reaction volume and incubated for 45 min. at 37 °C. The singly cut linerarized mixture was purified from an agarose gel by GENECLEAN™ and subjected to digestion with HindIII and FspI to produce the 2.5kb product containing FepA. The resulting insert was then ligated into EcoRI/HindIII digested pHSG575.

Clone	Primer Sequence	Restriction	Location in TonB
pSTON	5′-**GAAGGATTTC***ATT*GCGCATTGAAGGGCAGG-3′	Xmn I	R172
	5′-CT**AAGCTT***ACG*GCCGGTTGCGGT-3′	Hind III	250 nuc. 3′ of stop codon
pSTON104	5′-AG**GAATTC***AAA*AAGGTACAGGAGCAGCC-3′	EcoR I	K104
	5′-CT**AAGCTT***ACG*GCCGGTTGCGGT-3′	Hind III	250 nuc. 3′ of stop codon
pSTONRIG	5′-AG**GAATTC***CCG*CCACCGGAGCCGG-3′	EcoR I	P63
	5′-CT**AAGCTT***ACG*GCCGGTTGCGGT-3′	Hind III	250 nuc. 3′ of stop codon
pSTONFULL	5′-T**GAATTC***ATG*ACCCTTGATTTACCTCGC-3′	EcoR I	M1
	5′-CT**AAGCTT***ACG*GCCGGTTGCGGT-3′	Hind III	250 nuc. 3′ of stop codon

Table 2.4 Sequence, restriction site, and location of the primers used for cloning MalE:TonB fusions

2.6 pITS11: *fhuA* on pHSG575

FhuA was cloned onto pHSG575 by PCR amplification of BN1071 genomic DNA with the forward primer 5'-AG**CTGCAG**AAGGATATGTTTGGTACTAA-3', and the reverse primer 5'-TC**GGATCC**GGTGAACCGCTGAAAGAAGTTCAGTT-3' incorporating PstI and SacI restriction sites respectively. To ensure inclusion of the entire wild type promoter, the forward primer was designed to anneal 270 nucleotides 5' of the translational start site. Due to the unavailability of anti-FhuA antibodies, we were unable to assess the expression level of FhuA from this clone in comparison to chromosomal levels. Rather, the integrity of the clone was verified by cycle sequencing and restoration of wild type phenotypic properties of *fhuA*$^-$ strains harboring the plasmid.

2.7 pFhuNFepβ1 chimera; FhuA1-155:FepA149-724

The chimeric protein was constructed by sequential cloning of the FhuA N-terminus and the FepA β-barrel. Briefly, the N-domain of FhuA (residues 1-155) was PCR amplified from BN1071 genomic DNA with the forward primer 5'-AG**CTGCAG**CAAGGATATGTTTGGTAGTAA-3' and the reverse primer, 5'-C**GGATCC**ACGCTTGCTGACCATATTCAA-3' incorporating PstI and BamHI sites respectively. The approximately 800 bp product was then cloned into pUC18 creating pFhuN. In a separate reaction, the β-barrel of FepA was PCR amplified

from pITS449 with the forward primer 5'-TCGGATCCGGCGAGTGGCACGGCTCC-3' and the reverse primer 5'-TCGAGCTCAACGACGCGCACTTTGTCAA-3' incorporating BamHI and SacI sites respectively. The 1.7 kb product from this amplification was then cloned into pFhuN, creating ppUCFhuNFepβ1. The chimeric fusion was then transferred to pHSG575 by digestion with EcoRI and HindIII, creating pFhuNFepβ1. As described above for the cloning of pITS23, EcoRI and HindIII were used because the multiple cloning site of pHSG575 does not contain a SacI site. Thus, partial digestion of the chimera in pUC was required due to the presence of an internal EcoRI site at position 170 of FepA.

2.8 pFepNFhuβ chimera; FepA1-152:FhuA160-723

Analgous to pFhuNFepβ1, the chimeric protein joining the N-terminus of FepA and the β-barrel of FhuA was constructed by a sequential cloning procedure. Briefly, the N-terminus of FepA was PCR amplified from BN1071 genomic DNA with the forward primer 5'-ACCTGCAGTCTCACTTCCTACTTTTAACG-3' and the reverse primer 5'-TCGGATCCTTTTTTGGTAATGATGTTAACCAC-3' incorporating PstI and BamHI sites respectively. The approximately 900 bp product was cloned into pUC18 generating pFepN. In a separate reaction, the β-barrel of FhuA was PCR amplified from BN1071 genomic DNA with the forward primer 5'-TCGGATCCGGTGAACCGCTGAAAGAAGTTCAGTT-3' and the

reverse primer 5'-TC**GAGCTC**AACTTGTGAAATGGGCACGG-3' incorporating BamHI and SacI sites respectively. The 1.8kb product from this amplification was cloned into pFepN creating ppUCFepNFhuβ. The chimeric fragment was transferred to pHSG575 with EcoRI and HindIII digestion, creating pFepNFhuβ.

2.9 pTon23: *tonB* on pHSG575

The structural gene for TonB was cloned onto pHSG575 by PCR amplification of pRZ540 (*tonB*; Table 2.2). The forward primer was designed to anneal approximately 350 nucleotides 5' of the translational start codon so that the clone would retain the wild-type promoter and regulatory sequences in addition to incorporating a EcoRI site for cloning; 5'-**GAATTC**AAACGACCTTCATCATGCAGT-3'. The reverse primer annealed downstream of the stop codon and incorporated a HindIII site for cloning; 5'-CT**AAGCTT***ACG*GCCGGTTGCGGT-3'. The clone was verified by cycle sequencing, and phenotypically by the ability to restore wild-type functions in the *tonB* strains KDF571 and KDO23.

2.10 Isolation of genomic DNA

Two principal methods were employed for the isolation of genomic DNA from bacterial strains. The first (TritonX-100; NWFSC Molecular Biology protocols on the web) method was used when PCR and subsequent cloning of the

fragment was desired. Briefly, a 5 ml. overnight culture was pelleted and resuspended in 300µl STET buffer (8% Sucrose, 5% Triton X-100, 50mM Tris-Cl pH = 8.0, 50mM EDTA), and 30 µl of a Rnase/lysozyme mixture (10mg/ml lysozyme, 1mg/ml Rnase A in 50mM Tris-Cl pH = 8.0) was added and boiled for 1 min. 15 sec. The supernatant was phenol extracted, and proteins precipitated by the addition of 1/10 volume 4M LiCl. DNA was recovered by precipitation with 100% isoproponal.

The second method was utilized due to its ease and rapid purification of genomic DNA, and was employed when genomic DNA was to be PCR screened for product sizes (Wen-ping and Tsong 1993). Briefly, 1.5 ml. of a overnight culture was pelleted and resuspended in 200 µl of lysis buffer (40mM Tris-Acetate pH = 7.8, 20mM Na-Acetate, 1mM EDTA, 1% SDS) and cells lysed by vigorous pipetting. Proteins were removed by the addition of 70 µl of 5M NaCl, mixed well, and pelleted. The supernatant was extracted with chloroform and DNA recovered by precipitation with 100% ethanol.

2.11 Preparation of Competent Cells

A 5 ml. overnight LB culture of the strain to be rendered competent was subcultured (1/100) into 500ml. LB broth containing the appropriate antibiotics. Growth was monitored until the culture reached an $O.D._{600} \approx 0.5$ and chilled on ice for 10 minutes. Bacteria were pelleted by centrifugation (5000rpm 12min.) and

washed twice by resuspension in 200 ml. ice cold dH_20 and collected by centrifugation. The pellet was then washed once by resuspension in 10ml of 10% glycerol. Pellets were then resuspended with 10% glycerol to a final volume of 2ml, aliquoted (40ul), and frozen at -80 °C.

2.12 Site-directed mutagenesis

Site-directed mutants were prepared by the Quik-Change Site-directed Mutagenesis kit (Stratagene). Mutagenesis reactions contained 90ng of template DNA, 125ng of mutagenic primers, 10μM dNTPs, 1X Reaction buffer (Stratagene), and 2.5u of pfu turbo DNA polymerase in a 50μl reaction volume. Temperature cycling was performed with the following parameters; 1 cycle of denaturation at 98 °C for 2 min, followed by 18 cycles of denaturation (98 °C for 30 seconds), annealing (55 °C for 1 min.), and extension (68 °C 2min/kb of target). A final extension step was incorporated after the eighteen cycles to ensure complete synthesis. Following temperature cycling an aliquot was removed (10 μl) and electrophoresed on a 1% agarose gel to visualize the efficiency of the cycling process. To the remaining reaction, 1μl of the restriction enzyme DpnI was added and incubated for 1 hr. at 37 °C. The volume was adjusted to 100μl by the addition of autoclaved dH_2O, ethanol precipitated, and resuspended in 20μl of dH_2O. Typically, 3μl of this solution was transformed into an appropriate strain by electroporation (*E. coli* pulser; Bio-Rad) and selected by plating on LB-agar plates

containing chloramphenicol at 20 μg/ml. Mutations will be referred to in the following manner, X#Y, where X represents the wild-type amino acid to be mutagenized, # refers to the position of the residue in the primary sequence, and Y indicates the amino acid residue to which it was mutagenized.

2.13 Siderophore nutrition assay

Qualitative examination of siderophore uptake efficiency was determined through siderophore nutrition assays. Bacterial strains harboring wild type or mutant derivatives were innoculated from frozen permanents into LB media containing the appropriate antibiotic or combination of antibiotics for the strain and plasmid utilized (100ug/ml streptomycin, 100ug/ml ampicillin, 20ug/ml chloramphenicol). Cultures were grown overnight at 37 °C and subcultured 1/100 into LB and allowed to reach mid-log growth ($O.D._{600}$ 0.5-0.9). 100μl of the bacterial culture was plated in a six well culture cluster (Corning Incorporated) with 3ml. of Nutrient top agar, 90μM Apo-ferrichrome A, and antibiotics (100μg/ml streptomycin, 10μg/ml ampicillin, 20μg/ml chloramphenicol, accordingly for the strain/plasmid combination). The agar was allowed to solidify and a ¼" diameter sterile paper filter disk (Becton Dickinson Microbiology Systems, MD) was placed on top of the agar. Five microliters of a 50μM ferric-siderophore solution was dispensed onto the disk and incubated overnight at 37 °C. Results are expressed as the diameter of the observed growth halo in millimeters.

2.14 Colicin and bacteriophage sensitivities

Killing assays were utilized to assess the efficiency of protein toxin and bacteriophage sensitivity of FepA, FhuA, and their derivatives. Strains of interest were grown overnight in LB at 37 °C. 100μl of the bacterial culture was seeded onto LB plates with tryptone top agar containing the appropriate antibiotics for the strain/plasmid combination tested. Serial dilutions of colicins B, D, or M and bacteriophage T5 and ϕ80 were prepared in 96-well microtiter plates. Five microliters volumes were transferred to the plate using a Clonemaster (Immusine Corp., San Leandro, CA), and the plates incubated overnight at 37 °C. Results are expressed as the reciprocal of the highest dilution that still resulted in clearing of the bacterial lawn.

2.15 Preparation of Ferric Enterobactin

Enterobactin was purified from the supernatant of AN102 cultures (Wayne et al., 1976). Ferric enterobactin was prepared by dissolving 1-2mg of enterobactin in 0.5 ml methanol, mixed with 0.5 ml of 4mM $FeSO_4$ in dilute HCL, and incubated at room temperature for 1-2 hours to allow for complex formation. NaH_2PO_4 pH = 6.9 was added to a final concentration of 10mM and subjected to gel filtration on Sephadex LH20 equilibrated in 10mM phosphate buffer. The concentration of ferric enterobactin was calculated by measuring the absorbance at 495nm (mM = 5.6; Pollack et al. 1970) on a DU Beckman 640 spectrophomoter. The relative

purity of the preparation was determined by ratio of absorbance between 395nm and 495nm (395nm/495nm). Ferric enterobactin was stored on ice and repurified after 2-3 days by re-chromatographing the sample on Sephadex LH20. ^{59}Fe-enterobactin was prepared by the addition of 0.05mCi of $^{59}FeCl_3$ to $FeSO_4$ prior to the addition of enterobactin.

2.16 Siderophore Binding

The adsorption of ^{59}FeEnt and ^{59}FeFc was measured with metabolically inactive KDF541 expressing FepA or FhuA and their derivatives, respectively. Cultures were grown overnight in LB broth and subcultued 1/100 into MOPS minimal media to induce expression of iron regulated genes. Bacteria were grown for 6 h at 37 C to mid-log and then chilled on ice for 1 h, and an aliquot (containing 5 X 10^7 cells) was pipetted into a 50-ml test tube and incubated on ice. 25-ml volumes of ice-cold MOPS minimal media, containing varying concentrations of ^{59}Fe-siderophore, were poured into the tubes to achieve rapid and thorough mixing. After 1 min the binding reactions, which were performed in triplicate, were filtered through 0.45-um nitrocellulose, the filters were washed with 10ml of 0.9% $LiCl_2$ and counted in a Packard Cobra gamma counter. The initial adsorption reaction reached equilibrium within 5 s at physiological temperatures and 1 min on ice. The FepA and FhuA-deficient strain KDF541 was simultaneously tested as a negative control, and any nonspecific adsorption of ^{59}Fe-

siderophores by this strain was subtracted from the experimental samples. Whenever necessary because of low cpm bound, the assay samples were counted for an extended period of time (up to 30 min.) to decrease standard error. Binding data were analyzed using the Bound versus Total equation of Grafit 4.013 (Erithacus Ltd., Middlesex, UK).

2.17 Siderophore Transport Measurements

Transport manipulations were performed at 37 C. A volume of mid-log bacterial culture (50-100ul containing 5 X 10^7 cells) was pipetted into a 50-ml test tube and incubated in a 37 C water bath. Without delay, 25 ml of prewarmed MOPS minimal media, containing glucose (0.2%), appropriate nutritional supplements, and varying concentrations of ^{59}Fe-siderophores, were poured into the tube to achieve rapid and thorough mixing. The transport reactions were quenched by the addition of 1000-fold excess of nonradioactive ferric siderophores, immediately filtered through 0.45um nitrocellulose, and the filters were washed with 10 ml of 0.9% $LiCl_2$ and counted in a Packard Cobra gamma counter. Kinetic parameters were determined from the initial rates of uptake, which were calculated at each substrate concentration from two independent measurements mad in triplicate at 5 and 15 s: cpm bound to the cells at 5s were subtracted from the cpm associated with the cells at 15 s (10-s uptakes). For some mutants with low uptake rates (FepNFhu , FhuNFep , Fep) the uptake period was extended to 60 min

(Newton et al. 1999). In all transport experiments, the FepA and FhuA-deficient strain KDF541 was simultaneously tested as a negative control, and any non-specific adsorption of ^{59}Fe-siderophores was subtracted from the experimental samples. Transport results were analyzed according to the Michaelis-Menten equation, using Grafit 4.013.

2.18 Expression of FepA and mutant derivatives

Overnight LB cultures were subcultured 1/100 into MOPS minimal media and grown for 6 hours at 37 °C. Cells were pelleted and resuspended in SDS-PAGE sample buffer at 5 * 10^9 cells/ml, boiled for 5 minutes, and a 25µl aliquot was loaded onto 10% SDS-PAGE gels. After electrophoresis the gel was transferred to a nitrocellulose membrane and subjected to immunoblot analysis. Briefly, the membrane was incubated with blocking buffer (TBS + 1% Gelatin) to block unbound sites on the membrane, and treated with a α-FepA mAB (1:500 dilution in blocking buffer). The membrane was washed five times with TBS+0.05% Tween 20, and then incubated with ^{125}I-Protein A diluted in blocking buffer. After five washes with TBS-Tween, the membrane was exposed to X-ray film (Kokak) overnight and developed.

2.19 Measurements of Protein Concentration

The Micro BCA method (Pierce) was utilized to determine the protein concentration of purified proteins. Bovine Serum Albumin (BSA) served as the standard control, and for samples containing detergent an equivalent amount of buffer was added to the standard solutions.

The protein concentration of purified membranes was determined by boiling an aliquot of membranes in 1% SDS, and measuring the $O.D._{280}$. A standard value of 1 O.D. unit = 1mg/ml was used to estimate protein concentration.

2.20 Purification of the TonB C-terminus

ER2507/pSton was grown overnight in LB with ampicillin and streptomycin at 100ug/ml and subcultured at 1% into LB broth containing 0.2% glucose. Cells were grown to mid log (OD_{600} 0.5-0.8) and synthesis of the fusion induced by the addition of 0.5 mM IPTG. After 3 hours of induction, cells were collected by centrifugation and lysed in a French pressure cell at 14,000 psi. Cell enveloped were removed from the lysate by ultra-centrifugation, and the lysate was loaded directly onto an amylose column (Stratagene;15ml bed volume). The column was washed with 10 bed volumes of buffer A (200mM Tris-Cl, 0.1M NaCl, 1mM EDTA, 10mM BME) and protein eluted with buffer A containing 10mM maltose. The purified fusion protein was digested with Factor Xa (ratio 1mg

fusion/1ug Factor Xa) in 0.05% SDS. The liberated 8kD C-terminus was purified by gel filtration on Sephacryl S-100.

2.21 Purification of outer membrane proteins

Outer membrane proteins (wild type and mutant FepA, and OmpA) were purified from T-media cultures grown to stationary phase. The host strain used for the purification of FepA was the outer membrane protease (OmpT) deficient strain UT5600 (Table 2.1), whereas OmpA was purified from the *fepA* strain KDF541. Proteins were extracted from the outer membrane by differential extractions with Triton-X100 (Fiss et. al. 1992). Briefly, cell envelopes were extracted twice with IM solubilization buffer (10mM Tris-Cl pH=8.0, 2% Triton X-100, 10mM $MgCl_2$, 10mM Benzamadine) to solubilize and remove inner membrane proteins. The pellet was then extracted twice with OM solubilization buffer (10mM Tris-Cl pH=8.0, 2% Triton X-100, 5mM EDTA, 10mM Benzamadine) to solublize outer membrane associated proteins. FepA was purified from the solubilized mixture by affinity chromatography on Colicin B-sepharose (Payne et. al. 1997). OmpA was eluted from a DE-52 ion-exchange column by a linear (0-0.1M) salt gradient.

2.22 Purification of Colicins B and D

Colicins B and D were purified from DM1187/pCLB1 (obtained from M.A. McIntosh) and CA23 respectively by differential precipitations and

chromatography (Timmis, 1972; Pugsley and Reeves, 1977). Killing assays served as activity measurements during the purification procedure.

2.23 Preparation of Crude lysates of Colicin M and Colicin Ia

Crude lysates of Colicin M and Colicin Ia were prepared by mitomicyin C induction of cells harboring pColM or pColIa plasmids. Cells were grown overnight in LB cultures and subcultured 1/100 into 2L of LB broth. When cells reached an $O.D._{600}$ = 0.5, the SOS response was induced by the addition of mitomycin C at 1μg/ml and cultures grown in the dark for 2 hours. Cells were pelleted and resuspended in 30 ml. of phosphate buffered saline pH = 7.8, DNAse and Rnase were added and the cultures lysed by french pressure (2X at 14,000 p.s.i.). Cell envelopes were removed by ultracentrifugation and the lysates aliquoted and stored at -20 C until used in killing assays

2.24 Preperation of Bacteriophage T5 and 80

To prepare a working lysate of bacterophage phi-80, strain JS54 (ϕ80immLAM: Bejar and Bouche 1985) was grown overnight at 30 °C and subcultured 1/100 in 5 ml. LB containing 2mM $MgSO_4$. Upon reaching a $O.D._{600}$ of approximately 0.2, the culture was shifted to 42 °C for 15 min to induce the lytic cycle. Phage propagation was continued for 3 hr. at 37 °C, and $1/100^{th}$ volume of chloroform was added to lyse any remaining cells. The culture was

centrifuged at 10Krpm for 10 min. to remove cell debris and the supernatant aliquoted and stored at 4 °C. The titer of the lysate was determined by plating serial ten fold dilutions of it with a sensitive strain and counting the number of resulting plaques. Stock cultures of bacteriophage was then prepared by infecting a overnight culture of a sensitive host at a multiplicity of 1 and plating the mixture on LB-top agar. The next day virtually 100% lysis was evident, the agar was scraped off the plate and 1ml of chloroform was added and the sample vortexed. After centrifugation, the supernatant was stored at 4 °C. Phage stocks of T_5 were prepared in the same manner from a T_5 lysed lyophilized cell powder (American Type Culture Collection).

2.25 Conjugation of Proteins to Sepharose 6B

Sepharose 6B (50ml) was activated by dropwise addition of 6g CNBr in di-methylformamide, while maintaining the pH between 11.0 and 12.0. The resin was washed with distilled water and suspended in the appropriate conjugation buffer. For outer membrane proteins, 50mg of purified material was dissolved in conjugation buffer (0.2M $NaHCO_3$ containing 2% Triton X-100), added to the activated resin, and incubated overnight at 4° °C with gentle stirring. After conjugation the resin was washed with 2 liters of distilled water, 2 liters of 1M Acetic Acid, and 2 liters of distilled water. An aliquot of the first wash was saved for protein concentration determination to estimate the efficiency of conjugation,

which was usually > 95%. For non-outer membrane proteins Triton X-100 was omitted from the conjugation buffer.

2.26 Sucrose Density Gradient Fractionation of Inner and Outer Membranes

Cell envelopes were fractionated on sucrose density gradients as described (Smit et. al. 1975). Briefly, cell envelopes were prepared from an overnight T-media culture by french pressure. Cell envelopes were resuspended in 7.5 ml of 10mM Hepes buffer pH = 7.4 and floated on the top of a 0.77:1.44:2.02 M sucrose gradient. After centrifugation at 26 krpm for 16hr. the outer and inner membrane fractions were remove from the gradient with a needle and syringe.

2.27 Sulfo-EGS cross-linking

Bacteria grown in MOPS minimal media or sucrose gradient-purified outer membrane fractions were suspended at 10^9 cells/ml or 10mg/ml, respectively, in 4mM SulfoEGS, for 2 hr at 0 °C. After cross-linking, cells or OM proteins were solubilized in sample buffer and subjected to SDS-PAGE, and stained with Coomassie Blue or analyzed by ^{125}I Protein-A immunoblots utilizing α-FepA mAB45. When indicated, 5μM ferric enterobactin or ferrichrome was added to the cells prior to cross-linking. Cross-linked bands were excised from the gels, cleaved by incubation hydroxylamine, electroeluted (ISCO concentrator), and re-electrophoresed: The identity of the cross-linked proteins was determined by

sequnce analysis of their N-terminal 15 residues (Protein and Nucleic Acid Sequence Facility, Medical College of Wisconsin). Cells were treated identically when prepared for quantitative binding analysis, with the exception that, cells cross-linked in the presence of ferric enterobactin were warmed to 37 °C for 10 min. to allow complete transport of the siderophore.

2.28 Fluorescence Measurements

Emission spectrums were recorded using a SLM 8000 fluorimeter upgraded to 8100 functionality, equipped with a 450-watt xenon light source and a cooled PMT housing. The excitation wavelength was set at 295nm, in order to minimize the inner-filter effect and the intrinsic fluorescence of tyrosine. Tryptophan fluorescence of MalE-TonB69C (1.5uM) was performed at 25°C in 50mM Tris-Cl pH=7.4. For quenching studies, a concentrated stock solution of the quenching agent was added and allowed to equilibrate for two minutes before reading the spectrum. All spectra were corrected for dilution, and background fluorescence by the subtraction of appropriate blanks.

2.29 Colicin killing by ANS fluorescence

Cells were grown in MOPS minimal media for 5 hours, collected by centrifugation, and concentrated to 5 * 10^9 cells/ml by resuspension in MOPS media. Cells were diluted 10 fold in MOPS media and incubated at 37 °C for 10

min. The cell suspension was then transferred into a cuvette and placed in the fluorimeter with excitation and emission wavelengths at 360 and 470 nm respectively. After a steady baseline was obtained, ANS was added at a concentration of 120 μM, and upon regaining a steady baseline again, 4nM colicin B was added. For control strains lacking FepA, an extended incubation with colicin B produced no observable change in fluorescence levels. To confirm the negative control was physiologically active, and ANS was responding to the energy state of the cell, 10mM azide was added to the mixture and the fluorescence change observed.

2.30 Construction of KDO23:*fepA*$^{+}$*tonB*$^{-}$

KDO23 was derived from BN1071 by simultaneous selection against colicin B, M, and I_a. Colonies that survived this challenge were isolated and initially screened for killing by the toxins individually, and clones displaying resistance to all three were grown in T-media and analyzed by western blot to confirm the presence of FepA. ^{125}I-Protein A western blots with α-FepA mAB45 showed no difference in FepA expression between BN1071 and the clone of interest (data not shown). Final verification of the *tonB* phenotype was obtained by the restoration of colicin sensitivity and siderophore nutrition upon transformation of the clone with pRZ540 (*tonb*$^{+}$).

2.31 Characterization of the TonB mutation in KDO23

Genomic DNA was isolated from KDO23, and its isogenic parent BN1071, by the method of Chen and Kuo. PCR was performed with primers that anneal to the start codon, 5'-T**GAATTC**ATGACCCTTGATTTACCTCGC-3', and downstream of the stop codon, 5'-CT**AAGCTT**ACGGCCGGTTGCGGT-3'. The reaction was ran on a 1% agarose gel, and the size of the product estimated by comparison to the standard molecular weight markers run on the gel (λ 1kb: Gibco BRL). The amplified product from KDO23 was observed to be approximately 750 nucleotides indicating the mutation was a internal deletion of *tonB* (data not shown). Multiple attempts to clone the product into pUC18 for sequence analysis were unsuccessful. Others have reported the inability to clone TonB in multicopy plasmids suggesting that the deletion to TonB in KDO23 was in frame and produced a truncated from of TonB. In this light, it may be beneficial to discover the precise deletion to TonB in this strain, and future attempts should be performed in low copy vectors. In a similar procedure, the nature of a TonB mutation was determined in a separate *tonB* strain GUC-12. The mutation to TonB in GUC-12 was a deletion of a individual nucleotide at amino acid 43 of the coding sequence (Figure 2.1). The deletion knocked the coding sequence out of frame, and as a result introduced a stop codon at position 63 (Figure 2.2)

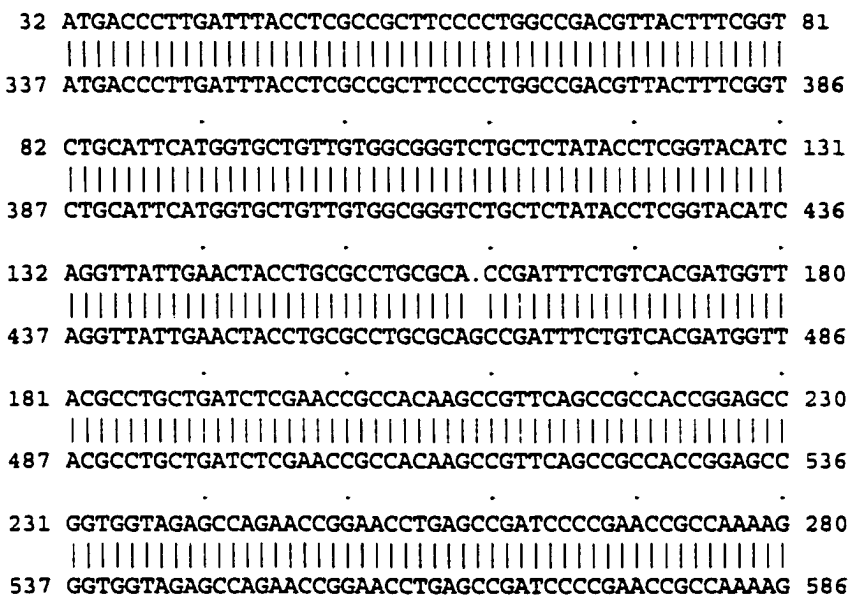

Figure 2.1: DNA sequence alignment between wild-type *tonB (*bottom) and *tonB* from GUC-12

ATGACCCTTGATTTACCTCGCCGCTTCCCCTGGCCGACGTTACTTTCGGTCTGCATTCAT
M T L D L P R R F P W P T L L S V C I H
GGTGCTGTTGTGGCGGGTCTGCTCTATACCTCGGTACATCAGGTTATTGAACTACCTGCG
G A V V A G L L Y T S V H Q V I E L P A
CC*TGCGCACCGATT*TCTGTCACGATGGTTACGCCTGCTGATCTCGAACCGCCACAAGCCG
P A H R F L S R W L R L L I S N R H K P
TTCAGCCGCCACCGGAGCCGGTGGTAGAGCCAGAACCGGAACCTGAGCCGATCCCCGAAC
F S R H R S R W - S Q N R N L S R S P N
CGCCAAAAGAAGCACCGGTGGTCATTGAAAAGCCGAAGCCGAAACCTAAGCCAAAACCGA
R Q K K H R W S L K S R S R N L S Q N R
AGCCGGTGAAAAAGGTACAGGAGCAGCCAAAACGCGATGTCAAACCCGTAGAGTCGCGTC
S R - K R Y R S S Q N A M S N P - S R V
CGGCATCACCGTTTGAAAATACGGCACCGGCACGCCTGACATCAAGTACAGCAACGGCTG
R H H R L K I R H R H A - H Q V Q Q R L
CAACCAGCAAGCCGGTTACCAGTGTGGCTTCAGGACCACGCGCATTAAGCCGTAATCAGC
Q P A S R L P V W L Q D H A H - A V I S

Figure 2.2: Translation of the *tonB* sequence from GUC-12, the area in which the mutation was introduced is underlined.

Chapter 3

Characterization of the C-terminal domain of TonB

Since the discovery of TonB, and the dependency of siderophore transport upon it, a description of its mechanistic action has remained elusive. The cellular location, topology, and organization of this protein have only further created an air of mystery surrounding its function. Bound to the inner membrane by an uncleaved signal sequence (Jaskula et. al. 1994; Karrlson et. al. 1993a; Roof et. al. 1991; Traub et. al. 1993), TonB extends into the periplasmic space by virtue of two rigid, and highly charged domains: a negatively charged Glu-Pro repeat is closely

followed by a positively charged Lys-Pro repeat, whose biochemical functions are, at best, speculative. The central domain is followed by a C-terminal globular domain that was proposed to fold in a β-α-β structure. However, the only structural information regarding TonB comes from the central region, in which NMR studies of a synthetic peptide, mimicking the dipeptide repeats, was observed to possess a rigid conformation capable of extending across the periplasmic space (Brewer et. al. 1990; Williamson et. al. 1994). The extension of the C-terminus in the vicinity of outer membrane receptors, *via* the rigid rod, superficially agrees with theories of how TonB functions (Evans et al. 1996; Klebba et al. 1993; Postle, 1990. Holroyd and Bradbeer. 1984; Moeck and Coulton. 1998). Genetic evidence initially raised the possibility that TonB interacted with periplasmic residues of the outer membrane receptors. TonB-dependent receptors all contain a moderately conserved region of sequence similarity at their N-termini, referred to as the TonB-box. The designation of this stretch of amino acids derives from mutations to it, Pro substitutions for Val or Leu, that abolish receptor function are partially restored when combined with mutations to the C-terminal region of TonB, Gln160 to Lys or Arg (Schoffler and Braun 1989; Bell et al. 1990; Kadner, 1990; Bradbeer, 1991; Braun et al. 1991). Any such interactions that may exist between TonB and outer membrane receptors are as yet undefined, but experimental evidence appears to agree with this view. Primarily, the binding of ferrichrome to FhuA reoriented the TonB-box (Ferguson et. al. 1998; Locher et al. 1998), as did binding of vitamin

B_{12} to BtuB (Merianos et. al. 2000), demonstrating that the periplasmic face of the receptors may change upon association with external ligand.

The importance of the C-terminal domain to TonB function was first observed with deletions to it. Deletion of the extreme C-terminal eight amino acids had no deleterious effect on TonB-dependent activity, whereas deletion of the C-terminal 15 amino acids abolished activity (Anton and Heller, 1991). Furthermore, upon deletion of the entire C-terminal domain (TonB Δ 174-239), TonB did not cross-link to FepA, or associate with outer membranes (Letain and Postle, 1997), suggesting this domain may be important for the interaction with outer membrane receptors or with the outer membrane itself.

3.1 Cloning, Overexpression, and Purification of the TonB C-terminus

To further delineate the function of the C-terminal domain of TonB in the transport process, and to gather information concerning its secondary structural characteristics, we purified it and characterized its phenotypic and structural properties. The C-terminal sixty-nine residues of TonB (170-239) were genetically fused to the periplasmic binding protein MalE, and the resulting fusion protein was purified by affinity chromatography on a amylose resin (Guan et. al. 1987; Maina et. al. 1988; Kellerman and Ferenci 1982). Upon induction of cells with IPTG, a pronounced band corresponding to the calculated molecular weight of the fusion protein (51kDa; Figure 3.1) was visible. The fusion was purified in high yield

(50mg/L of culture) and high purity (>95%), as judged by SDS-PAGE electrophoresis (Figure 3.2).

To remove the maltose binding protein portion of the fusion we took advantage of an internal Factor X_a cleavage site, located in a spacer arm between the two polypeptides. However, protelytic cleavage of the fusion protein occurred only when 0.05% SDS was added to the reaction, suggesting that the cleavage site was buried within the protein structure of the fusion protein (Figure 3.3). The digestion products were resolved on a gel filtration column to purify the 8 kDa TonB fragment (TonB69C) to high purity (>95%; Figure 3.3).

3.2 Intrinsic Fluorescence

Although fluorescence cannot directly indicate the secondary structural characteristics of a polypeptide, important information may be obtained regarding the micro-environment of a particular tryptophan residue. The C-terminus of TonB contains a single tryptophan residue at position 213, located within the aforementioned proposed βαβ motif. TonB69C displayed a characteristic tryptophan fluorescence, with a maximum emission at 318 nm (Figure 3.4). Upon denaturation of the fragment with guanidine hydrochloride, the emission maximum shifted to 352nm and the fluorescence intensity decreased by 45%. The emission maximum of the denatured fragment was similar to that observed for free

tryptophan in aqueous solution indicating that, in the native state, W213 is folded within a non-polar environment of a globular protein structure.

3.3 Effect of quenchers on W213 fluorescence

Tryptophan fluorescence is sensitive to quenching by a variety of substances. Quenching ordinarily occurs upon direct collision of the quenching agent with the emitting molecule, in this case tryptophan. Therefore, the accessibility of tryptophan quenching by reagents that are positively charged, negatively charged, and hydrophobic uncharged can provide useful information concerning the environment of the residue in the folded structure. We evaluated the accessibility of W213 quenching by acrylamide, iodide, and cesium. Collisional quenching is described mathematically by the Stern-Volmer equation (Equation 1.1), and more accurately, the stern-volmer constant K_{sv}. When exposed to acrylamide, stern-volmer analysis yielded K_{sv} values of 5.8 and 8.4 for native and denatured TonB69C respectively (Figure 3.5; Table 3.1). The negatively charged species Iodide produced values of 2.6 and 4.4, whereas quenching by the positively charged cesium ion gave values of 0.37 and 1.4 for native and denatured respectively (Figure 3.5; Table 3.1). Emission spectra of TonB69C in the presence of 0.4M NaCl showed no perturbation, indicating that the increased ionic strength did not alter the protein structure (data not shown). The quenching studies indicate that W213 is located within a hydrophobic region of the protein structure that is, to

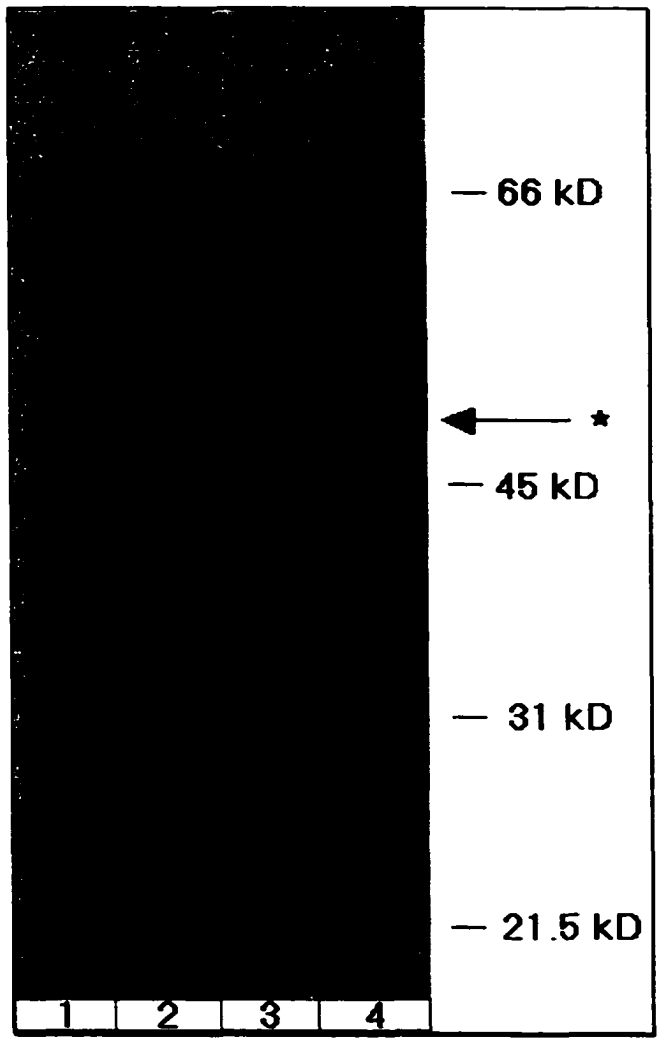

Figure 3.1 Overexpression of MalE-TonB69C. Mid-log phase cells were induced with 0.5mM IPTG and 1 x 10^8 cells were removed and separated on a 10% SDS-PAGE gel at Lane 1) 0 hour of induction 2) 1 hour of induction 3) 2 hours of induction 4) 3 hours of induction. The approximately 51 kD protein corresponding to MalE-TonB69C is indicated. Molecular weight markers are shown for reference.

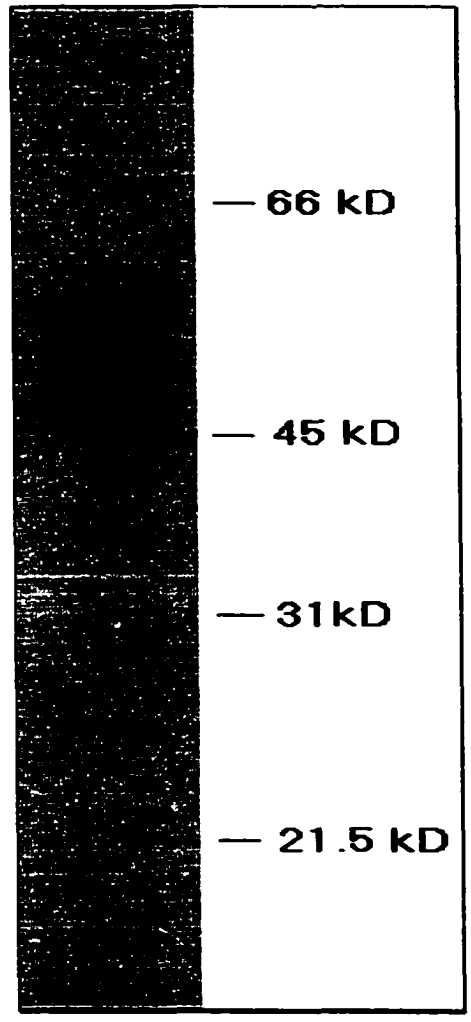

Figure 3.2 Purification of the MalE-TonB69C. Shown is 10ul of a fraction eluted from the amalyose column (total volume 7 ml.)

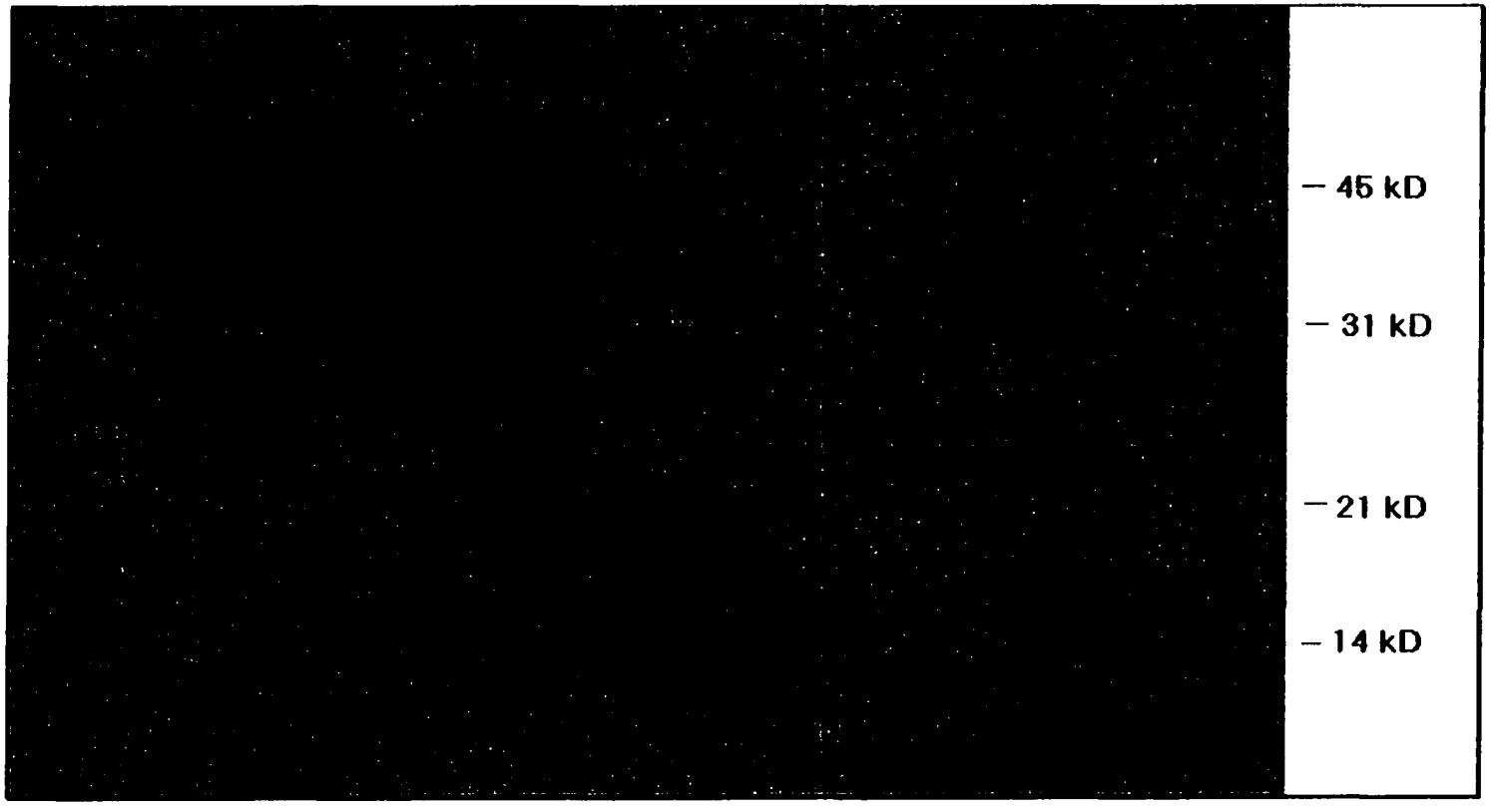

Figure 3.3 S-100 Elution profile of TonB-CTD purification. Factor Xa digested fusion protein was subjected to Sephacryl S-100 gel filtration chromatography. 10 ul of column fractions (total volume 1 ml.) were added to sample buffer and ran on 16% SDS-PAGE. The approximate position of molecular weight standards is shown for reference.

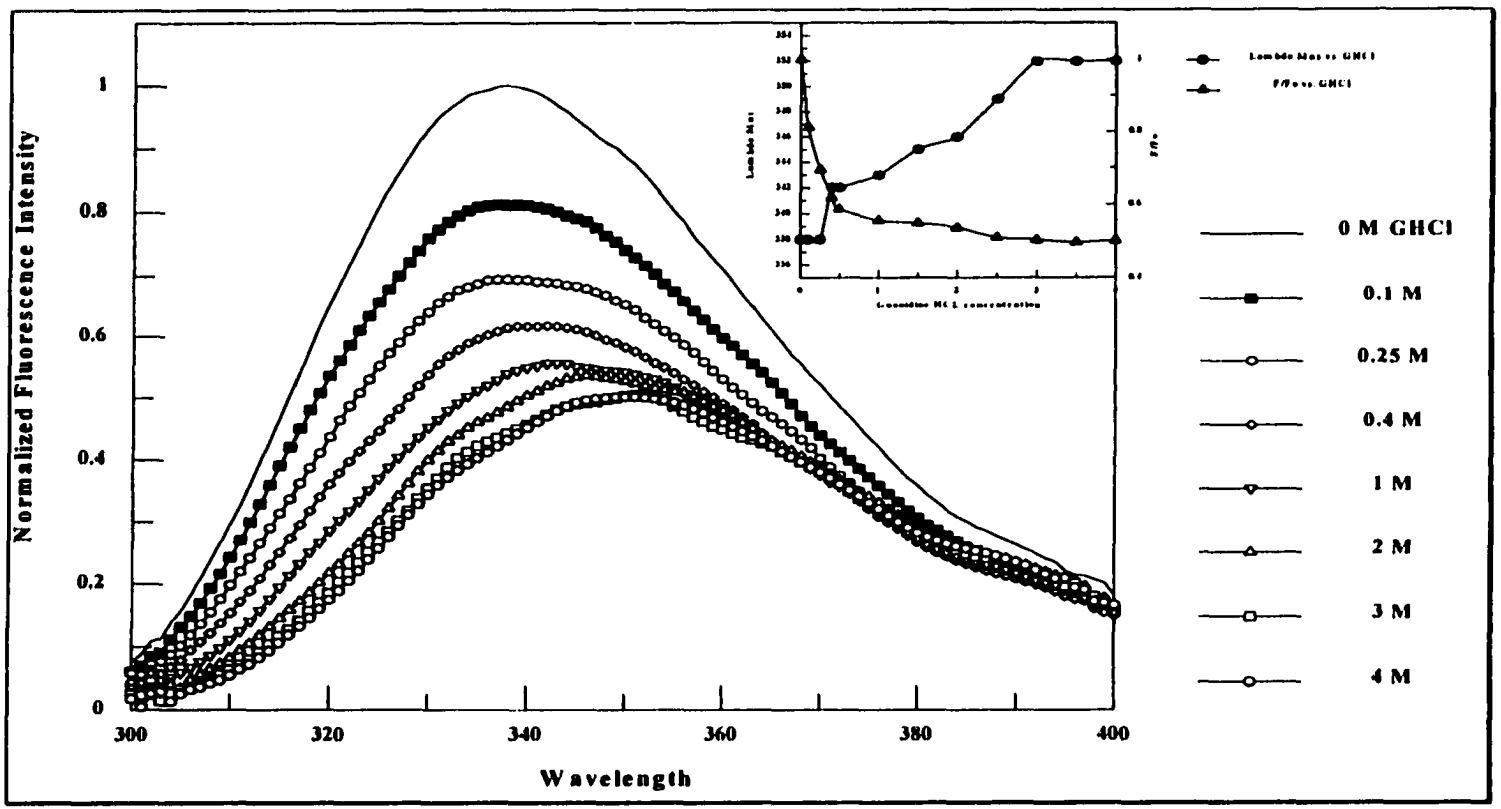

Figure 3.4. Guanidine HCl titration of the TonB C-terminus. Fluorescence emission spectra of a single tryptophan residue (W213) was monitored in the presence of the denaturant GHCl. A red shift in the maximal wavelength of emission and a marked decrease in fluorescence intensity was observed. The inset graph shows two alternative approaches of data analysis for the titration.

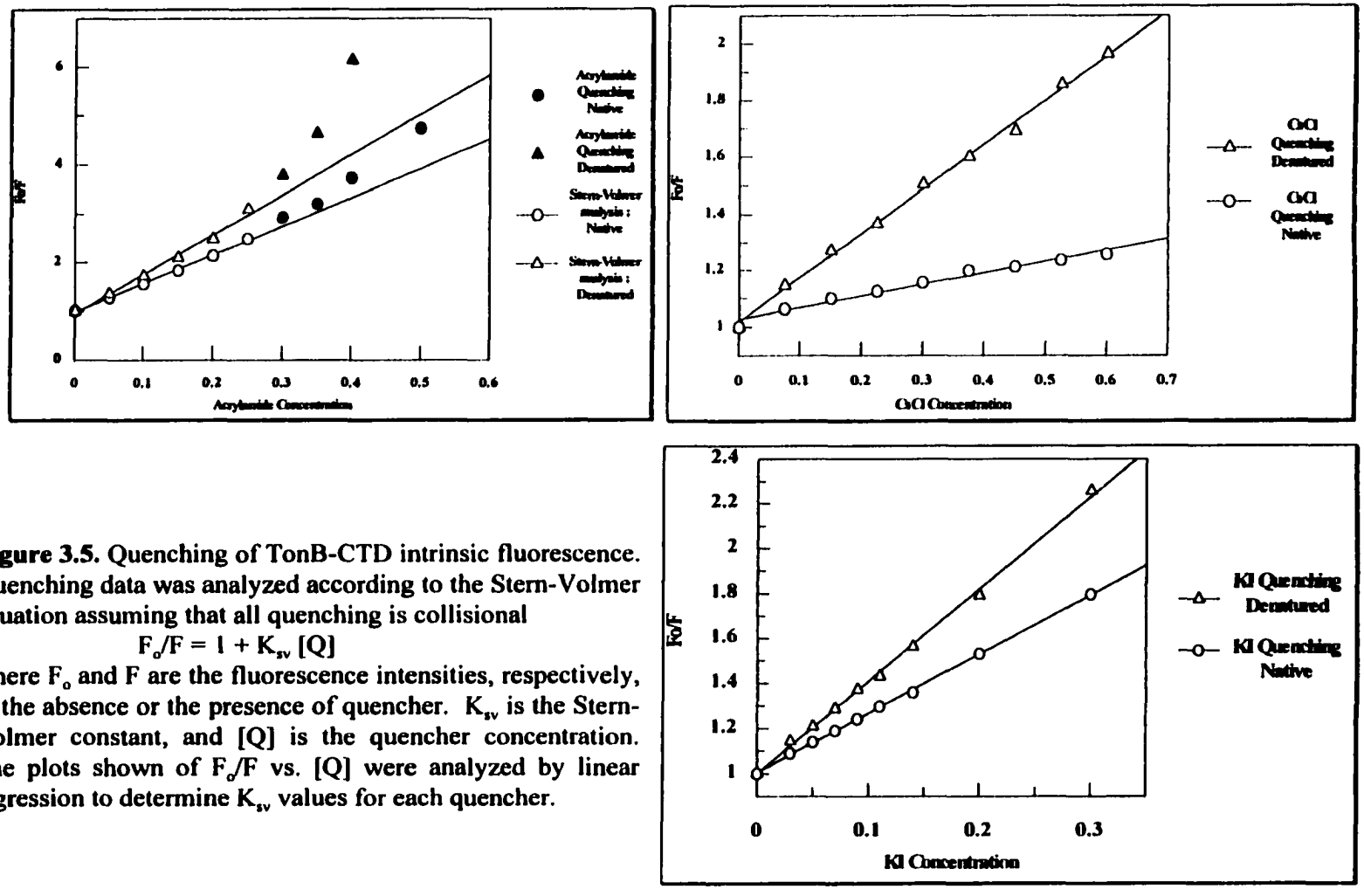

Figure 3.5. Quenching of TonB-CTD intrinsic fluorescence. Quenching data was analyzed according to the Stern-Volmer equation assuming that all quenching is collisional

$$F_o/F = 1 + K_{sv}[Q]$$

where F_o and F are the fluorescence intensities, respectively, in the absence or the presence of quencher. K_{sv} is the Stern-Volmer constant, and [Q] is the quencher concentration. The plots shown of F_o/F vs. [Q] were analyzed by linear regression to determine K_{sv} values for each quencher.

	Acrylamide	Iodide	Cesium
Native	5.9 M^{-1} ± 0.4	2.6 M^{-1} ± 0.2	0.4 M^{-1} ± 0.05
Denatured	8.2 M^{-1} ± 0.4	4.1 M^{-1} ± 0.1	1.6 M^{-1} ± 0.001

Table 3.1. Stern-Volmer constants (K_{sv}) for the quenching of TonB69C W213.

an extent, exposed to the aqueous environment. Furthermore, the higher susceptibility of W213 quenching to Iodide as compared to Cesium suggest a high degree of positively charged residues nestled closely to W213 in the folded structure.

3.4 Functional properties of MalE-TonB69C

To investigate the effect of MalE-TonB69C on TonB-dependent processes, a *fepA*$^{+}$ *tonB*$^{-}$ strain (Table 2.1), isogenic to BN1071, was isolated for characterization of the fusion protein in a wild type and *tonB* background. Overexpression of MalE-TonB69 was unable to complement the *tonB* mutation in KDO23 suggesting that TonB must remain intact with its N-terminal membrane spanning domain for productive function (Table 3.2). However, when overexpressed in a wild-type background, the fusion effectively inhibited ferrichrome and ferric enterobactin uptake in siderophore nutrition assays (Table 3.2), suggesting the C-terminal portion of TonB competes with wild type TonB for function. No difference was observed in susceptibility to colicins B or D by strains overexpressing MalE-TonB69C (Table 3.2). Two alternative explanations exist to describe this dichotomy. First, colicins possess so called one-hit kinetics, meaning transport of a single colicin molecule is sufficient to result in cell death. Therefore, the level of inhibition by MalE-TonB69C may not be observed in colicin killing assays since the transport of only one molecule is required. Alternatively, the

	Growth response to Siderophores		Colicin Killing	Antibiotic Susceptibility[a]						
Bacterial Strain / Plasmid	**Fe-Ent.**	**Fc**	**Col B**	**B**	**Cm**	**N**	**Te**	**Er**	**NB**	**Rf**
KDO23	0	0	0	0	21	14	20	0	0	9
KDO23/pRZ540	15	13	5	0	19	0[b]	18	0	0	8
KDO23/pMal-p2	0	0	0	0	18	14	20	0	0	9
KDO23/pSTon	0	0	0	0	21	14	21	0	0	10
KDO23/pSton + 1mM IPTG	0	0	0	0	21	14	21	0	0	10
BN1071	16	14	5	0	19	15	19	0	0	8
BN1071 + 1mM IPTG	16	14	5	0	18	14	20	0	0	8
BN1071/pRZ540	16	13	5	0	20	0	20	0	0	8
BN1071/pRZ540 + 1mM IPTG	16	13	5	0	20	0	20	0	0	9
BN1071/pMalp-2	16	14	5	0	19	15	20	0	0	9
BN1071/pMalp-2 + 1mM IPTG	15.5	14	5	0	20	16	20	0	0	9
BN1071/pSTon	14	14	5	0	20	15	20	0	0	9
BN1071/pSTon + 1mM IPTG	0	0	5	0	20	15	20	0	0	9

Table 3.2. Phenotypic Properties of MalE-TonB69C.

a -. Chloramphenicol (Cm), erythromycin (Er), rifampicin (Rf), bacitracin (B), Tetracycline (Te), Novobiocin (NB), and Neomycin (N).

f - pRZ540 is kan^r.

mechanism of TonB for colicin import may differ from its function during siderophore uptake. Antibiotic susceptibility, a TonB-independent process that measures the integrity of the outer membrane, was unaffected by overexpression of MalE-TonB69C (Table 3.2)

3.5 Interaction of MalE-TonB69C with proteins

Genetic studies raised the possibility that TonB physically interacts with the siderophore receptors of the outer membrane. Mutations to a N-terminal region of sequence homology, the TonB box, could be partially rescued by mutations to the C-terminal domain of TonB (Schoffler and Braun 1989; Bell et al. 1990; Kadner, 1990; Bradbeer, 1991; Braun et al. 1991). Subsequently, *in vivo* formaldehyde cross-links between TonB and FepA or FhuA, and disulfide complexes formed between cysteine mutations to the TonB-box of BtuB and the C-domain of TonB further implicated the role of physical contact (Cadieux and Kadner, 1999; Cadieux et. al. 2000). To investigate the ability of MalE-TonB69C to interact with other proteins, we covalently coupled FepA, FepAΔ12-17 (which lacks the TonB box), colicin B, OmpA, and lysozyme to cyanogen bromide-activated sepharose. In binding assays employing column-immobilized proteins, MalE-TonB69C adsorbed to all proteins tested, except the unconjugated resin (Figure 3.6- 3.13), whereas MalE did not (data only shown for ColB and FepA columns). A slight non-specific adsorption was observed between the fusion and lysozyme conjugated

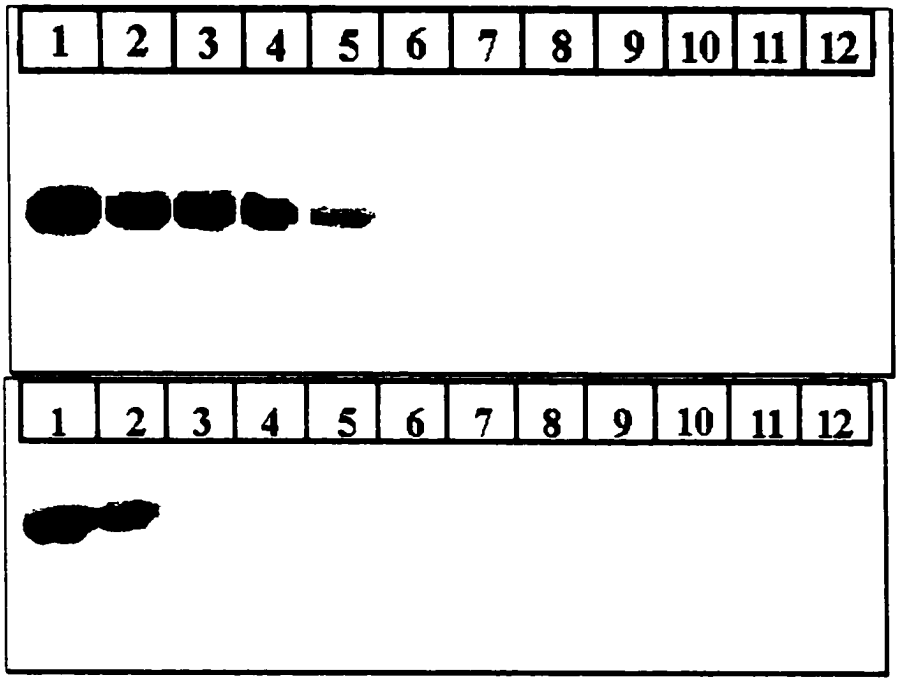

Figure 3.6 Retention of MalE-TonB69C by Sepharose. 4mg of purified MalE-TonB fusion protein was loaded onto a sepharose column, washed with 10 column volumes of 50mM Tris-Cl pH = 7.4, and eluted with a linear salt gradient from 0 to 0.5M NaCl. Top panel: 1, column load; 2, column flow; 3-12, wash fractions. Bottom panel: 1, column load; 2, column flow; 3-12, salt gradient fractions.

Figure 3.7 MalE-TonB69C - FepA interaction. 4mg of purified MalE-TonB69C was loaded onto a sepharose conjugated FepA column, washed with 10 column volumes of 50mM Tris-Cl pH =7.4, and eluted with a linear salt gradient from 0 to 0.5M NaCl. Top panel: 1, column load; 2, column flow; 3-12, wash fractions. Bottom panel: 1, column load; 2, column flow; 3-14, salt gradient fractions.

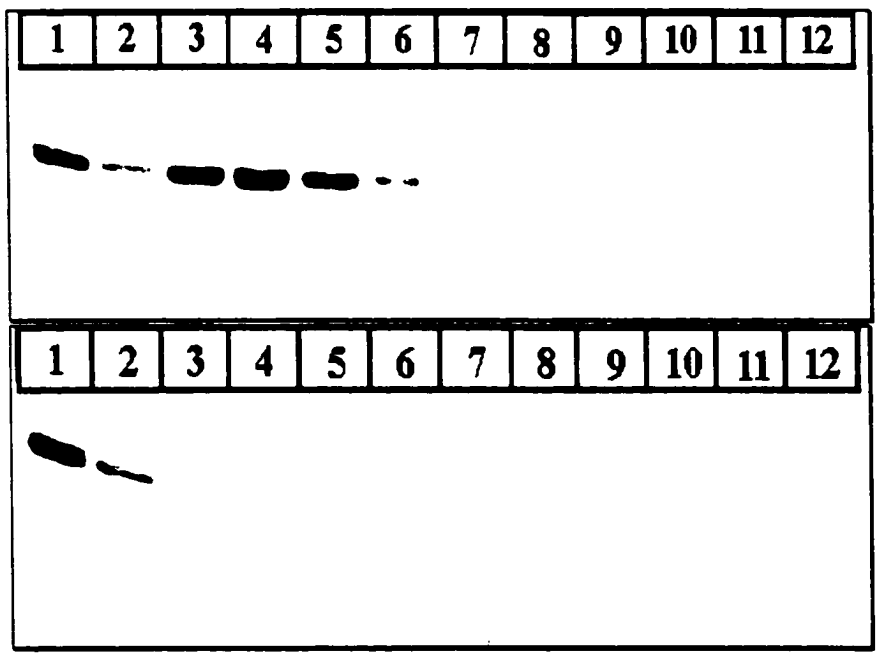

Figure 3.8 MalE - FepA interaction. 4mg of purified MalE was loaded onto a sepharose conjugated FepA column, washed with 10 column volumes of 50mM Tris-Cl pH = 7.4, and eluted with a linear salt gradient from 0 to 0.5M NaCl. Top panel: 1, column load; 2, column flow; 3-12, wash fractions. Bottom panel: 1, column load; 2, column flow; 3-12 salt gradient fractions.

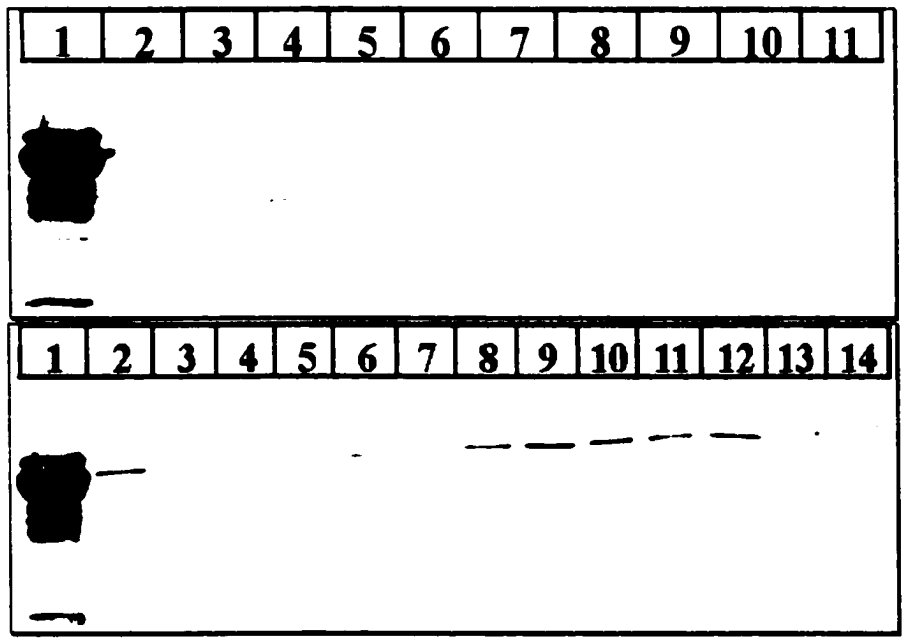

Figure 3.9. MalE-TonB69C - Colicin B interaction. 4mg of purified MalE-TonB fusion protein was loaded onto a sepharose conjugated colicin B column, washed with 10 column volumes of 50mM Tris-Cl pH = 7.4, and eluted with a linear salt gradient from 0 to 0.5M NaCl. Top panel: 1, column load; 2, column flow; 3-11, wash fractions. Bottom panel: 1, column load; 2, column flow; 3-14, salt gradient fractions (lanes 3-14)

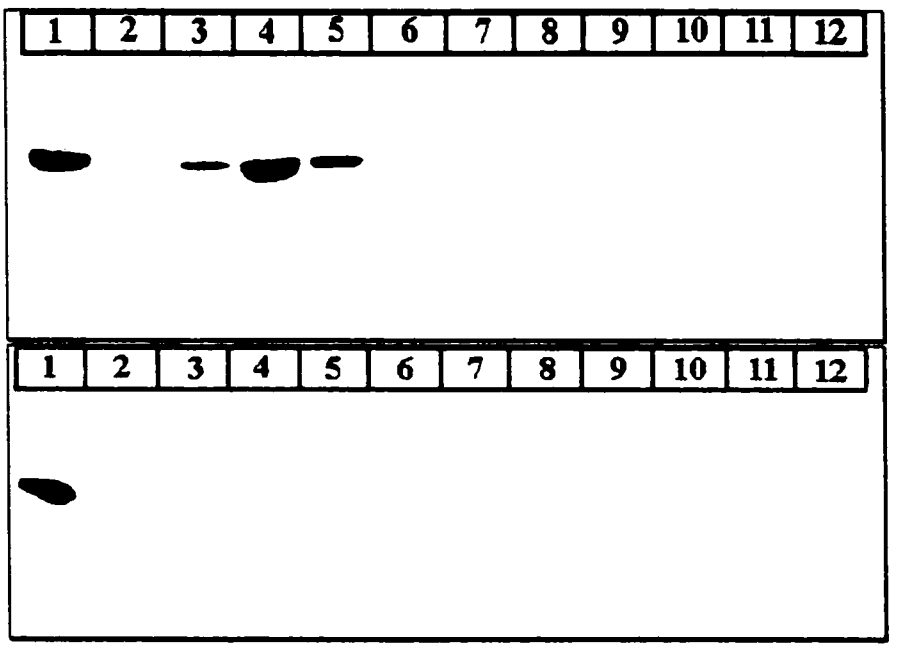

Figure 3.10. Colicin B - MalE interaction. 4mg of purified MalE was loaded onto a sepharose conjugated colicin B column, washed with 10 column volumes of 50mM Tris-Cl pH = 7.4, and eluted with a linear salt gradient from 0 to 0.5M NaCl. Top panel: 1, column load; 2, column flow; 3-12, wash fractions. Bottom panel: 1, column load; 2, column flow; 3-12, salt gradient fractions.

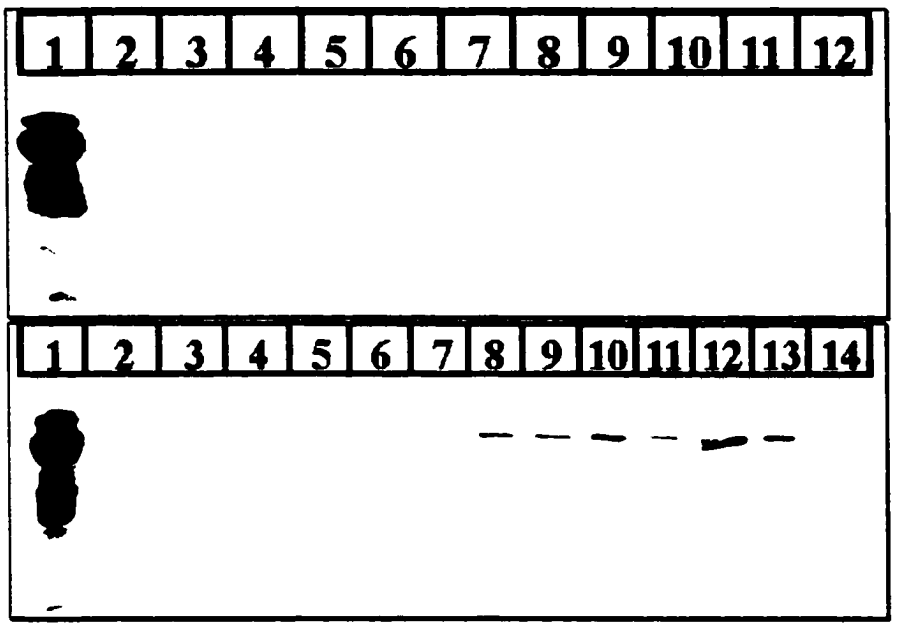

Figure 3.11. MalE-TonB69C - FepA Δ13-17 Interaction. 4mg of purified MalE-TonB fusion protein was loaded onto a sepharose conjugated FepAΔ13-17 column, washed with 10 column volumes of 50mM Tris-Cl pH = 7.4, and eluted with a linear salt gradient from 0 to 0.5M NaCl. Top panel: 1, column load; 2, column flow; 3-12, wash fractions. Bottom panel: 1, column load; 2, column flow; 3-14, salt gradient fractions.

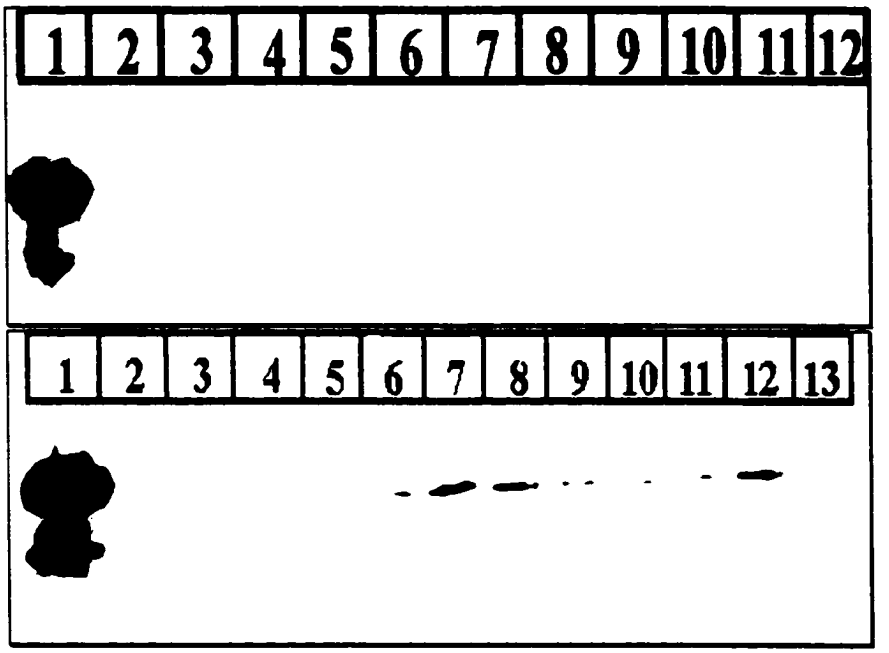

Figure 3.12 MalE-TonB69C - OmpA interaction. 4mg of purified MalE-TonB fusion protein was loaded onto a sepharose conjugated OmpA column, washed with 10 column volumes of 50mM Tris-Cl pH = 7.4, and eluted with a linear salt gradient from 0 to 0.5M NaCl. Top panel: 1, column load; 2, column flow; 3-12, wash fractions. Bottom panel: 1, column load; 2, column flow; 3-13, salt gradient fractions.

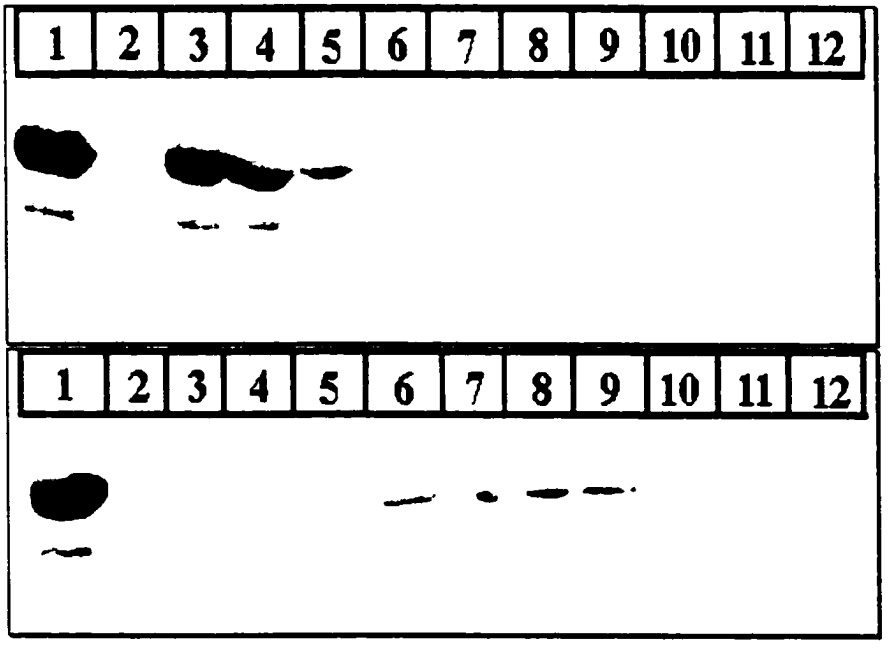

Figure 3.13. MalE-TonB69C - Lysozyme 4mg of purified MalE-TonB fusion protein was loaded onto a sepharose conjugated lysozyme column, washed with 10 column volumes of 50mM Tris-Cl pH = 7.4, and eluted with a linear salt gradient from 0 to 0.5M NaCl. Top panel: 1, column load; 2, column flow; 3-12, wash fractions. Bottom panel: 1, column load; 2, column flow; 3-12, salt gradient fractions.

sepharose. The fusion protein was eluted from the columns with a mild salt gradient (0-0.5M NaCl) suggesting the interaction was of moderate affinity. Nonetheless, the adsorption of MalE-TonB69C to columns containing immobilized OmpA indicate that TonB has a general affinity for outer membrane proteins that does not rely upon a specific interaction with the TonB box of siderophore receptors.

3.6 Cellular localization of the C-terminus

Although the physiological importance remains unknown, the peculiar partitioning of full-length TonB between outer and inner membranes appears to derive from the properties of the C-terminal domain (Letain and Postle 1997). To investigate the ability of the C-terminal domain of TonB to localize the MalE fusion to outer membranes, cell envelopes obtained from cells overexpressing the fusion protein were fractionated on sucrose density gradients. The presence of the C-terminal 69 amino acid residues was sufficient to localize a portion of the fusion protein to the outer membrane (Figure 3.14). MalE, expressed from either the chromosome or vector plasmid, did not localize to the outer membrane, although a small amount of MalE-LacZ′ was observed to partition to the outer membrane (Figure 3.14). A larger extent of membrane localization was observed when the C-terminal 135 amino acids of TonB were fused to MalE (Figure 3.14), indicating that

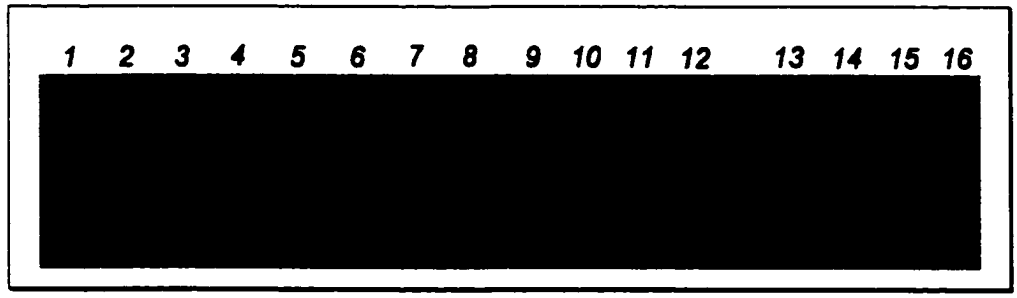

Figure 3.14. Membrane localization of MalE-TonB69C. Inner and outer membranes from ER2507 and ER2507 expressing TonB fusions were fractionated on sucrose gradients. 30ug of membranes were analyzed by western immunoblots with α-MalE mAB, and developed with ^{125}-I-protein A. lanes 1-4. ER2507(*malE*) whole cells, cell lysate, IM and OM, respectively; lanes 5-8. ER2507/pMalp2 (MalE) whole cells, cell lysate, IM, and OM; lanes 9-12. ER2507/pSTON (MalE-TonB69C) whole cells, cell lysate, IM and OM; lanes 13-16. ER2507/pSTON104 (MalE-TonB135C) whole cells, cell lysate, IM, and OM.

portions of the C-terminus required for proper membrane localization are missing in the MalE-TonB69C fusion.

3.7 Liposome insertion of TonB69C

The C-terminal domain dependent localization of TonB to the outer membrane suggests the association with or insertion of this domain into the lipid bilayer. Two techniques were utilized to assess the ability of TonB69C to become membrane associated or membrane inserted. When exposed to DOPC/EPG liposomes, the purified TonB C-terminus displayed a 10% decrease in fluorescence intensity with no shift in the λ_{max} of emission (Figure 3.15). The alteration to fluorescence intensity indicates a structural rearrangement of TonB69C upon association with liposomes. Generally, an increase in the fluorescence intensity would be expected upon insertion into the more hydrophobic lipid bilayer, resulting in a reduction in solvent exposure for the fluorescing residue. However, the fluorescence change upon association/insertion with membranes represents differences between the folded and membrane associated states. Thus, a hydrophobic environment in the folded conformation would not necessarily show an increase in fluorescence upon insertion into a membrane. The single tryptophan residue of TonB69C was indeed in a relatively hydrophobic environment, as evidenced by guanidine hydrochloride titration (Figure 3.4). To discriminate between membrane insertion/association, nitroxide spin labeled lipids were

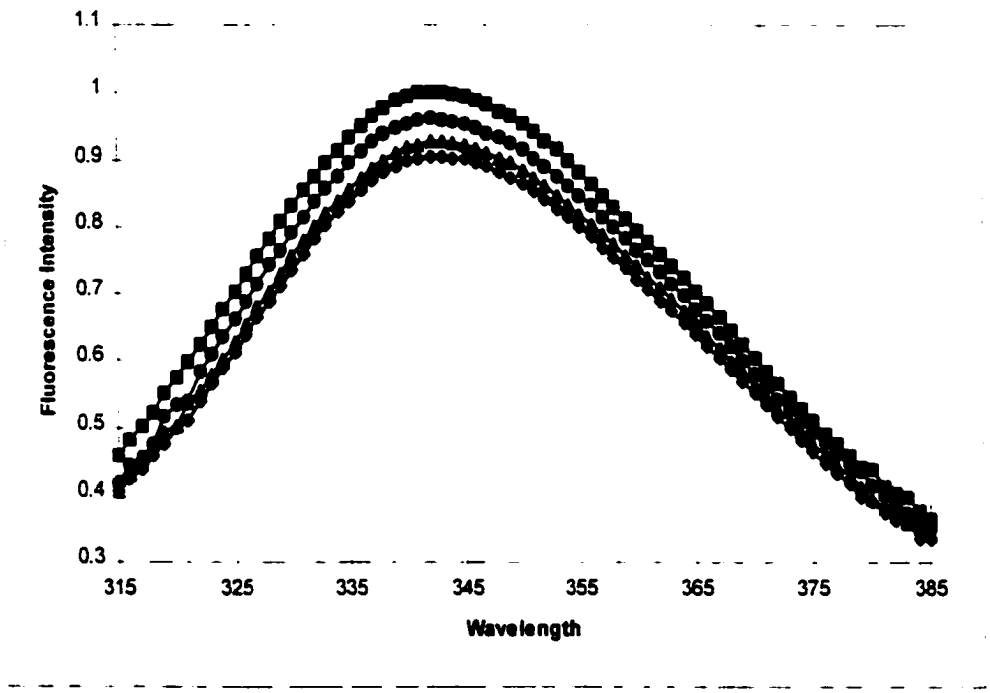

Figure 3.15 Insertion of TonB69C into DOPC/EPG liposomes. ■ No liposomes; ● 1µl of 1/10 DOPC/EPG liposomes; ▲ 5µl of DOPC/EPG liposomes; ◆ 2µl of concentrated DOPC/EPG liposomes

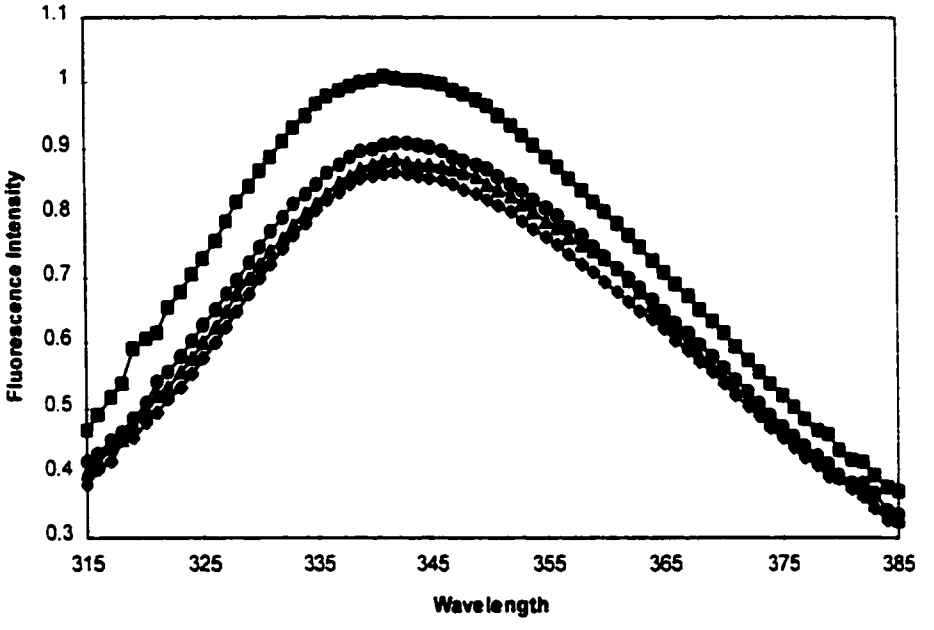

Figure 3.16 Insertion of TonB69C into DOPC/EPG liposomes. ■ No liposomes; ● 1μl of 1/10 Nitroxide liposomes; ▲ 5μl of 1/10 Nitroxide liposomes; ◆ 2μl of concentrated Nitroxide liposomes

employed. The nitroxide moiety of the lipids can quench fluorescence intensity upon insertion of fluorophores into the membrane, and they are typically used to estimate depth of insertion of membrane-inserting toxins (Shepard et. al. 1998). When exposed to nitroxide containing liposomes, an increase of five percent in the quenching was observed in comparison to the non-nitroxide containing liposomes (Figure 3.15). The additional increase in quenching upon exposure to nitroxide lipids strongly suggests the purified C-terminus of TonB inserts into the liposomes.

Chapter 4

Deletion and Chimeric Constructions of FepA and FhuA

The crystallographic depictions of FepA and FhuA were unable to address several pertinent questions regarding the siderophore binding and transport processes. The explanation of TonB dependence, for instance, was not evident upon inspection of the structures, although a change in structure of the N-terminal extreminity of FhuA during ferrichrome binding superficially supported the idea of conformational signaling between the receptor protein and TonB. The localization of the "TonB box" of siderophore receptors within this region of the N-terminal

extreminity concurs with the notion of signal transduction between an occupied receptor and TonB (Kadner 1990; Postle 1990; Postle 1993; Skare et. al. 1993; Moeck et. al. 1997; Cadieux and Kadner 1999; Merianos et. al. 2000). In this light, it was unexpected that a mutant FhuA protein, devoid of the N-terminal globular domain, efficiently transported ferrichrome and remained TonB-dependent (Braun et. al. 2000). What then, is the function and/or disposition of the N-domain during the transport reaction? Does the conformation of the N-domain change, creating a substrate customized pathway for the siderophore to pass, or is it completely expelled during the transport reaction? The latter faces, among other things, a large energetic barrier to overcome since some fifty potential hydrogen and ionic bond interactions exist between the N-domain and the barrel wall (Ferguson et al. 1998; Locher et al. 1998; Buchanan et al. 1998). The former seems more plausible, but transient channels of such size have not been observed in membrane proteins. Furthermore, how does such a substrate customized channel form, and what aspect of the protein structure regulates its opening?

Neither was the process of ligand recognition explained by the crystal structures. The siderophore receptors of *Escherichia coli* discriminate between numerous ferric siderophore complexes, that, despite similar size (600-1000 Da) and chelation geometry (hexa-coordinate) are distinct in charge and chemical composition (Neilands 1982; Neilands 1985; Raymond et. al. 1994). Each ferric siderophore enters through its own specific outer membrane transporter. Does

specificity originate in cell surface loops, or residues within the N-domain at the entrance to the membrane channel? Experiments on a mutant FhuA protein devoid of the N-domain were relevant to this issue, as well as the ligand transport process (Braun et. al. 2000). However, these studies did not provide thermodynamic or kinetic descriptions of the binding and transport process. As such, no definitive conclusions arose from this work regarding the ligand recognition process. For instance, was the impaired uptake of ferrichrome a result of reduced binding affinities, or alternatively, an alteration in the transport kinetics? Without kinetic descriptions of the binding and uptake process answers to these questions remained obscure. To experimentally address these questions. I designed experiments with the following objectives: (i) to verify the phenotype of the N-domain deletion of FhuA, (ii) to determine if similar mutations of FepA transport ferric enterobactin, (iii) to consider the functional exchangeability of the FepA and FhuA N-termini, (iv) to provide thermodynamic and kinetic descriptions of the binding and transport reactions by such mutant receptors.

4.1 Design of FepA and FhuA deletion and chimeric proteins

Biochemical studies with deletion mutants of FepA and FhuA provided the first evidence that the receptors contained diffuseable pores (Rutz et. al. 1992; Killman et. al. 1993; Killmann et. al. 1996). These observations led to the idea that siderophore receptors function as ligand-gated porins whose channels are regulated

by surface exposed loops. A more robust approach created deletion mutants of each surface exposed loop of FepA, dissected the relative importance of each loop in recognition and transport of ferric enterobactin (Newton et. al. 1999). Similarly, deletion of the central "gating-loop" of FhuA reduced the rate of ferrichrome uptake and converted FhuA into a non-specific diffusion channel (Killmann et. al. 1993; Killmann et. al. 1996). Chimeric proteins of FhuA consisting of the central part of FhuA and the N- and C-terminal parts of the coprogen receptor (FhuE), or the N- and/or C-terminal parts of the ferrioxamine B receptor (FoxA) transport ferrichrome (Killmann and Braun 1998). Although, conclusions drawn from these chimeric constructions of FhuA were undermined by the ability of FhuE and FoxA alone to transport ferrichrome, albeit not efficiently.

I constructed two sets of mutant proteins to investigate the role of the N-terminal domain in ferric-siderophore binding and transport. Furthermore, I engineered deletion mutants that removed the entire N-terminal globular domain, creating receptor proteins that contained only the C-terminal β-barrel portion of the protein. For FepA, I generated two such deletions for biochemical characterization. The first, FepAΔ17-151(Fepβ), removed most of the N-domain but left residues 1-16, which include the TonB-box region, fused to G151. The second, FepA Δ3-151 (Fepβ2), also removed the N-domain, but eliminated the TonB-box. For FhuA, I made a clone identical to the one previously described (FhuAΔ5-160; Fhuβ; Braun

et. al. 2000), for validation of the prior findings, and comparison to the FepA deletion clones

The creation of chimeric proteins in which the N-domain of one receptor was genetically fused to the C-terminal β-barrel domain of the analogous receptor allowed me to assess the functional exchangeability of the N-termini of FepA and FhuA. The protein engineering preserved three fundamental properties of siderophore receptor structure: the globular N-domain, the C-terminal β-barrel domain, and the β-turn that joins them. Construction of the chimeric clones avoided the insertion or deletion of amino acids: FepNFhuβ contained the N-domain and β-turn of FepA linked to the β-barrel of FhuA; FhuNFepβ contained the N-domain of FhuA linked to the β-turn and β-barrel of FepA (Figure 4.1).

4.2 Expression and Localization of Deletion and Chimeric Receptors

Western immunoblots employing α-FepA monoclonal antibodies 26 and 45 (Murphy et. al. 1990) verified the proper expression of the mutant and chimeric derivatives. The former antibody recognizes an epitope in the N-terminal globular domain of FepA bound by residues 27 and 37 (Murphy et. al. 1990). The latter binds in loop four of the C-terminal barrel domain around residue 329 (Murphy et. al. 1990; Cao et. al. 2000). With the exception of FhuNFepβ, which showed a small amount of degradation, all chimeric and deletion constructions were stably expressed near wild-type levels (Figure 4.2; Table 4.1). The reduced amounts of

FhuNFepβ, as compared to FepNFhuβ, are consistent with the relative difference in expression from the FhuA and FepA promoter. In addition, Fepβ was expressed at lower amounts than Fepβ2, perhaps because the former construct deletes residues in the N-terminal extremity that are important for proper secretion. Quantitative determinations of expression levels indicated that the protein engineering did not adversely affect the synthesis or secretion of the other mutant derivatives (Table 4.1). Fractionation of cell envelopes on density gradients confirmed the mutants were properly localized within the outer membrane (Figure 4.3). To address the possibility that the mutant receptors contained gross structural abnormalities within the outer membrane, their conformation was evaluated *in vivo*. Flow cytometric analysis of cell surface loops utilizing two monoclonal antibodies that recognize surface exposed epitopes of FepA (mAB 33 and 45; Netwon et. al. 1999) indicated that the conformation of the mutant receptors were similar to that of native FepA (Table 4.1). When combined, these approaches suggest that the deletion of, or introduction of an aberrant, N-domain does not appreciably alter the expression, OM localization, or cell surface accessibility of the resulting chimeric proteins.

4.3 Ligand Recognition by Deletion and Chimeric Receptors

The deletion and chimeric proteins functioned with unexpected selectivity and efficiency as dictated by their surface loops and β-barrels. The absence, or presence of the incorrect N-domain did not influence siderophore recognition.

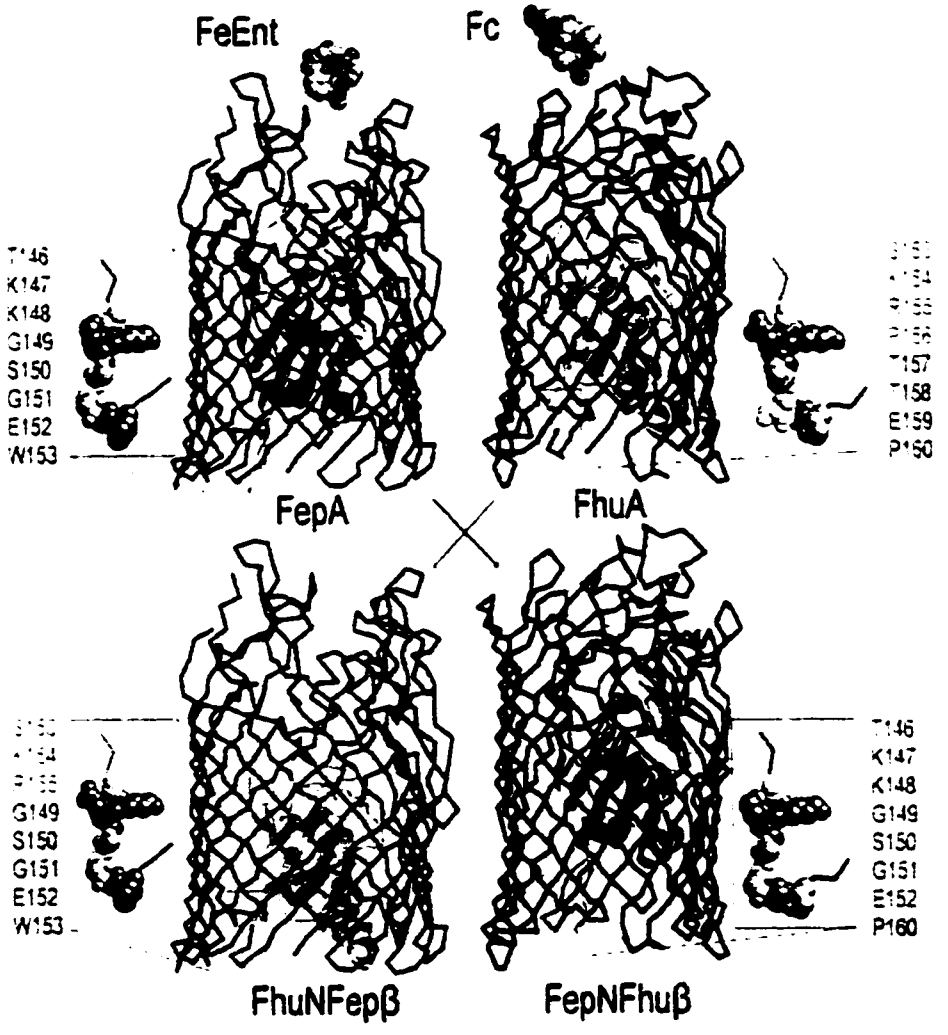

Figure 4.1 Cloning design and architecture of the chimeric clones FhuNFepβ and FepNFhuβ

Strain/Plasmid	Ferric Enterobactin						Protein Ligands		MAbs		Antibiotic			Exp.[b]
	Binding		Transport				ColB	ColD						
	K_d	Cap.	Nutr.[a]	K_m	V_{max}	k_3			33	45	N	B	E	
KDF541	NB	0	0	NT	0	0	R	R	0.15	0.13	14	0	0	0
KDF541/pFepA	0.4	64.0	18	0.40	411	6.4	10^5	4×10^4	7.8	14.1	14	0	8	1.2×10^5
KDF541/pFhuNFepβ	0.6	1.6	25[c]	1.7	1.6	0.9	10^3	4×10^1	7.6	8.3	14	0	8	1.5×10^4
KDF541/pFepβ	0.2	4.3	20[c]	1.45	1.4	0.3	4×10^4	4×10^3	8.9	13.8	14	8	10	9.4×10^4
	Ferrichrome						ColM	T5						
AN193	NB	0	0	NT	0	0	R	R	ND	ND	14	0	8	0
AN193/pFhuA	0.6	23	19	0.6	87	4	2×10^2	2×10^6	ND	ND	14	0	8	ND
AN193/pFepNFhuβ	0.6	1.6	19	2.5	9.8	6.5	R	10^5	0.2	0.18	14	0	8	9.4×10^4
AN193/pFhuβ	1.0	3.0	21	3.6	25	8.3	R	10^5	ND	ND	16	8	8	ND

Table 4.1. Phenotypic properties of deletion and chimeric clones. a - Diameter of growth halos from siderophore nutrition assays. b - Expression (copies/cell) was measured from ^{125}I-protein A western blots as compared to normalized standards, and expressed as receptors/cell. c - very faint growth halos were observed, see Figure 4.5. For FeEnt, the mean standard errors for K_d and capacity were 16% and 4%, respectively. For Fc, mean standard errors for K_d and capacity were 15% and 2%. NB, no binding. For FeEnt, the mean standard errors for K_m and V_{max} were 17% and 4%, respectively. For Fc, the mean standard errors for K_m and V_{max} were 27% and 6%. The turnover number for each protein (k_3; molecules transported/min) was calculated by dividing V_{max} by capacity. NT, no transport.

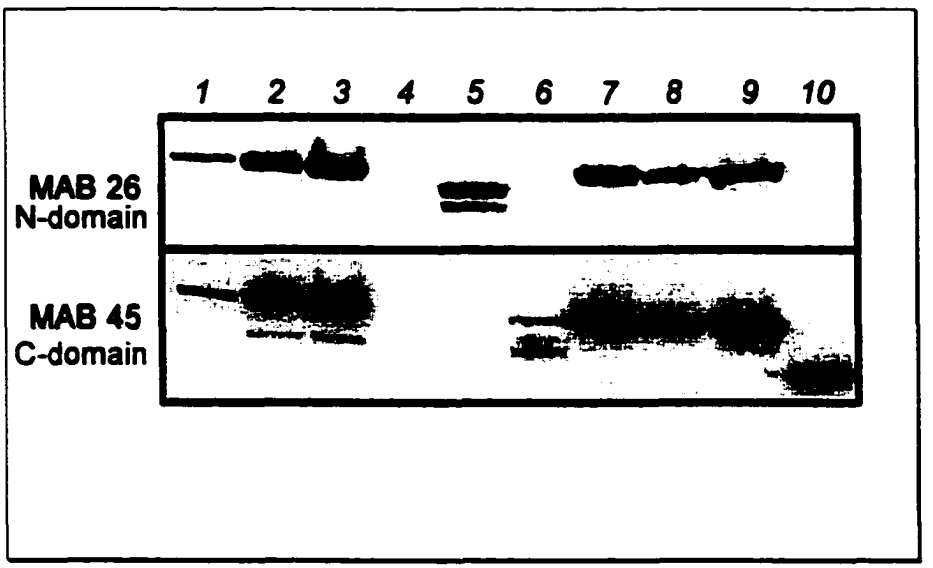

Figure 4.2 Expression of Chimeric and Deletion Mutants. Western immunoblots stained with either mAB 26 (top) or mAB 45 (bottom) and developed with ^{125}I-Protein A. Lanes 1-3, 1.3, and 5μg of purified FepA respectively. Lanes 4-10 each contain lystates of 2.5 *10^8 bacterial cells, except lane 9, which contains 10^8. Lane 4, KDF541 (*fepA, fhuA*); Lane 5, KDF541/pFepNFhuβ; Lane 6, KDF541/pFhuNFepβ; Lane 7, KDF541/pITS23 (*fepA*$^+$); Lane 8, BN1071 (*fepA*$^+$,*fhuA*$^+$); Lane 9, KDF541/pITS449 (*fepA*$^+$); Lane 10, KDF541/pFepβ

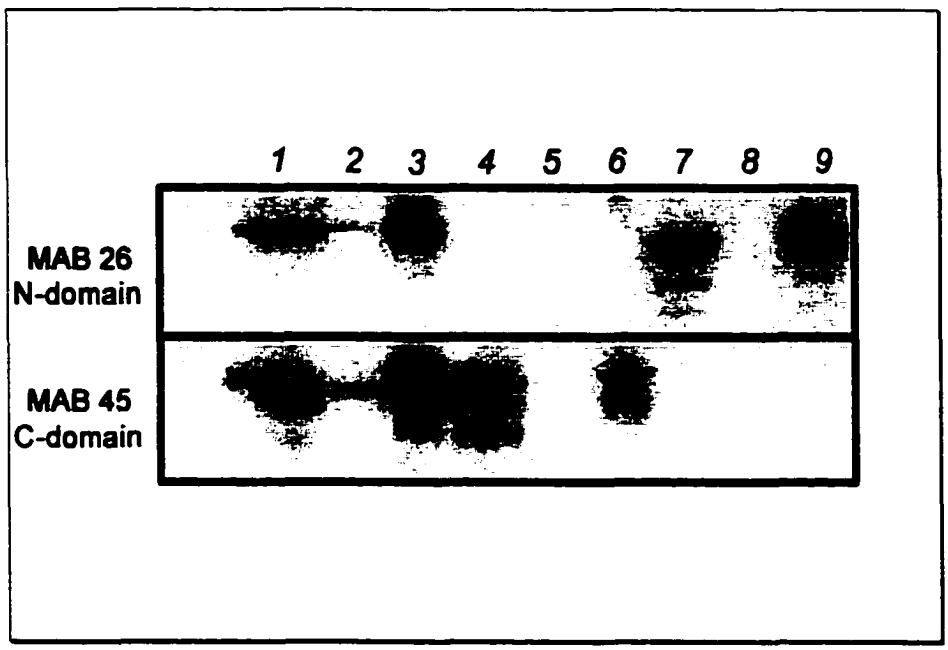

Figure 4.3 Localization of chimeric proteins. Inner and outer membranes were separated by sucrose density-gradient fractionation, and 30μg of each sample was analyzed by western blot with mAB 26 (top) or mAB 45 (bottom). Lanes 1-3, KDF541/pITS23 cell lysate, inner membrane, and outer membrane respectively; Lanes 4-6, KDF541/pFhuNFepβ lysate, IM, and OM; Lanes 7-9, KDF541/pFepNFhuβ lysate, IM, and OM.

FhuNFepβ bound ferric enterobactin (FeEnt) but not Ferrichrome (Fc), wheras FepNFhuβ bound Fc but not FeEnt. FepA absorbs FeEnt with subnanamolar affinity, which was preserved in the FhuNFepβ chimera. The K_d of its binding reaction with FeEnt was 0.2nM (Table 4.1; Figure 4.4). The reverse hybrid, FepNFhuβ, bound Fc with an affinity equivalent to that of the wild-type receptor FhuA: The K_d of its binding reaction with Fc was 0.6nM (Table 4.1; Figure 4.4). So, despite the presence of a heterologous N-domain, the receptors retained the selectivity of their β-barrels, while maintaining wild-type affinity. The empty β-barrels of FepA and FhuA also avidly bound their appropriate ferric-siderophore, further indicating that the surface loops select among the ligands bacteria encounter in their environment. The data support previous findings that implicated the importance of aromatic amino acids in FeEnt binding. These aromatic residues localize to the exterior-most portions of cell surface loops surrounding the entrance to the FepA channel (Cao et. al. 2000). Within the crystal structure of FhuA, ferrichrome lodged deep within the vestiblue, participating in hydrogen bond contacts with three N-domain residues (R81, Y116, and G99; Locher et. al. 1998; Ferguson et. al. 1998). Direct interactions between ferrichrome and the N-domain of FhuA suggest the participation of the N-domain in ligand recognition and binding. However, the subnanamolar binding affinity of the two mutant proteins lacking the N-domain, Fhuβ (for Fc) and Fepβ (for FeEnt), indicate that in both receptor proteins the N-domain does not significantly influence ligand recognition

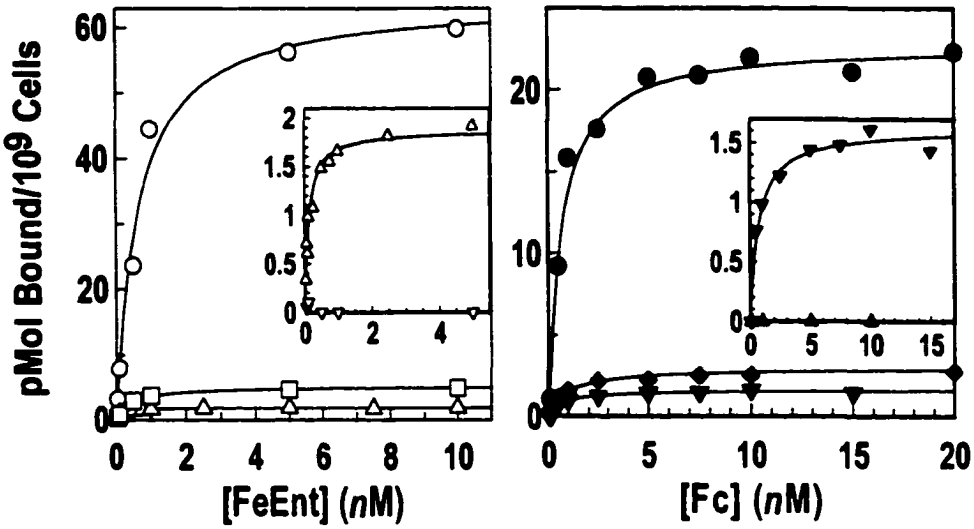

Figure 4.4 Ferric Enterobactin (FeEnt) and Ferrichrome (Fc) binding by chimeric and deletion proteins. The adsorption of [^{59}Fe]Ent (open symbols) and [^{59}Fe]Fc (closed symbols) was measured with metabolically inactive KDF541 expressing FepA or FhuA (○), FhuNFepβ (△), FepNFhuβ (▽), Fepβ (□), and Fhuβ (◇) on pHSG575.

or binding. In contrast, the data suggest that the N-domain does not participate at all in ligand binding, and if it does, the contributions are minimal and secondary to the interaction with surface loops.

Although it was not required for ligand recognition, the N-domain of FepA and FhuA were needed for maximal binding. Mutant constructions lacking a N-domain, or containing an aberrant one, adsorbed ferric siderophores at much lower capacities as compared to the wild-type receptors (Table 4.1; Figure 4.4). The reduction in capacity levels could not be explained by reduced expression levels (Table 4.1; Figure 4.2), improper localization (Table 4.1; Figure 4.3), or degradation (Figure 4.1), rather, biochemical descriptions of their binding capabilities indicated that only a fraction (≈10%) of the mutant receptors bound ferric siderophores. Thus, a correct N-domain, which was not necessary for siderophore recognition, was required for optimal binding.

4.4 Interactions of mutant receptors with protein toxins and bacteriophages

The β-barrels of the mutant receptors also dictated their interactions with protein toxins and bacteriophages. Reiterating the results observed for siderophore binding, cells expressing Fepβ or FhuNFepβ were rendered sensitive to colicins B and D, but not M or bacteriophages that are recognized by FhuA. Similarily, Fhuβ or FepNFhuβ recognized and transported bacteriophage T5 and phi80, but were resistant when challenged against the toxins that utilize FepA, colicins B and D

(Table 4.1). Although the β-barrels allowed for recognition and transport, the efficiency of killing by these toxins was somewhat reduced, suggesting that the toxins further interact with the globular N-domain while implementing their toxicity (Table 4.1). In contrast to data obtained by Braun and co-workers (Braun et. al. 2000), we did not observe colicin M killing of cells harboring FhuA barrel constructs. This discrepancy most likely stems from the low activity of our colicin M preparation ($1 * 10^{-2}$; Table 4.1)

4.5 Transport of ferric siderophores by mutant receptors

The occlusion of the beta-barrel domain by the globular N-domain raises a puzzling question: What is the function and structural disposition of the globular domain during the transport reaction? Passage of ferric-siderophores requires a minimum diameter of about 15 Å, which, when viewed in space filling representation, does not exist in either FepA or FhuA. In addition, siderophore receptors recognize and transport synthetic antibiotics, so called "Trojan-Horse" antibiotics, that often double the size of the iron complex without affecting its recognition or uptake (Minnick et. al. 1992; Diarra et. al. 1996; Reissbrodt et. al. 1997; Fung-Tomoc et. al. 1997; Kline et. al. 2000; Roosenberg et. el. 2000). Furthermore, although colicins generally possess a slender and elongated shape, their passage even through an open porin channel faces severe steric constraints. Does the N-domain exit the barrel during transport, or change conformation within

the pore to form an opening that allows for the passage of siderophores? Transport of iron chelates by the mutant receptors should provide insight into these alternatives. Although the chimeric proteins avidly bound the ferric-siderophore dictated by its surface loops and β-barrel domain, the presence of a aberrant N-domain within the barrel makes it unlikely that the bound siderophore would be internalized. For example, transport of Fc through FepNFhuβ is unexpected, since this chimeric protein possesses an N-domain that was adapted for transport of a negatively charged catechol siderophore, ferric enterobactin. Yet when analyzed by siderophore nutrition assays, ferrichrome stimulated the growth of cells expressing Fhuβ or FepNFhuβ at levels comparable to that of cells containing wild-type FhuA (Figure 4.5). The observations were further explained with quantitative determinations of the uptake kinetics: despite a slightly lower overall uptake affinity for Fc by FepNFhuβ than FhuA (K_m values of 2.5 and 0.6nM respectively; Table 4.1; Figure 4.6) the turnover numbers of Fc uptake were comparable (k_3 values of 6.5/min and 4/min respectively; Table 4.1). In addition, the plug-less derivative of FhuA, Fhuβ, transported Fc with a similar affinity (K_m = 3.6 nM) and at a faster rate (k_3 = 8.3/min) than the wild-type protein. Therefore, neither the presence of a N-domain, or the introduction of the FepA N-domain into the FhuA β-barrel impaired uptake. Uptake experiments with FepA barrel derivatives corroborated these conclusions, despite a reduced efficiency of these clones for FeEnt uptake (Table 4.1; Figure 4.6). Both Fepβ and FhuNFepβ displayed FeEnt

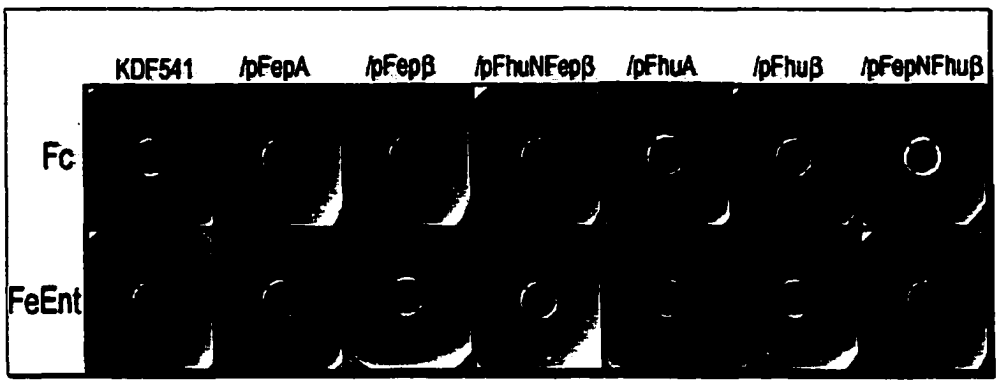

Figure 4.5 Siderophore nutrition assays of chimeric and deletion proteins. Bacterial cultures harboring FepA, FhuA, and their derivatives were seeded onto a agar lawn. A sterile filter disk was placed on top of the solidified agar and 5μl of 50μM ferrichrome (top panel) or ferric enterobactin (bottom panel) was applied to the disk and incubated overnight at 37 °C. No growth halos were observed when the chimeric and deletion constructions were expressed in KDF571 (*tonB*), indicating they remained TonB dependent for transport.

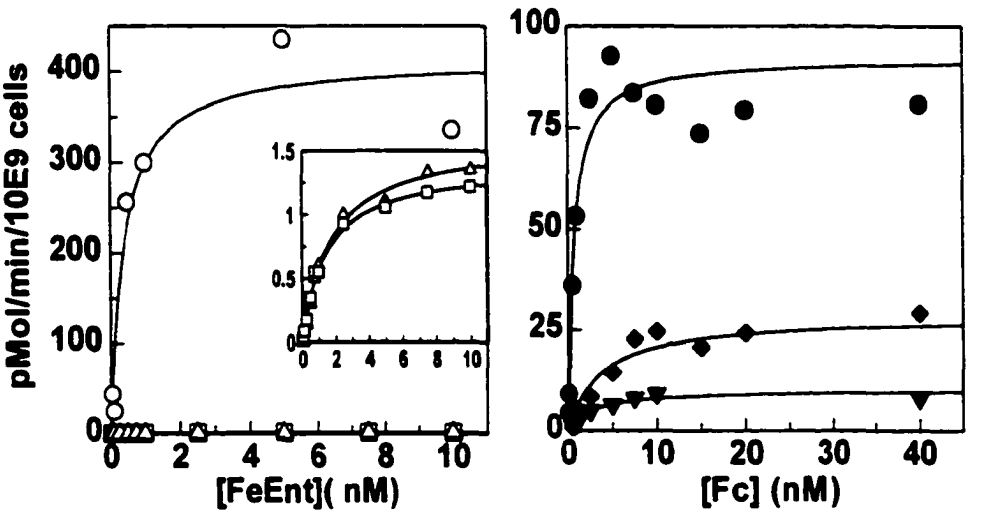

Figure 4.6 Ferric Enterobactin (FeEnt) and Ferrichrome (Fc) transport by chimeric and deletion proteins. The uptake of [^{59}Fe]Ent (open symbols) and [^{59}Fe]Fc (closed symbols) was measured with KDF541 expressing FepA or FhuA (O), FhuNFepβ (Δ), FepNFhuβ (∇), Fepβ (□), and Fhuβ (◇) on pHSG575. The inset graph on the left reduces the scale of the y axis to show the saturation curves of Fepβ and FhuNFepβ.

uptake, albeit slower than wild-type FepA (k_3 values of 0.3/min, 0.9/min, and 6.4/min respectively; Table 4.1; Figure 4.6). The reduced transport rates explained the marginal abilities of Fepβ and FhuNFepβ in siderophore nutrition tests with ferric enterobactin (Figure 4.5). When the deletion and chimeric constructions were transferred to the *tonB*⁻ strain KDF571 (Rutz et. al. 1992) no uptake of ferric-siderophores (Figure 4.6) or sensitivity to protein toxins and bacteriophages (Table 4.1) was observed, indicating the receptors remained TonB-dependent despite the removal of the TonB-box containing N-domain. Uptake of ferric-siderophores through the empty barrels of FepA and FhuA undermine previous theories aimed at describing the function of TonB (Evans et al. 1996; Postle, 1990; Holroyd and Bradbeer, 1984; Moeck and Coulton, 1998; Kadner 1990). Specifically, transmembrane signaling and/or functional interactions between bound receptors and TonB, through the TonB box, are erroneous since the empty barrels of FepA and FhuA do not contain these regions.

4.6 Probing the conformation of the chimeric proteins

We became concerned with the tertiary structure of the hybird proteins upon learning of the almost identical activities of the empty barrel and its counterpart containing a heterologous N-domain. The similar activities raised the possibility that, within the chimeric constructions, the N-domain was not properly folded and assembled within the barrel. Rather, it remained suspended within the periplasmic

space. We utilized three independent methods to assess the overall tertiary structure of the chimeric proteins.

4.6.1 Native Electrophoresis of the chimeric proteins

The β-barrel proteins of the outer membrane are resistant to denaturation by SDS, and they possess a compact native structure that imparts an enhanced migration in PAGE. Denaturation of the β-barrels by heating in ionic detergents eliminates this compact state, reverting the abnormal electorphoretic mobility. In their native states, both FepA and FhuA exhibit this compact nature and increased mobility in electrophoresis (Murphy et. al. 1990; Locher and Rosenbusch 1997). However, in contrast to the general porins like OmpF/C, the siderophore receptors are less stable, and hence more sensitive to denaturation. For these reasons, native electrophoresis of the chimeric proteins should be a revealing measure of their overall tertiary structure. For example, it would be expected that the native electrophoretic migration of the chimeric protein would be increased if the N-domain remained suspended from, and not properly folded within the barrel. When electrophoresed in LDS at 4 °C, both FepNFhuβ and FhuNFepβ displayed the same rapid mobility as FhuA and FepA, respectively (Figure 4.7). Suggesting that the chimeric proteins fold properly and possess the same compact nature of the wild-type receptors.

4.6.2 Immunochemical investigations to chimeric protein structure

The large repertoire of available monoclonal antibodies directed against epitopes of FepA are a powerful tool for probing the conformational state of the OM receptor (Murphy et. al. 1990; Rutz et. al. 1991; Rutz et. al. 1992; Newton et. al. 1999). In this instance, monoclonal antibodies with epitopes mapping to the N-domain were targeted to evaluate their accessibility in the chimeric proteins. In Enzyme Linked Immunosorbent Assays (ELISAs) the accessibility of four different FepA monoclonals that recognize epitopes in the N-domain were indistinguishable when analyzed against FepNFhuβ and wild-type FepA (Figure 4.8). The antibodies did not react with their epitope unless the protein was denatured before adsorption to the plates, indicating that the N-domain of FepNFhuβ was sequestered within the barrel in a similar manner in which the N-domain is within the barrel of wild-type FepA (Figure 4.8). The lack of monoclonal antibodies directed at the N-domain of FhuA prevented a similar analysis of FhuNFepβ. However, the proper localization of cell surface loops was measured cytofluormetrically with FepA monoclonals directed towards epitopes located in the C-terminal domain. Analogous to FepNFhuβ in ELISA, the accessibility of cell surface loops in FhuNFepβ was indistinguishable from wild-type FepA in flow cytometry (Table 4.1), again, suggesting the tertiary structure of the chimeric protein remained intact.

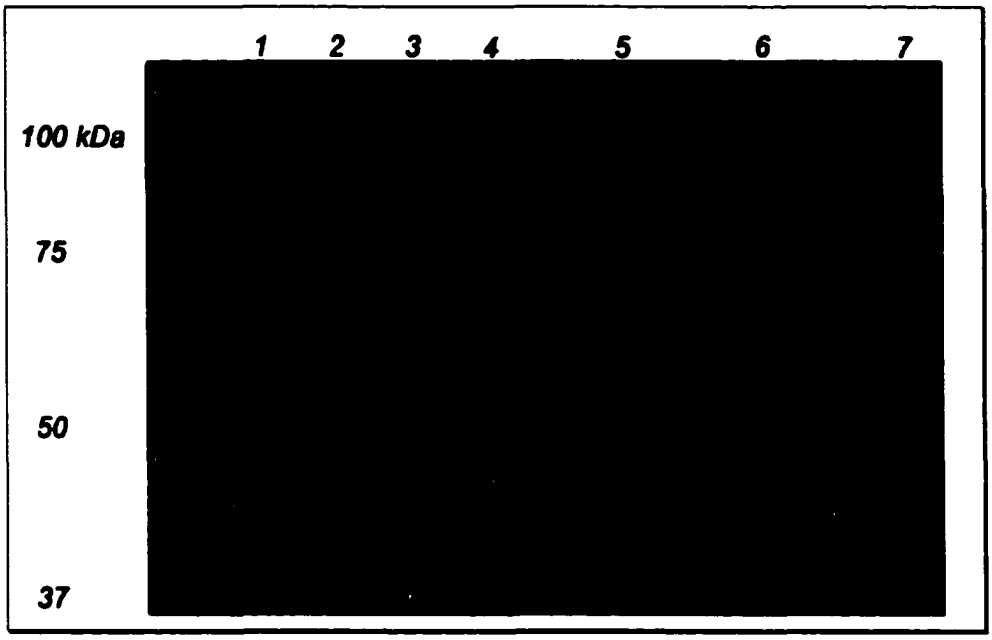

Figure 4.7. Non-denaturing LDS-PAGE of chimeric proteins. The left panel is a non-denaturing LDS-PAGE stained with coomassie blue; the right panel is a western immunoblot of a non-denaturing LDS-PAGE, stained with a mixture of mAB26 and mAB45. Lanes 1 and 2, non-denatured and denatured purified FepA respectively. Lanes 3 and 4, non-denatured and denatured purified FhuA respectively. Lanes 5-7, non-denatured outer membrane fragments (30μg) from KDF541 harboring pITS23, pFhuNFepβ, and pFepNFhuβ respectively. Molecular weight standards are shown for reference.

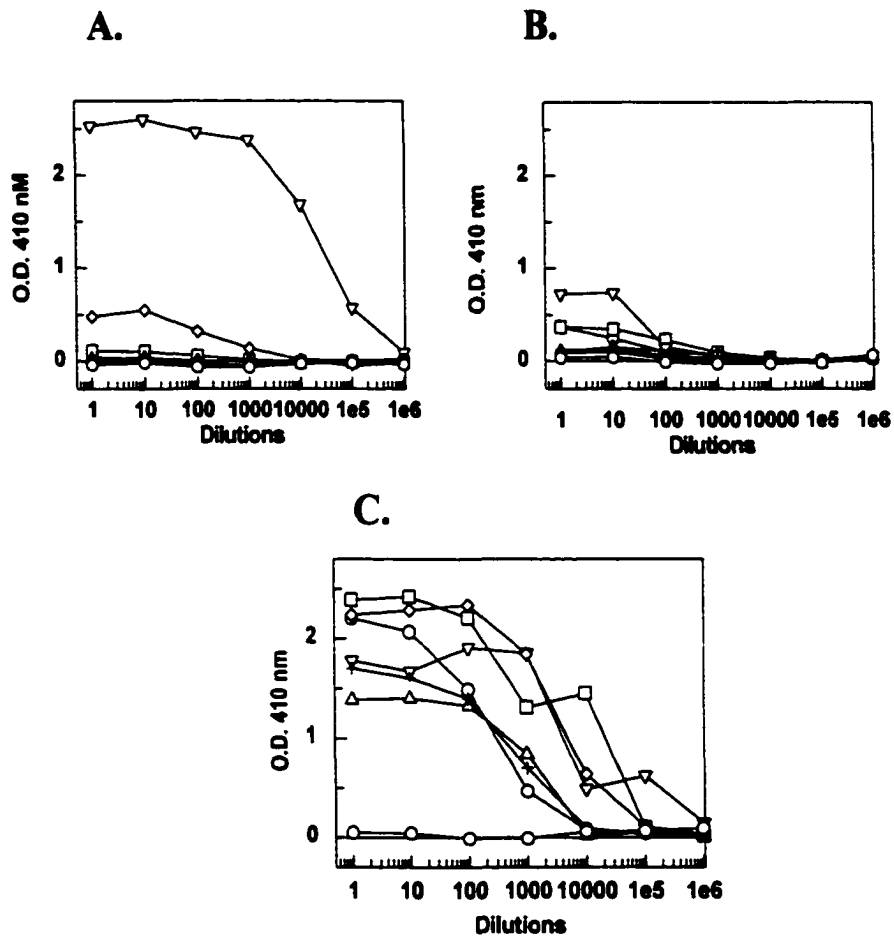

Figure 4.8. Analysis of FepNFhuβ by ELISA. Outer membranes from KDF541 carrying pITS23 (A), pFepNFhuβ (B), or purified, denatured FepA (C) were adsorbed to microtiter plates and analyzed with FepA mABs 1 (○), 12 (◇), 27 (□), 41 (△), 33 (+), and 45 (▽), or normal mouse serum (○). The first four recognize different epitopes in the N-domain of FepA, whereas the latter two bind epitopes in surface loops of the barrel.

4.6.3 Permeability of chimeric proteins to antibiotics

The gram-negative bacterial outer membrane serves as a selective permeability barrier, permitting the uptake of nutrients and vitamins (<600 Da) and excluding the diffusion of larger, toxic molecules such as antibiotics and detergents (Nikaido and Vaara 1995). The diffusable properties of the outer membrane are directly related to the size of porin channels located within it. Among general and specific porins, the inward orientation of a unique cell surface loop (L3), the transverse loop, contributes significantly to the size exclusion limits of the pores formed by these proteins. In the case of siderophore receptors, the potentially large pore that would form from a 22-stranded beta-barrel must be sealed to maintain the integrity of the permeability barrier. The N-domain may therefore serve an analogous function to that of the transverse loop in general and specific porins, constricting the size of the pore formed by the C-terminal barrel domain. The susceptibility of bacterial strains harboring either deletion or chimeric derivatives to antibiotics that exceed the diffusion limits of the OM would therefore serve as an effective indicator of the structure of the mutant receptors. As shown in Table 4.1, neither FepNFhuβ or FhuNFepβ conferred an increased susceptibility to large antibiotics, whereas strains expressing Fhuβ or Fepβ displayed an enhanced susceptibility to bacatricin (1500 Da; Table 4.1). Together the three approaches strongly suggest that the chimeric receptors assemble within the OM with their N-termini properly folded within the heterologous β-barrel domains.

Chapter 5

Sulfo-EGS Cross-linking of FepA

Chemical cross-linking is widely used in biochemical investigations to analyze the structure and associations of cell membrane proteins. It is well suited for the search of oligomeric species (Locher and Rosenbusch 1997), for analysis of neighboring membrane proteins (Mikkelsen and Wallach 1976; Trommer et. al. 1975; Palva and Randall 1976), and to probe the topology of membrane bound proteins (Nicolson and Singer 1971; Frye and Edidin 1970). The selection of an appropriate cross-linking reagent for the study of membrane proteins is crucial and

often depends on the type of information sought. Bi-functional reagents result in the covalent linkage between two target molecules. They contain two reactive groups separated by a non-reactive backbone spacer of defined length. Numerous cross-linking reagents are available to choose from that possess reactive groups towards specific amino acids (i.e. cysteine) or functional groups (i.e. primary amines).

Formaldehyde cross-linking studies suggested that TonB may interact with the siderophore receptors of the outer membrane (Skare et. al. 1993; Larsen et. al. 1997; Moeck et. al. 1997). However, the non-specific nature of this reagent, and low quantities of complex observed raised questions about its validity. In addition, glutaraldehyde cross-linking studies with FhuA indicated the possibility of oligomeric states of the receptor (Locher and Rosenbusch, 1997). We sought to analyze the cross-linking properties of FepA by use of a reagent with well defined targets that are amendable to study by established techniques.

5.1 In vivo Cross-linking of FepA

To probe for oligomeric states and analyze neighboring membrane proteins of FepA, I initiated cross-linking studies with the homo-bifunctional crosslinking reagent Sulfo-EGS [Ethylene glycolbis(sulfosuccinimidylsuccinate)]. Sulfo-EGS was the reagent of choice for numerous reasons: (i.) it is water soluble and membrane impermeant. (ii.) The size of Sulfo-EGS (664 Da) prevents its diffusion

across the water-filled channels of the outer membrane restricting its action to targets on the surface of the outer membrane. (iii.) The homo-bifunctional cross-linking groups of Sulfo-EGS react specifically with primary amines (e.g. Lysine). (iv.) A defined spacer length (16.1 Å) between the two reactive groups provided the knowledge of relative distances between the cross-linked species.

When bacteria or outer membranes containing FepA were exposed to Sulfo-EGS, two prominent cross-linked bands appeared containing FepA, of approximate molecular masses 100 (band 1) and 120 kDa (band 2; Figure 5.1). Monomeric FepA exhibits an electrophoretic mobility in SDS-PAGE of 81kDa, indicating that the cross-linked complexes contain FepA linked to species of approximately 20 and 40kDa. Formation of the cross-linked products was independent of the presence or absence of TonB (data not shown), eliminating the possibility that either of the cross-linked complexes contained TonB. Multimeric complexes (dimeric, trimeric, etc.) of FepA were not observed in western blots of the cross-linked samples. The absence of bands corresponding to multimeric forms does not rule out the possibility that such complexes may exist since the nature and arrangement of such a complex is unknown. For example, dimeric or trimeric forms of FepA may not posses accessible lysine residues that reside within close enough proximity to result in productive cross-linking of the oligomeric complex(s). Rather, the data simply indicate that Sulfo-EGS is not able to define such a complex.

5.2 Effect of Ferric Enterobactin on cross-linking

Previous biophysical studies implicated the importance of cell surface loop conformational change in siderophore binding and transport (Liu et al. 1994; Klug et al. 1998; Payne et al. 1997; Cao et al. 2000). However, the validity of these conclusions was challenged in the crystallographic structures of free and liganded-FhuA, because no conformational change occurred in the cell surface loops of the ligand-bound and ligand free FhuA structures. To address this apparent paradox, I performed cross-linking studies in the presence and absence of ferric enterobactin, in search for different conformational states of FepA.

When pre-incubated with saturating amounts of ferric enterobactin prior to the addition of cross-linker, bacteria expressing FepA showed a different cross-linking pattern (Figure 5.1). The presence of ferric enterobactin abolished cross-linked band 2, and drastically reduced the amount of band 1. Changes in the cross-linking pattern depended upon the binding of ferric enterobactin to FepA, and not the presence of the ferric-siderophore itself, as cross-linking studies in the presence of another ferric-siderophore, ferrichrome, were indistinguishable from wild-type cells without the addition of exogenous ligand (data not shown). Two explanations exist for the disappearance of cross-linked products in the presence of ferric enterobactin. First, binding of the siderophore may induce conformational changes in the cell surface loops that alter the orientation of the target such that it is no longer accessible for productive cross-linking. The second possibiliy is that binding

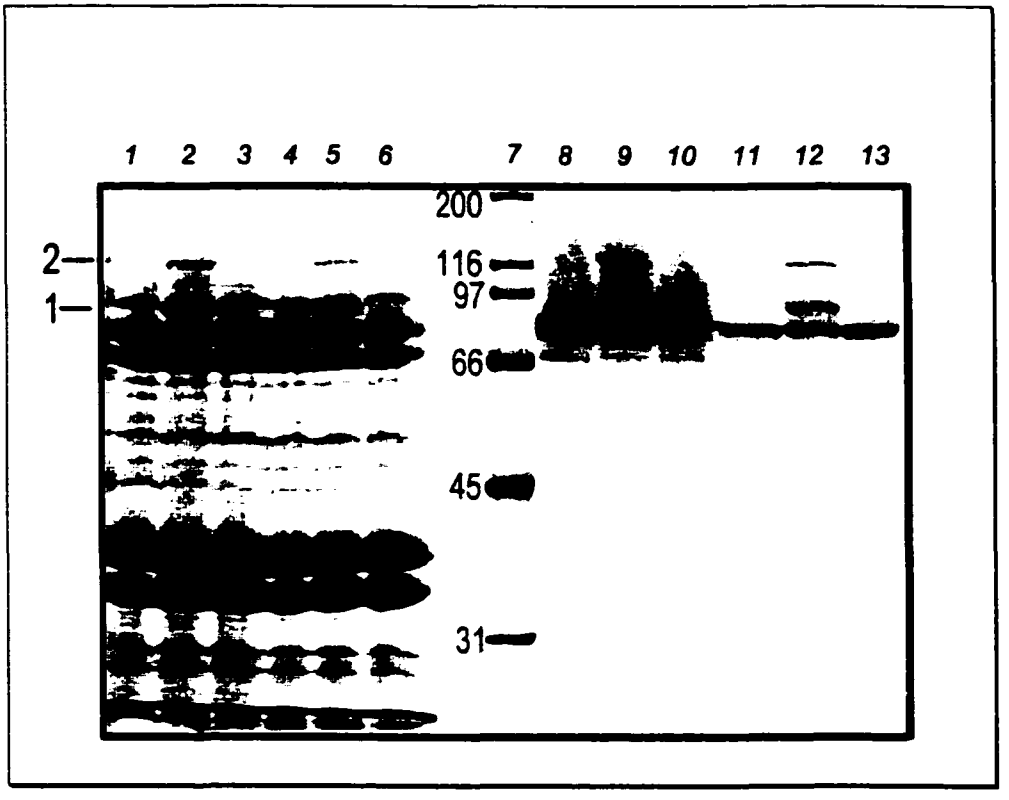

Figure 5.1. Sulfo-EGS Cross-linking of FepA. Left panel: Outer membranes from BN1071 (lanes 1-3) or KDF541 pITS23 (lanes 4-6) were treated with Sulfo-EGS, subjected to SDS-PAGE, and stained with Coomassie Blue. Lanes 1 and 4, no cross-linking; lanes 2 and 5, cross-linked by Sulfo-EGS; Lanes 3 and 6, cross-linked in the presence of 5μM FeEnt. Lane 7, moleuclar mass standards. Right panel: outer membranes from KDF541/pITS23 (lanes 1-3), or live cells of KDF541/pITS23 were either untreated (lanes 8 and 11), or cross-linked with Sulfo-EGS in the absence (lanes 9 and 12) or presence (lanes 10 and 13) of 5μM FeEnt.

of ferric enterobactin physically blocks the reactive lysine residue, rendering it inaccessible to the cross-linking reagent. This situation may occur if the reactive lysine residue is itself involved in the binding reaction, or if it is situated within close enough proximity to the binding pocket to block accessibility when bound.

5.3 Determination of the Lysine residue that participates in cross-linking

To better understand differences in the cross-linking patterns of free and bound-FepA, I identified the FepA lysine residue involved in productive cross-linking with Sulfo-EGS. Determination of the involved lysine residue may seem straight forward, because mutation or deletion of it will eliminate the observed cross-linked products. However, the task of locating the responsible lysine residue was daunting because FepA contains thirty-one lysine residues, and from inspection of the crystal structure approximately twenty-three of these reside on the cell surface. To narrow down and expedite the search for lysine candidates, I first performed cross-linking reactions with existing loop deletion mutants (Newton et. al. 2000). Dr. Newton engineered a series of loop deletions that individually remove each of the eleven cell surface loops of FepA. Deletion of cell surface loops 2 (residues 98 - 123), 4 (residues 315 - 326), 7 (residues 467 - 497), 8 (residues 546 - 560), and 11 (residues 681 - 691) abolish the formation of cross-linked products (Figure 5.3). Changes to the cross-linking profile of loop deletions Δ2, Δ4, and Δ8 were likely due to structural alterations of the loops themselves,

A.

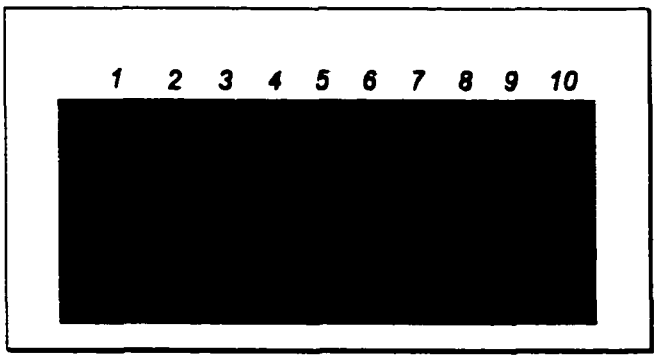

B.

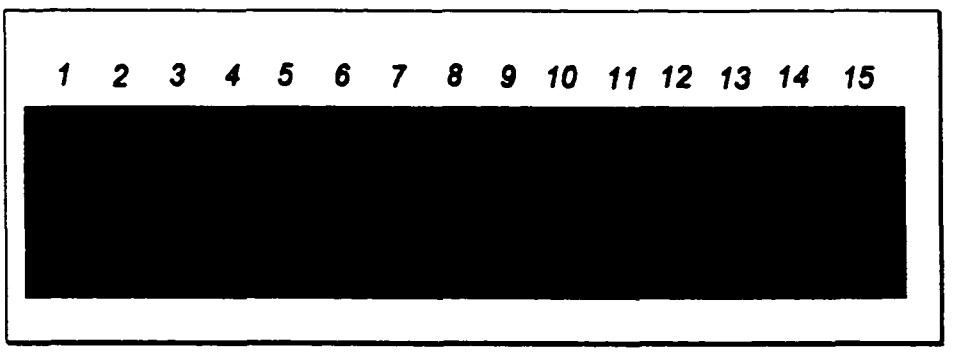

Figure 5.2. Cross-linking of the FepA loop deletions. Panel A. Live cells from KDF541 harboring pITS23 (1-2), Δ2 (3-4), Δ3 (5-6), Δ4 (7-8), Δ5 (9-10), were untreated (lanes 1,3,5,7,9) or cross-linked (2,4,6,8,10) with Sulfo-EGS. Panel B. Live cells from KDF541 harboring pITS23 (1-4), Δ7 (4-6), Δ8 (7-9), Δ9 (10-12), Δ11 (13-15), were untreated (1,4,7,10,13), or cross-linked in the absence (lanes 2,5,8,11,14), or presence of FeEnt (lanes 3,6,9,12,15)

because these loop deletions contain no lys residues. ΔL7 and ΔL11 remove three lysine residues from the primary structure of FepA; In ΔL7, Lys467 and Lys483, and in ΔL11, Lys681. I changed these candidate residues to alanine to remove the reactive primary amine group. The phenotypic properties of these mutations were indistinguishable from the wild type protein, with the exception of a slight (10 fold) reduction in colicin B sensitivity to cells harboring the K483A mutation (Table 5.1). Analysis of the cross-linking patterns of these mutant proteins (Figure 5.3) showed that K483A abolished the cross-linking reaction, whereas K467A and K681A produced wild-type cross-linking patterns. These data suggested that the primary amine of lysine 483 is responsible for the cross-linked bands produced by Sulfo-EGS.

Does the location of lysine 483 in loop 7 of FepA suggest anything about the nature of the cross-linking reaction? Upon close inspection of the crystal structure with particular attention to the location of lysine 483, a fascinating discovery arises. The discovery confirms the idea of conformational movement of the surface loops. Lysine 483 is located within a highly flexible region of cell surface loop seven of the FepA structure. In addition, only the beta carbon of its side chain was solved in the crystal structure, presumably because of the flexibility of this side chain (Figure 5.4). Its disposition in space is directly above and near the center of the channel formed by the beta-barrel domain (Figure 5.4). This region is in the approximate area in which a weak iron signal was observed in

attempts to solve ligand bound structures of FepA (Buchannan et al. 1999). The location may suggest that the lysine residue itself is within close proximity to, or part of, one of the binding sites (most probably B1)(Payne et al. 1997; Cao et al. 2000), and hence blocks cross-linking due to its disposition to the bound siderophore. However, the measurement of atomic distances from lysine 483 to atoms of FepA along the rim of the barrel and surface loops suggest a different story. Distances from the beta carbon of lysine 483 to the four sides of the FepA structure are 19.5 Å, 20.9 Å, 23.9 Å, and 19.3 Å respectively (Figure 5.4). These atomic distances not only make it unlikely that lysine 483 could participate in cross-linking to neighboring membrane proteins, they make it impossible. The spacer length between reactive residues in Sulfo-EGS is 16.1 Å, far shorter than the smallest distance from the beta carbon of lysine 483 to the external face of the surface loops (19.3 A; Figure 5.4). Although, the inclusion of the remaining side chain residues, and the flexibility of the loop itself, may decrease these distance measurements it remains unlikely that the reactive lysine residue of OmpA would lie within the cutoff distance of 16 Å. Supporting this view is the observation that cell surface loops of OmpA extend above the membrane bilayer far less than the loops of FepA, as such a more accurate measurement of the distance between lysine 483 and the external rim of FepA would contain residues within the loops that are closer to the membrane bilayer. The orientation and location of lysine 483, and its involvement in cross-linking, suggest that in the native environment

Strain	*Colicin B*	*Colicin D*	*Fe-Ent Nutrition*
KDF541	R	R	0
pITS23	$1 * 10^5$	$4 * 10^4$	16
pITS23/K167A	$2 * 10^5$	$4 * 10^4$	16
pITS23/K328A	$2 * 10^5$	$4 * 10^4$	16
pITS23/K332A	$2 * 10^5$	$4 * 10^4$	16
pITS23/K375A	$1 * 10^5$	$4 * 10^4$	16
pITS23/K406A	$2 * 10^5$	$4 * 10^4$	16
pITS23/K467A	8 * 104	$4 * 10^4$	16
pITS23/K483A	$2 * 10^4$	$2 * 10^3$	16
pITS23/K503A	$2 * 10^5$	$4 * 10^4$	16
pITS23/K535A	$2 * 10^5$	$4 * 10^4$	16
pITS23/K560A	$2 * 10^5$	$4 * 10^4$	16
pITS23/K634A	$2 * 10^5$	$4 * 10^4$	16
pITS23/K635A	$2 * 10^5$	$4 * 10^4$	16
pITS23/K639A	$2 * 10^5$	$4 * 10^4$	16
pITS23/K681A	$1 * 10^5$	$2 * 10^4$	16

Table 5.1. Phenotypic properties of the FepA lysine mutants.

A.

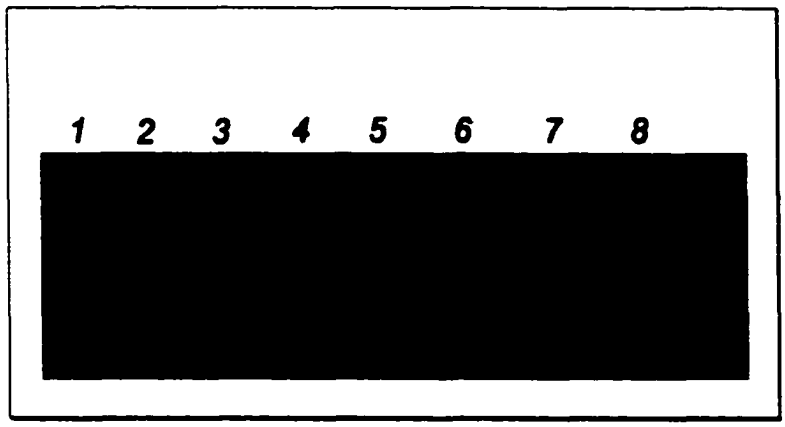

B.

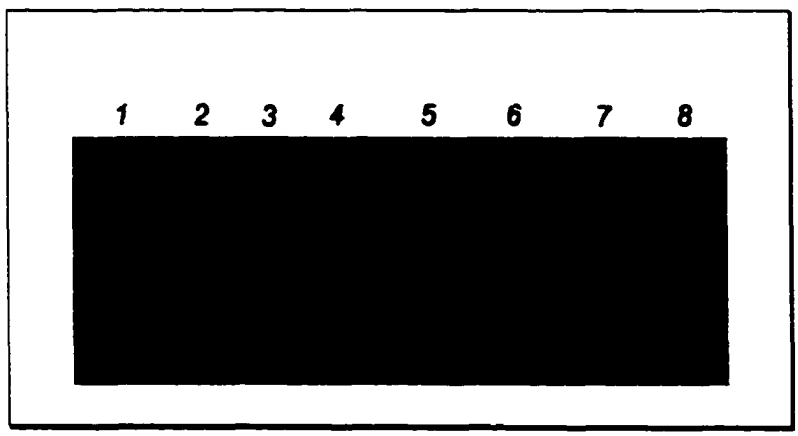

Figure 5.3. Sulfo-EGS cross-linking of FepA lysine mutants. A. Cell lysates in the absence and presence of cross-linking reagent respectively. lanes 1-2, KDF541; 3-4, KDF541/pITS23; 5-6 KDF541/pITS23/K467A; lanes 7-8, KDF541/pITS23/K681A. B. Cell lysates of KDF541/pITS23, lanes 1-4, and KDF541/pITS23/K483A lanes 5-8, in the absence of crosslinker, lanes 1,5; in the presence of cross-linker, lanes 2, and 6; in the presence of ferric enterobactin and absence of cross-linker, lanes 3 and 7; in the presence of ferric enterobactin and cross-linker, lanes 4 and 8.

Atomic Distance from K483 to:

Distance	Residue
20.9	A212
23.9	Q335
19.3	V643
19.5	Q641

Figure 5.4. Location of lysine 483 (red) in the crystal structure, and atomic distances (in angstroms) between the alpha carbon of it and amino acid residues at the external rim of the surface loops.

of the outer membrane the surface loops of FepA adopt an extended conformation. The extended conformation places the reactive residue within cross-linking distance of neighboring proteins in the membrane bilayer, and upon binding of the ferric-siderophore the loops contract. Purification of FepA from its native environment of the outer membrane may result in collapse of the surface loops, explaining why no conformational change in the loops were observed in free and liganded crystal structures (Ferguson et al. 1998; Locher et al. 1998; Buchanan et al. 1998). Experiments with both FepA and FhuA had previously suggested that the conformation of the purified protein is different from that in its native environment, the exact details of this difference was not known (Zhou et al. 1993; Zhou et al. 1995; Locher and Rosenbusch 1997; Payne et. al. 1999; Cao et al. 2000). For example, binding of ferric enterobactin by purified FepA is seventy-five fold increased from binding of the siderophore by live cells (15nM and 0.2nM respectively; Zhou et al. 1993; Zhou et al. 1995; Payne et. al. 1999; Newton et. al. 1999; Cao et al. 2000). Similar conclusions were drawn when two independent methods of ferrichrome binding by purified FhuA were reported (Locher and Rosenbusch 1997). The cross-linking results provide the first direct indication that cell surface loops collapse upon solubilization of the receptor from its native membrane environment.

5.4 Determination of Protein Content in Cross-linked Bands 1 and 2

An added advantage of using Sulfo-EGS in cross-linking investigations of FepA is that the cross-linker is cleaveable upon incubation with hydroxylamine (Abdella et. al. 1979). Therefore, upon generation of cross-linked products they can be isolated and cleaved to produce the individual components of the cross-linked complex. The cleaved products are then analyzed by SDS-PAGE, and N-terminal sequencing, to assign identity to the components of the cross-linked products. Purification of cross-linked products by excision from SDS-PAGE gels of whole cell lysates was not possible, because numerous proteins were visible in coomassie stained SDS-PAGE, and would contaminate the retrieval of products directly out of the gel. To avoid these impurities, I cross-linked proteins from sucrose density gradient-purified outer membranes, because no detectable protein content was visible in lanes un-treated with cross-linking reagent (Figure 5.6).

5.4.1 Isolation and determination of the 120kDa Band 2

To identify the protein components of crosslinked band 2, preparative scale cross-linking reactions were performed on outer membranes and electrophoresed on trough gels. After staining with coomassie blue, the 120 kDa band was excised from the gel matrix with a razor blade, and the gel sliver was incubated in the presence of hydroxylamine to cleave the cross-linking reagent. The cleaved products were electroeluted from the gel matrix and re-electrophoresed. The

cleaved and electroeluted cross-linked product yielded three protein components upon re-electrophoresis (Figure 5.6). In addition to FepA, two of the most abundant outer membrane proteins were also present, OmpA and OmpF/C, as determined by Edman degdradation of their N-termini. The discrepancy in the concentrations of FepA, OmpF/C, and OmpA in lane 3 of Figure 5.5 occurs because the molecular weight of FepA (81kDa) is almost three fold higher than the molecular weights of OmpF/C and OmpA. Accordingly, in SDS-PAGE of a dissociated 1:1 complex of FepA:OmpA, for example, a nearly three fold lower intensity for the OmpA band is expected. The results suggested that, when unbound, the surface loops of FepA adopt an extended "open" conformation that is within crosslinking distance of the two other major outer membrane proteins. Upon binding of ferric enterobactin, the surface loops coalesce or "close" around the ferric-siderophore complex, and the conformation of the closed complex moves the surface loops farther from OmpF/C and OmpA than the spacer arm of the cross-linking reagent can reach, thus preventing complex formation. Presumably the crystal structure of FepA captured the closed complex, that closely imitates the bound form of the receptor.

5.4.2 Isolation and determination of the 100kDa Band 1

In procedures identical to those used for determining the protein content of Band 2, the only protein product observed after cleavage and re-electrophoresis of

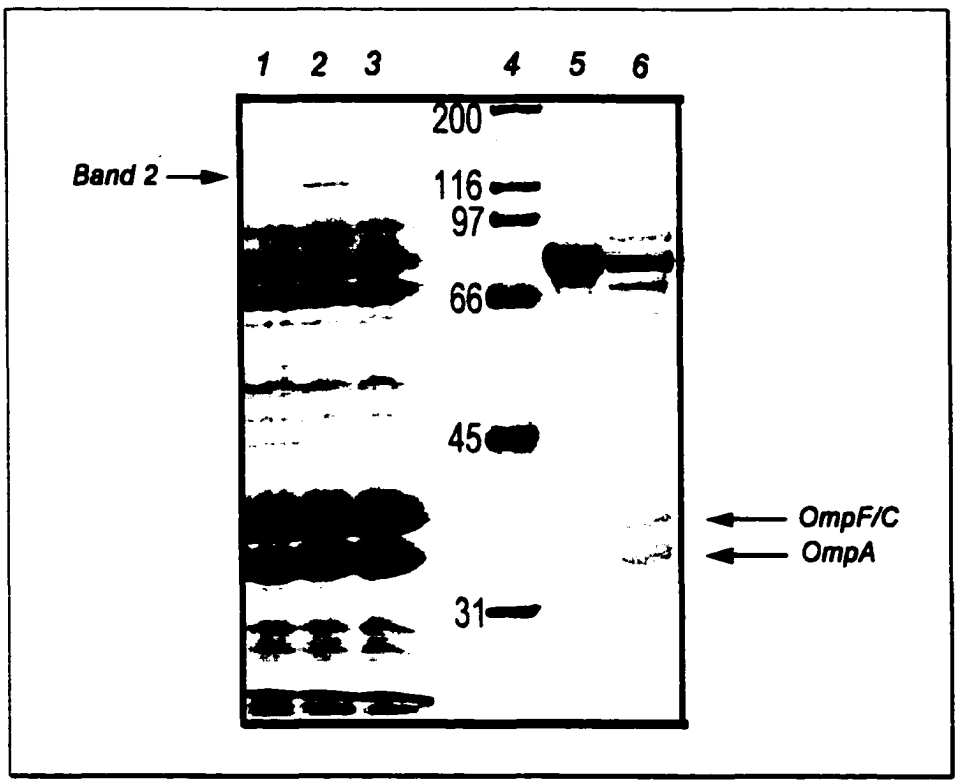

Figure 5.5. Protein content of cross-linked band 2. Outer membranes from KDF541/pITS23 were subjected to cross-linking and visualized by staining with coomassie blue. Lane 1, no cross-linking; lane 2, cross-linked; lane 3, cross-linked in the presence of ferric enterobactin. Lane 4, molecular weight standards. Lane 5, purified FepA. Lane 6, Band 2 in lane 2 was cut from the gel and cross-links cleaved by incubation with hydroxylamine and re-electrophoresed.

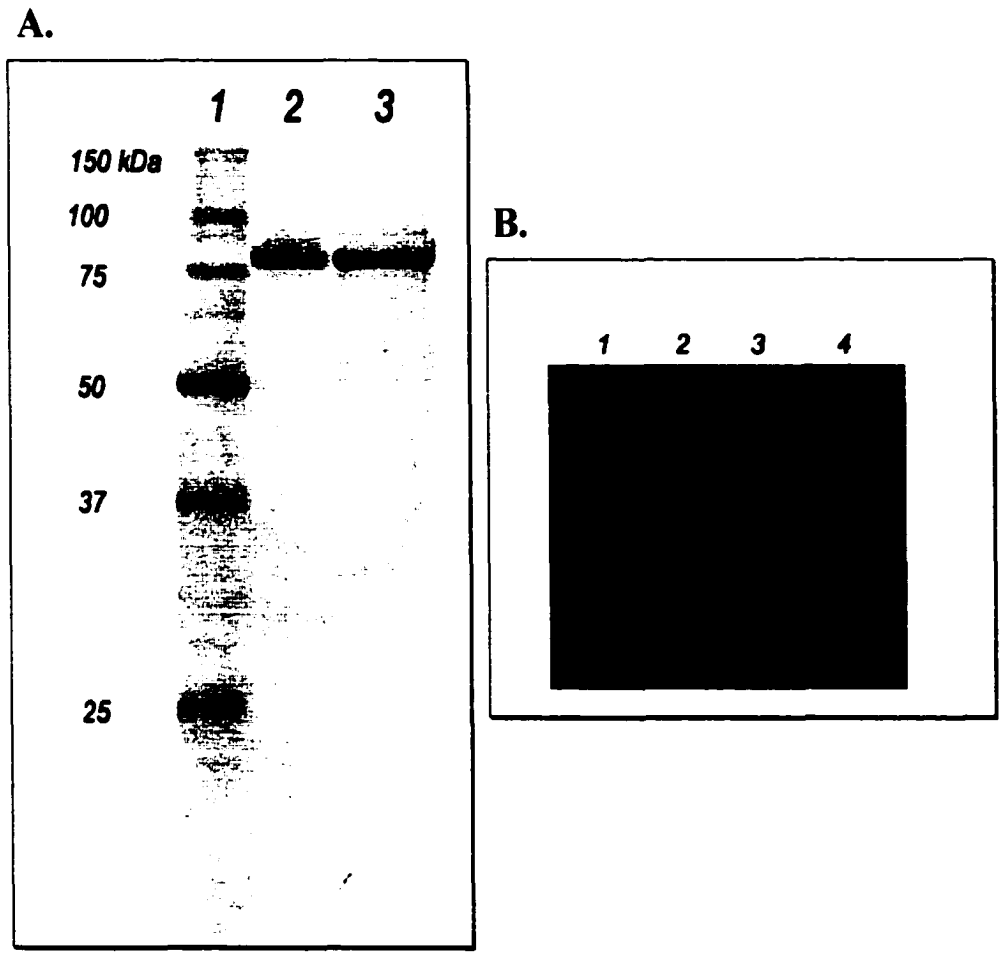

Figure 5.6. Protein content of Band 1. A. Commassie Blue stained gel of molecular weight standards and purified FepA, lanes 1 and 2 respectively. Lane 3 is the re-electrophoresis of band 1 from outer membrane cross-linking reactions after cleavage with hydroxylamine. B. Western blot of cell lysates from KDF541/pITS23, lanes 1-2, and KDF541/pITS23/pMF19, lanes 3-4. In the absence, 1 and 3, and presence, 2 and 4, of cross-linking reagent.

cross-linked band 1 was FepA (Figure 5.6). There were sufficient quantities of FepA in the dissociated complex to allow for the visualization of an approximately 20 kDa protein in SDS-PAGE gels, yet only FepA was observed (Figure 5.6). Indicating that the other component of the 100kDa complex was not proteinaceous. If the 100kDa cross-linked complex does not consist of FepA linked to another outer membrane protein, then what are its components? One possible explanation is that the reactive lysine on FepA is cross-linked to lipopolysaccharide, the primary component of the outer leaflet of the outer membrane. Alternatively, it is possible that FepA is cross-linked to itself, and this internal link, upon denaturation, produces an anomalous migration in SDS-PAGE.

Escherichia coli K-12 strains and derivatives used in the laboratory contain lesions in the biosynthetic pathway for producing full length LPS molecules on the surface of the outer membrane. Hence, strains contain only a portion of the LPS molecule (Lipid A and KDO core), and are commonly referred to as rough strains. Introduction of the plasmid pMF19, which codes for a functional rhamnosyltransferase essential for O16 synthesis (Feldman et. al. 1999), the host strain synthesizes full length LPS and becomes smooth. The full length polysaccharide coat of LPS varies from 100 to 200, giving it a much greater molecular weight (18,000 to 36,000 kDa) than rough LPS. I performed cross-linking studies on strains harboring the pMF19 plasmid, and analyzed them for an increase in the molecular weight of band 1 (Figure 5.6). But this was not the case;

the cross-linking pattern of cells expressing the pMF19 plasmid showed no increase in the molecular weight of band 1, indicating that the cross-linked product was not a FepA:LPS complex.

Proteins migrate in SDS-PAGE on the basis of size and shape. Extended or non-spherical shapes of proteins may cause anomalous migration patterns, in which the protein does not run corresponding to its molecular weight. This phenomenon was observed for one of the components of the ferric-siderophore transport system, TonB. The central region of TonB contains a $(Glu\text{-}Pro)_n$-$(Lys\text{-}Pro)_m$ repeat motif, that was shown by NMR studies to assume an extended linear conformation (Brewer et. al. 1990). The deduced amino acid sequence of TonB predicts a protein of approximately 26 kDa in size. However, in SDS-PAGE TonB migrates to a position of approximately 36-40 kDa in molecular weight. The anomalous migration is attributed to the extended repeat motifs, and deletion of them reverts the anomalous migration pattern (Larsen et. al. 1993). A similar phenomenon may occur if internal cross-links form within FepA. Experimental evidence for this idea may come from mutagenesis of the other participant lysine residue that forms internal cross-links with K483. However, the task of discovering this residue is once again daunting, due to the number of lysine residues cell surface accessible in FepA. One could target those lysine residues within 16 Å of K483 for mutagenesis, since this residue is known to participate in forming cross-links. However, without knowledge of the precise differences in the conformation

of cell surface loops *in vivo* and in the crystal structure, the selection of such residues is complicated. Nevertheless, I targeted eleven additional lysine residues for mutagenesis, and evaluated their cross-linking profiles: K167A, K328A, K332A, K375A, K406A, K503A, K535A, K560A, K634A, K635A, and K639A (Table 5.1). All of the lysine mutations retained wild type colicin killing and siderophore nutrition assays (Table 5.1). Cross-linking profiles of these mutant receptors showed no observable difference from the wild-type profile, indicating they do not constitute the proposed partner with K483 in forming internal FepA cross-links (Figure 5.7). A more exhaustive approach, in which all FepA lysine residues are individually mutagenized, may identify another participant lysine residue in the proposed internal crosslinks, but that experiment is beyond the scope of this thesis.

5.5 Cross-linking of FepA mutants and chimeric proteins

Cross-linking studies in the presence and absence of ferric enterobactin, combined with the elucidation of the participant lysine residue involved, supported the previous conclusion that conformational changes are an important aspect of the ligand binding process. Two conformations of the receptor protein were observed; an open unbound receptor, and a bound closed receptor. The cross-linking profile is therefore indicates unique loop conformations in both the bound and unbound state. To determine if loop conformations were altered in either FepA mutant or

A.

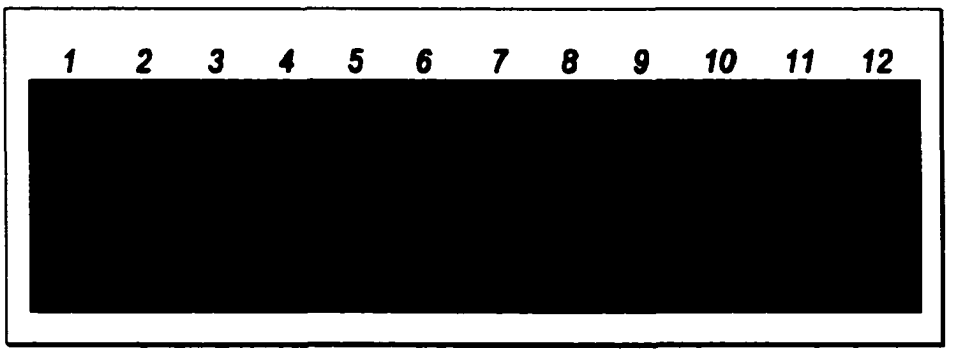

B.

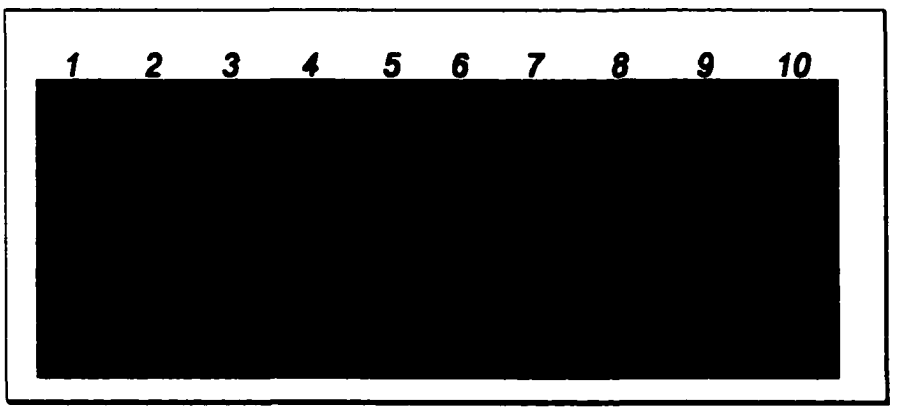

Figure 5.7. Cross-linking of FepA lysine mutants. Panel A. Cell lysates in the absence (lanes 1,3,5,7,9,11) and presence (lanes 2,4,6,8,10,12) of cross-linking reagent. Lanes 1and 2, KDF541/pITS23/K167A; lanes 3 and 4, KDF541/pITS23/K328A; lanes 5 and 6, KDF541/pITS23/K332A; lanes 7 and 8, KDF541/pITS23/K375A; lanes 9 and 10, KDF541/pITS23/K406A; lanes 11 and 12, KDF541/pITS23/K503A. Panel B. Cell lysates in the absence (lanes 1,3,5,7, and 9) and presence (lanes 2,4,6,8, and 10) of crosslinker. Lanes 1 and 2, KDF541/pITS23/K535A; lanes 3 and 4, KDF541/pITS23/K560A; lanes 5 and 6, KDF541/pITS23/K634A; lanes 7 and 8, KDF541/pITS23/K635A; lanes 9 and 10, KDF541/pITS23/K639A

chimeric constructions, we analyzed their cross-linking profile. Initial cross-linking studies with FepA loop deletions, which were intended to narrow the search for the participant lysine residue, validated this approach. For example, deletions of loops 2, 4, and 8 resulted in no cross-linked products, despite containing no lysine residues within these amino acid deletions. Quantitative binding assays of these loop deletions showed that, for Δ2 and Δ11, the binding affinity of FepA for ferric enterobactin was decreased 7,000 and 1,000 fold respectively, and binding was completely destroyed upon deletion of loop 8 (Newton et. al. 1999). When combined, the binding affinity and cross-linking profile of these deletions suggest that these loops are important in maintaining the structural integrity of the open conformation.

When Fepβ was subjected to cross-linking with Sulfo-EGS, band 2 was abolished and the amount of band 1 is greatly reduced (Figure 5.8). In fact, the cross-linking profile of Fepβ was remarkably reminiscent to cross-linking reactions of the wild-type receptor in the presence of ferric enterobactin (compare lane 6 with lane 8 in Figure 5.8). In addition, the amount of band 1 remaining in Fepβ cross-linked cells is approximately 5-10% of the quantity observed in wild-type cells. The results physically define the importance of the N-domain in siderophore binding. Receptors with deletions to the N-domain adsorbed siderophores at much lower capacities than the wild-type receptor (Table 4.1), leading to the conclusion that only 5-10% of the deletion clones were functional. Cross-linking studies of the

plug-less FepA construct explain this conclusion, in that, insertion of the plug domain functions to optimize and extend cell surface loops into the open conformation. Such an effect may occur by protein•protein interactions between the globular domain and the barrel or alternatively the loops themselves, promoting the formation of the open conformation. Cross-linking reactions with chimeric constructions of FepA and FhuA corroborated this conclusion. Insertion of the correct N-domain is necessary for optimal binding and hence formation of band 2 in the cross-linking reaction (Table 4. 1; Figure 5.8).

5.6 Activity of Cross-linked FepA: Binding of Ferric Enterobactin

Cross-linking studies of FepA defined two separate conformational states of the receptor, and the importance of the N-domain in defining them yet the experiments did not define the importance of these conformational states in binding and transport. For example, in the open state, is receptor closing required to promote binding, or is simply the formation of the open state sufficient? Binding studies of cross-linked receptors discriminated between these two possibilities. When cross-linked, FepA is presumably locked into the open conformation by covalent modification to OmpA or OmpF/C, and unable to close upon the addition of ferric enterobactin. Analysis of the binding data is complicated by the presence of approximately one-third of the wild-type protein that remains upon treatment of cells with Sulfo-EGS (Figure 5.1). However, a comparison of the binding of wild-

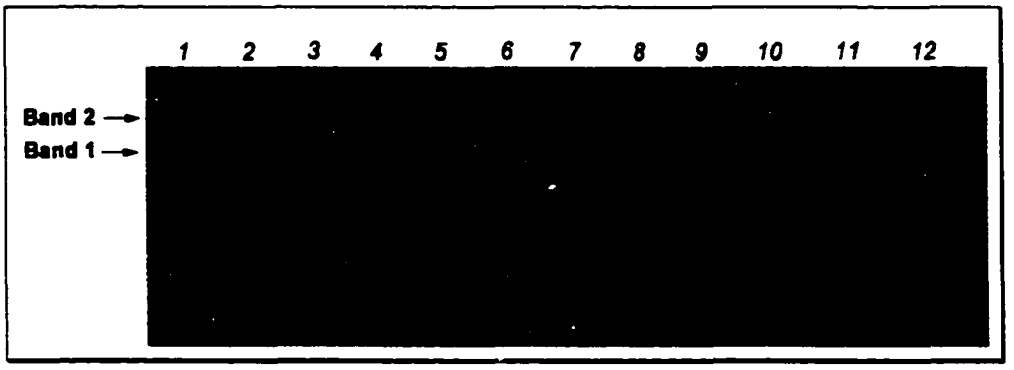

Figure 5.8. Sulfo-EGS cross-linking of deletion and chimeric clones. Western blot developed with a cocktail of α-FepA mABs 26 and 4. Cell lystaes of KDF541/pFepNFhuβ (lanes 1-3), KDF541/pITS23 (lanes 4-6), KDF541/pFepβ, or KDF541/pFhuNFepβ (lanes 10-12) were either untreated (lanes 1, 4, 7, and 10), or cross-linked with Sulfo-EGS in the absence (lanes 2, 5, 8, and 11) or presence (lanes 3, 6, 9, and 12) of 5μM FeEnt.

type and mutant cells that were cross-linked in the presence and absence of ferric enterobactin give some indication of the ability of the cross-linked products to bind ferric enterobactin (Table 5.2). When analyzed in binding assays, cross-linked cells displayed a sixty fold lower binding affinity for ferric enterobactin with a fifty percent drop in capacity (Table 5.2; Figure 5.9). Binding measurements of the cross-linked K483A mutant, which produces no observable cross-links, results in a eighty-seven fold decrease in the binding affinity with no change in the capacity levels (Table 5.2; Figure 5.10). Amino acid residue K483 is itself involved in the binding reaction, as this mutant shows an eleven fold loss of affinity for ferric enterobactin (Figure 5.10). The eighty-seven fold decrease in the binding affinity of mutant cross-linked samples is due to a combinatory affect. The K_d is increased by mutation of the K483 residue itself, and also by the formation of non-productive cross-links to FepA. By definition, non-productive cross-links are those that derivatize one lysine residue of FepA, but the second reactive group of the cross-linking reagent does not react with another lysine residue. These non-productive cross-links affect the binding reaction by placing the bulky cross-linking reagent on the cell surface, presumably blocking numerous binding residues. Cross-links that are non-productive would not appear in western blots of the cross-linked mutant unless 5-10 occur because the molecular weight of the cross-linking reagent is only 647 Da. The number of non-productive cross-links is low (<3) since no shift in the molecular weight of FepA K483A was observed in cross-linked

Strain	*Capacity*	K_d *(nM)*	*Fold Decrease (WT)*	*Fold Decrease (Mutant)*
pITS23	50	0.13	0	-
pITS23 X-Linked	25	8	60	-
pITS23 + Ent.	53	0.2	0	-
pITS23 + Ent. X-linked	20	0.8	6	-
pITS23 K483A	47	1.3	12	0
pITS23/K483A X-linked	45	11.4	87	8
pITS23/K483A + Ent.	47	1.4	10	0
pITS23/K483A + Ent. X-linked	38	1.5	10	0

Table 5.2 Adsorption of ferric enterobactin to wild-type and K483A mutant FepA cells cross-linked in the presence and absence of FeEnt.

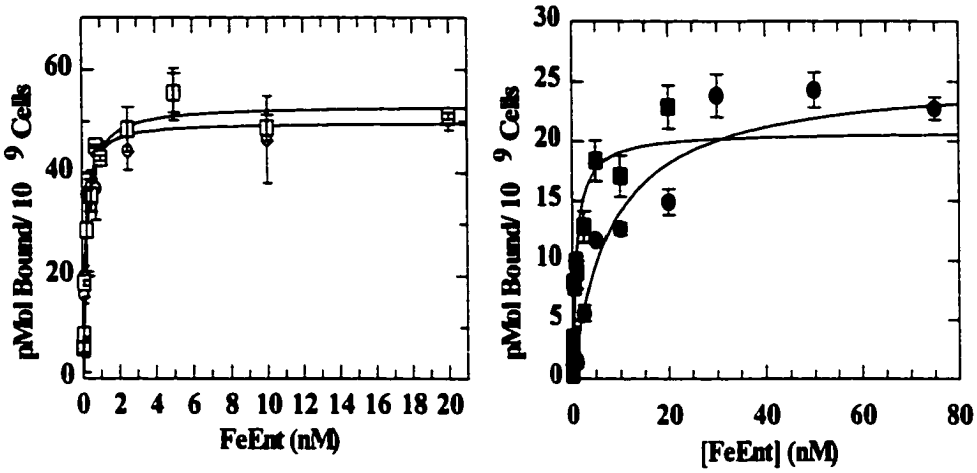

Figure 5.9. Ferric Enterobactin binding by cross-linked cells. The adsorption of [^{59}Fe]Ent was measured with metabolically inactive KDF541 expressing pITS23 without (open symbols) or with cross-linking (closed symbols) either in the absence (O) or presence ferric enterobactin (□) during the cross-linking reaction.

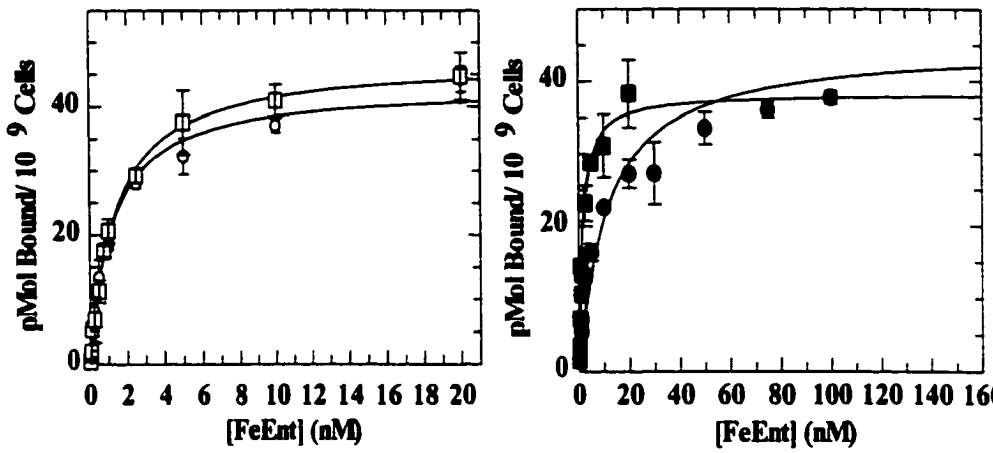

Figure 5.10. Ferric Enterobactin binding by FepA K483A cross-linked cells. The adsorption of [^{59}Fe]Ent was measured with metabolically inactive KDF541 expressing pITS23/K483A without (open symbols) or with cross-linking (closed symbols) either in the absence (O) or presence ferric enterobactin (□) during the cross-linking reaction.

samples (Figure 5.3). In contrast, when cells were cross-linked in the presence of ferric enterobactin the binding properties are virtually indistinguishable from the wild-type protein, indicating that the non-productive cross-links are protected by ferric enterobactin binding. Taken together, the results suggest that the K_d of the wild type receptor increases some 60-65 fold upon the formation of non-productive cross-links, and for the mutant K483A, this value increases to 85 fold upon the addition of the 12 fold increase for mutation to the K483 residue. The cross-linked products observed in SDS-PAGE at 100 and 120 kDa respectively appear to have a very low, if any, binding affinity for ferric enterobactin. The inability of the open conformation to bind ferric enterobactin suggests the conformational change that occurs upon receptor closing is required for binding.

5.7 Activity of Cross-linked FepA: Colicin Killing by ANS fluorescence

The ability of the cross-linked FepA species to function in colicin binding and uptake was investigated through the use of a fluorescence killing assay. The assay utilizes the fluorescent probe 8-anilino-1-napthalenesulfonic acid (ANS), whose fluorescent emission properties are sensitive to the energized state of the cell (Helgerson and Cramer 1976; Nieva-Gomez and Gennis 1977). The fluor experiences an increased binding affinity for membranes upon de-energization of the cell, resulting in an enhanced fluorescence (Nieva-Gomez and Gennis 1977). Colicin B, a member of the pore-forming family of toxins, implements its cytotoxic

activity by insertion of a pore-forming domain into the inner membrane of *E. coli*. Thus, changes in the fluorescence profile of ANS-treated cells monitors the rate of colicin B dependent de-energization of *E. coli*. When cells expressing FepA were treated with colicin B, a linear increase in the fluorescence intensity of ANS was observed (Figure 5.11). The increase in fluorescence was due to both the energetic state of the cell, and the FepA-dependent translocation of colicin B across the outer membrane: *fepA*$^-$ cells showed no increase in ANS fluorescence upon the addition of colicin B. However, subsequent addition of azide, an energy uncoupler, did cause enhancement of ANS fluorescence (Figure 5.11). The change in fluorescence with respect to time during the linear increase reflects the relative rate of colicin killing. It is of importance to note that the assay does not directly measure transport of colicin B by FepA, but the overall killing reaction. Nonetheless, when comparing mutant and cross-linked FepA, it is only these alterations to FepA that change the overall reaction scheme. Therefore, a comparison of the slope obtained for the change in fluorescence versus time of FepA, mutant derivatives, and cross-linked cells reflects the relative efficiency of these constructs in the recognization and transport of colicin B.

When cross-linked cells were exposed to colicin B an 11-fold decrease in the killing rate occurred: The rates of killing for wild-type and cross-linked cells were 110 $\Delta F/\Delta s$ and 10 $\Delta F/\Delta s$ (Table 5.3; Figure 5.11), respectively. To determine if crosslinked FepA still recognized and transported colicin B, comparisons of the

killing rates between wild-type and the non-productive cross-linking mutant, K483A, were initiated. The mutant receptor displayed a two fold reduction in the killing rate relative to the wild-type protein; rates of 50 $\Delta F/\Delta s$ and 110 $\Delta F/\Delta s$ respectively (Table 5.3; Figure 5.12). This reduction in colicin killing of the mutant receptor suggests that K483 participates in colicin B binding. The fact that K483 participates in ferric-enterobactin binding is consistent with this conclusion (Figure 5.10; Table 5.1). When subjected to cross-linking prior to the colicin killing test, K483A exhibited an additional five fold decrease (Table 5.2; Figure 5.12). Both the wild type and K483A cross-linked samples showed the same rate of colicin killing, suggesting that the ten-fold rate reduction of the cross-linked wild-type receptor was due to the formation of non-productive cross-links. Furthermore, ferric-enterobactin binding protected the wild type but not K483A from the detrimental effects of the cross-linker (2-fold), suggesting that virtually 100% of the K483A residues in the wild-type receptor reacts with Sulfo-EGS, although not all form productive cross-links. The data reiterate conclusions derived from the binding studies of cross-linked samples: FepA, restricted to the open conformation by covalent cross-links, cannot efficiently transport colicin B. When combined, the phenotypic measurements of cross-linked FepA support the need for a conformational change to a closed conformation during the transport reaction.

Strain/Plasmid - Cross-linking Conditions	Rate of ANS Fluorescence Change ($\Delta F/\Delta s$)
KDF541	0
KDF541/pITS23	110
KDF541/pITS23 X-linked	10
KDF541/pITS23 + FeEnt X-linked	20
KDF541/pITS23/K483A	50
KDF541/pITS23/K483A X-linked	10
KDF541/pITS23/K483A + FeEnt X-linked	9

Table 5.3. Colicin B killing rates for wild type and K483A mutant cells cross-linked in the presence or absence of ferric enterobactin.

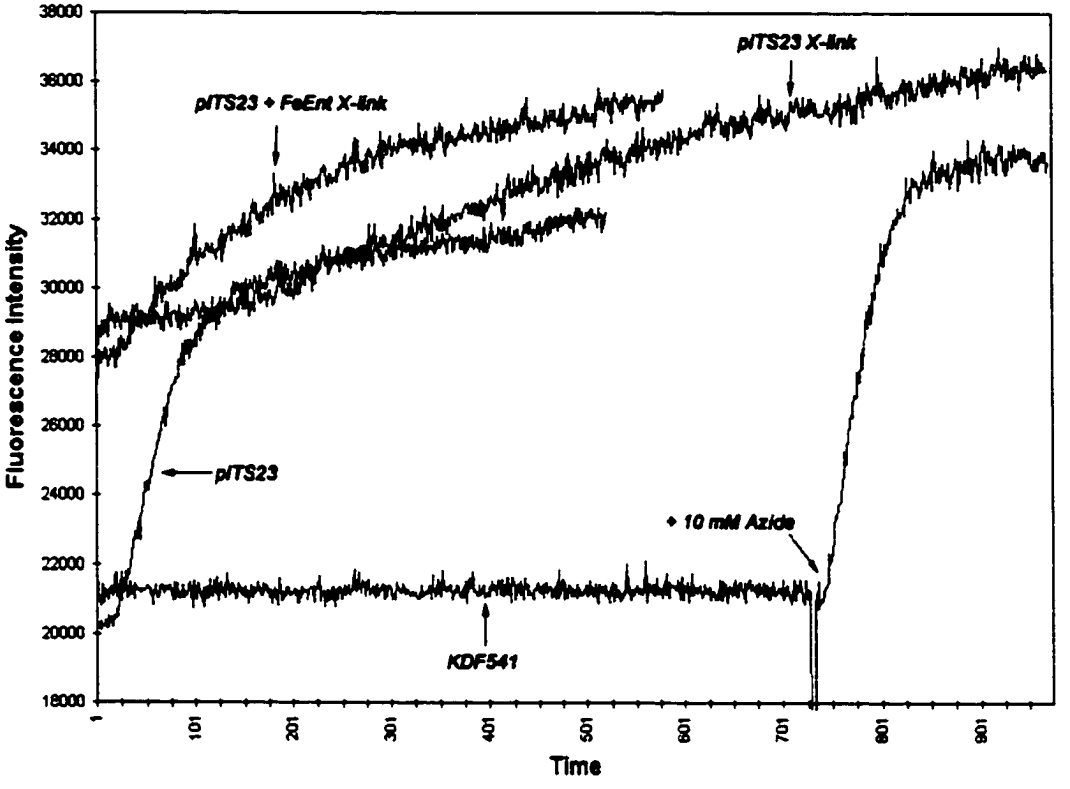

Figure 5.11. Colicin B killing of KDF541 cells expressing pITS23 cross-linked in the presence and absence of FeEnt, measured by ANS fluorescence.

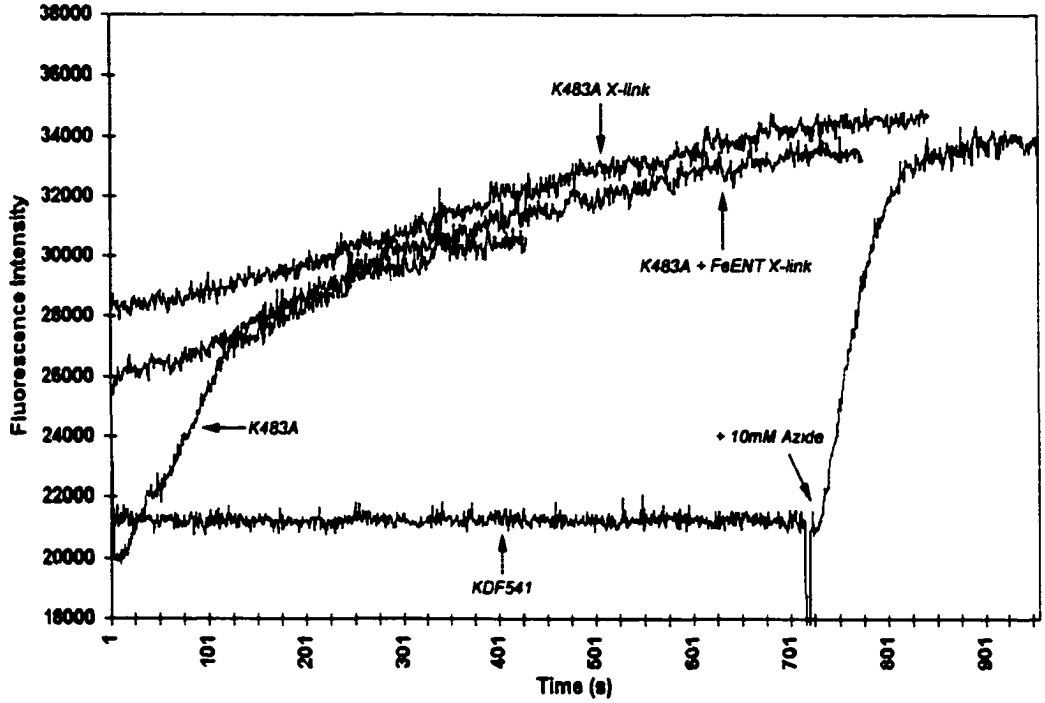

Figure 5.12. Colicin B killing of KDF541 cells expressing pITS23/K483A cross-linked in the presence and absence of FeEnt, measured by ANS fluorescence.

5.8 Effect of energy inhibitors on the cross-linking profile

The energy and TonB dependence of siderophore transport was recognized some thirty years ago (Pugsley and Reeves, 1977; Bradbeer, 1993), yet, the nature and involvement of these two factors in the transport process remains obscure and controversial. For example, TonB is commonly referred to as an energy transducer, even though no experiments directly link TonB with energy. The Sulfo-EGS cross-linking profile was independent of the presence of TonB; I studied the cross-linking profile in the presence of energy inhibitors, in order to obtain a better understanding of the TonB and energy dependence of FepA function. Transport across the outer membrane depends on cytoplasmic membrane-derived proton-motive force (PMF: Bradbeer 1993). Accordingly, I investigated cross-linking in the presence of PMF-deflating reagents. These so-called proton-ionophores deflate PMF by moving protons in the periplasmic space across the inner membrane, into to the cytoplasm. Two such PMF deflating agents, 2,4-dinitrophenol (DNP) and carbonyl cyanide m-chlorophynylhydrazone (CCCP), produced no differences in the cross-linking profile (Figure 5.13). ATP synthase directs ATP formation by catalyzing the reaction between ADP and inorganic phosphate. The energy required for this reaction derives from the ability of ATP synthase to utilize the periplasmic proton gradient. Alternatively, in times of need, ATP synthase may work in the reverse direction, hydrolyzing cellular ATP pools to produce a proton-gradient (Bradbeer 1993). Thus, the reverse action of ATP synthase may generate short-lived proton

gradients even in the presence of PMF deflating reagents. To eliminate this possibility and assure PMF deflation, the cross-linking reactions were performed in an *unc*$^-$ background. Historically, ATP synthase mutants were referred to as uncoupled or *unc* mutants, because the mutation in ATP synthase uncoupled oxidation from phosphorylation. The cross-linked profile remained unaltered when experiments were performed in a *fepA*$^-$ *unc*$^-$ background (ANC11; Table 2.1), in the presence of either DNP or CCCP (Figure 5.15). The results suggest, but do not rule out, that energy input is not necessary for attaining the "open" binding competent state. The possibility that PMF is involved still remains because, in these experiments the cells were depleted of energy after synthesis and presumably insertion of FepA into the outer membrane. With this view, attaining the "open" state upon insertion into the membrane is dependendent on PMF, but not necessary for maintaining it.

Analogous to the flow of water being restricted by a dam, inhibitors of the electron transport chain (potassium cyanide and sodium azide) block the production of the energized membrane state by interfering with cellular respiration. In a continued search for energy poisons that alter the cross-linking profile, I tested the ability of two inhibitors of the electron transport chain to affect cross-linking. Cyanide and azide both block oxidative phosphorylation by reacting with the reduced form of cytochrome oxidase. When treated with azide prior to cross-linking, the amount of band 1 was significantly reduced with a concomitant

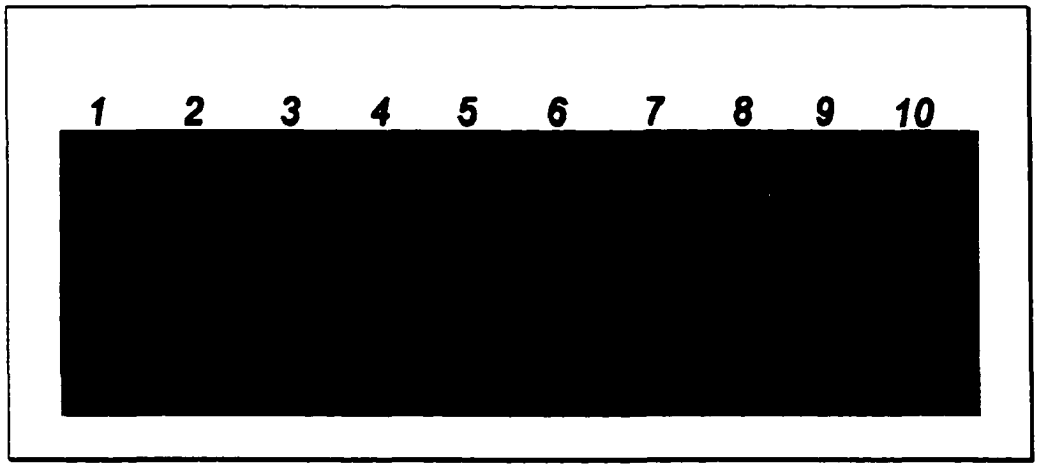

Figure 5.13. Cross-linking in the presence of energy inhibitors. KDF541/pITS was treated with energy inhibitors and either untreated (lanes 1,3,5,7, and 9), or cross-linked with sulfo-EGS (lanes 2,4,6,8, and 10). Lanes 1 and 2, no energy inhibitor present; lanes 3 and 4, 20mM cyanide; lanes 5 and 6, 0.1mM CCCP; lanes 7 and 8, 2mM DNP; lanes 9 and 10, 10mM Azide.

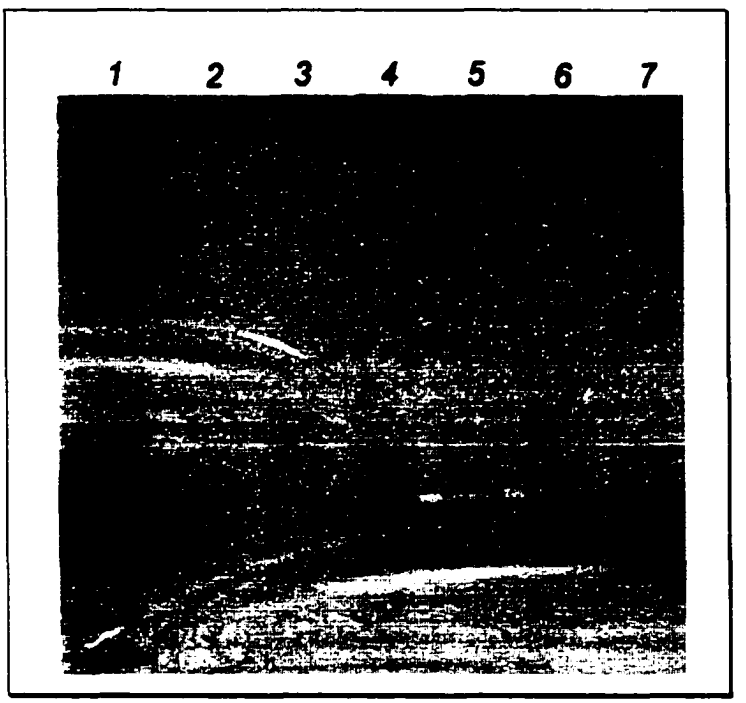

Figure 5.14. Suflo-EGS crosslinking of purified bovine serum albumin in the presence and absence of energy inhibitors. Twenty-five micrograms of BSA was untreated (lane1), or cross-linked in the absence (lane 2) or presence of. Lane 3. 20mM Cyanide; lane 4. 0.1mM CCCP; lane 5. 2mM DNP; lane 6. 10mM Azide; lane 7. 100mM Azide.

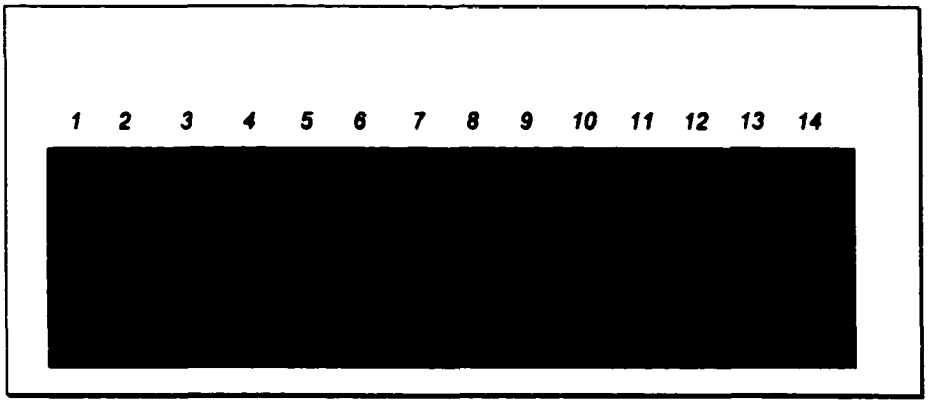

Figure 5.15. Sulfo-EGS cross-linking of FepA in the presence of energy inhibitors in a unc background. ANC718 (lanes 1 and 2) or ANC718/pITS23 (lanes 3-14) were untreated (lanes 1, 3, 5, 7, 9, 11, and 13) or cross-linked (lanes 2, 4, 6, 8, 10, 12, and 14) with Sulfo-EGS in the presence of 0.1mM CCCP, lanes 3 and 4; 1mM CCCP, lanes 5 and 6; 2mM DNP, lanes 7 and 8; 100mM DNP, lanes 9 and 10; 10mM Sodium azide, lanes 11 and 12; 100mM Sodium azide, lanes 13 and 14.

increase in the amount of band 2 (Figure 5.13). In contrast, when pre-treated with cyanide, band 2 was completely abolished, with a slight reduction in the amount of band 1 (Figure 5.13). To rule out the possibility that the energy poison itself interferes or reacts with the cross-linking reagent, purified bovine serum albumin (BSA) was cross-linked in the presence and absence of the energy inhibitors (Figure 5.14). Although a slight inhibition of BSA cross-linking was observed (<5%), the extent of direct inhibition by the energy poison was minimal when compared to the reduction observed in live cells. Furthermore, a concomitant increase of band 2 in the presence of azide, and similar amounts of band 1 in presence and absence of cyanide suggest that alterations to the cross-linking profile are specific to the energy state of the cell rather than a direct affect to K483 in the cross-linking reaction.

Chapter 6

Discussion

The acquisition of iron is essential for sustaining microbial growth and pathogenicity. In order to overcome the environmental limitations for obtaining this nutritional necessity, bacteria have evolved specialized and elaborate pathways for obtaining it. The siderophore receptors of the Gram-negative bacterial outer membrane are one such example. These receptors avidly bind and actively transport ferric-complexes across the outer membrane. However, a description of their selectivity, recognition, and transport of the iron-bearing ligand have remained

elusive. In addition, the role of an essential inner membrane protein, TonB, in the transport process remains ambiguous and enigmatic.

Studies with the C-terminal domain of TonB preceded the solving of its crystallographic structure (Chang et. al. 2001), however the structure allows a critical analysis of the information obtained. The C-terminal domain of TonB crystallized as a homo dimer, and it remains unclear if this dimeric structure is physiologically relevant or a product of the purification/crystallization procedures. Past studies of C-terminal truncations appear to agree with the dimeric structure (Anton and Heller 1991). In these studies, deletion of the C-terminal eight amino acids of TonB had no effect on function whereas deletion of the terminal fifteen amino acids abolished function. In the crystal structure, the C-terminal fifteen amino acids of TonB is part of a 4 stranded β-sheet that stabilizes the dimeric form (Figure 1.4). Deletion of the amino acids included in this β-strand would indubitably disrupt formation of the dimeric complex, suggesting that TonB functions in the dimeric state. In this respect, it is easy to conceive how expression of the C-terminal domain in the periplasam could inhibit TonB function in a wild type background, forming non-functional mixed dimers between the fragment and full-length TonB. This conclusion is supported by the recent observation of others that expression of similar C-terminal portions of TonB inhibit ferrichrome uptake (Howard et. al. 2001). Alternatively, the C-terminal fragment may compete with the wild type protein for interaction with a component of the transport system. The

fluorescent spectroscopic description of tryptophan 213 agrees quite well with its position in the crystal structure. Denaturant unfolding and quenching studies suggest that W213 is located within a hydrophobic pocket of the protein structure with neighboring basic amino acids in this region. Indeed, W213 of the C-domain is within this exact environment of the protein in the crystal structure (Figure 6.1).

A description of the TonB dependency to the siderophore transport reaction, to date, remains elusive. Studies with TonB69C and N-domain deletions of FepA and FhuA bore some relevance to this issue. Specifically, concepts of transmembrane signaling and physical interactions between TonB siderophore receptors, through a region of sequence homology at their N-termini, are misleading. Transport of siderophores by the empty barrels of FepA and FhuA, which do not contain these regions, undermine these ideas. In addition, the interaction of the C-terminal domain of TonB with the non TonB-dependent porin OmpA suggests TonB possesses a general affinity for outer membrane proteins. This interaction may occur at the rim of the periplasmic face of outer membrane proteins, or alternatively with their β-barrel domains. The partitioning of TonB into the outer membrane, and the spontaneous insertion of TonB69C into liposomes may suggest that this interaction occurs within the lipid bilayer of the outer membrane. Outer membrane protein β-barrels share strong homology within their transmembrane segments which could explain the general affinity of TonB for all classes of outer membrane porins. This view is supported by the dimeric

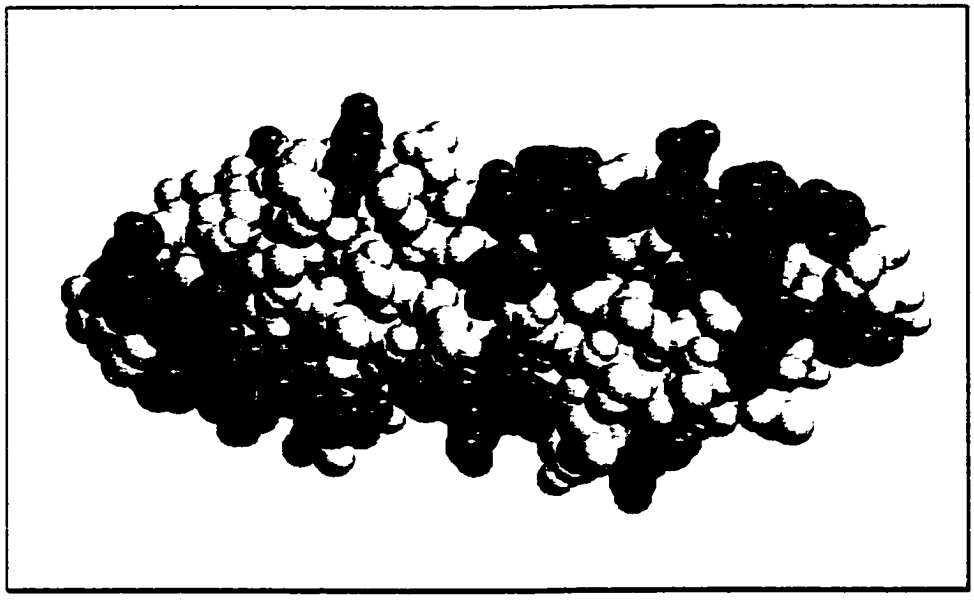

Figure 6.1. Crystal Structure of the C-terminal domain of TonB depicting the relative position of W213 (red) in relationship to acidic (purple) and basic (green) amino acids.

structure of TonB, which is assuredly too large to enter and interact with residues within the channel formed by the β-barrel domain. It is tempting to propose, based on sequence homology between ExbB and MotA, that TonB rotates analogous to that of the flagellar motor, and this spinning creates regions of suction near the interface of the outer membrane and periplasmic space. This action may, in turn, promote the expulsion of the N-domain from the barrel domain opening a pore for the siderophore to pass. With this view, the reorientation of the N-domain upon siderophore binding may serve to appropriately position the N-domain for removal. The model would also alleviate stoichiometry concerns between TonB and siderophore receptors, as well as providing an explanation of the energy dependence. Experiments designed at observing this rotational motion of TonB may provide a better understanding of how this protein functions.

The crystallographic depictions of FepA and FhuA were able to describe the architectural organization of the siderophore receptors, but were unable to address pertinent questions regarding their function. For example, the siderophore receptors of the outer membrane discriminate between numerous iron-complexes that, despite similar size and chelation geometry, differ in charge and chemical composition. Does selectivity originate in cell surface loops, or from residues within the N-domain at the channel entrance? Direct contacts between N-domain residues and ferrichrome were observed in liganded structures of FhuA suggesting that the N-domain contributed to the selectivity and efficiency of siderophore

binding. However, equilibrium binding studies of mutant receptors lacking the N-domain unequivocally demonstrated that the selectivity, and affinity, derive from residues within the surface loops. The ability of Fepβ and Fhuβ to discriminate between ferric enterobactin and ferrichrome, and bind them with wild-type affinity confirms this point. The preserved subnanamolar binding affinity between the N-domain deletions and their respective iron-complex indicate that the N-domain does not participate in ligand recognition, and if it contributes to binding the interaction is secondary and minimal to the interaction with surface loops. In addition, the selectivity of N-domain deletions for protein toxins and bacteriophages further reiterate this point.

The complete obstruction of the channel formed by the β-barrel ensured that rearrangement or displacement of the N-domain was a necessity of the transport reaction. Energetic considerations led most to propose that the N-domain would alter its structure to form a substrate-customized pathway for the ligand to pass into the underlying periplasam. Conformational changes within the N-domain upon ligand binding superficially supported this view, as well as the idea of receptor signaling to TonB. Quantitative measurements of the transport kinetics of ferric-siderophore uptake by the chimeric constructions undercut the notion of substrate customized channels and strongly suggest the complete expulsion of the N-domain during the transport reaction. According to the view of substrate-customized channels, the chimeric protein FepNFhuβ could not transport ferrichrome since the

protein contains a N-domain that was adapted for the negatively charged catechol siderophore, ferric enterobactin, yet the chimera efficiently internalized the neutral hydroxamate siderophore, ferrichrome, with turnover numbers similar to the wild type protein. Furthermore, functionality of the empty barrels alone further implies the N-domain exits the barrel during the transport reaction. In fact, transport by the chimeric receptors suggests the opposite, siderophores enter through a non-specific route that is neither created or regulated by the N-domain. The expulsion of the N-domain from the barrel, contaminant with siderophore internalization, requires the breakage of numerous hydrogen and ionic bond interactions between the N-domain and barrel wall. This energetic barrier might explain the energy dependence of the transport reaction. Alternatively, the loss of hydrogen bond and ionic interactions may be compensated for by formation of new bonding interactions upon exposure of the domain to the periplasmic space. Evidence supporting complete removal of the N-domain during the transport reaction also explains the uptake of siderophore-antibiotic conjugates, which often double the size of the iron complex without affecting its uptake. A large diffusion channel comparable to those that exist in the empty barrels of FepA and FhuA are necessary to permit uptake of these Trojan horse antibiotics across the outer membrane.

If the N-domain does not participate in ligand selection or creation of a substrate-customized channel, then what is its function? We propose that the N-domain serves to promote optimal binding by compelling the surface loops to an

extended conformation that is optimized for maximal binding.. Acquiring this binding-optimized conformation is dependent upon insertion of the correct N-domain within the barrel. The reduced binding capacity of β-barrels without or with an aberrant N-domain substantiate this idea, as does the cross-linking profile of Fepβ. The direct role of the N-domain in obtaining the open conformation is unknown, but could occur by protein-protein interactions between the N-domain and the surface loops or alternatively the barrel itself. The presence of the globular N-domain within the channel may serve other purposes than simply optimizing the surface loops for binding. For example, it may aid in preserving the integrity of the permeability properties of the outer membrane. The bacterial outer membrane serves as a protective permeability barrier tolerating the diffusion of nutrients smaller than 600 Da, while preventing the diffusion of larger, toxic, hydrophobic molecules the bacterium may encounter in the intestinal tract of animals. The obstruction of the large channel, which when open would render the bacterium sensitive to detergents and the like, is a rational design for restricting diffusion across the channel. Other porins of the outer membrane use a similar strategy to restrict the permeability properties of the channel they form. The unique inward orientation of a single cell surface loop, the transverse (L3) loop, restricts the channel size in general and substrate-specific porins.

Despite numerous biophysical studies implicating the importance of loop dynamics in the binding and transport reaction, the crystal structure of FhuA

sparked controversy regarding this view. In structures of ferrichrome bound FhuA, no appreciable difference in cell surface loop conformation was observed. However, one must consider the conformation of the protein in its native environment of the outer membrane, free from the constraints of crystallography. Cross-linking studies of FepA provide more evidence for cell surface loop conformational changes. When exposed to Sulfo-EGS, FepA forms cross-links with the major outer membrane proteins OmpF/C and OmpA. Two conditions influenced the cross-linking profile; binding of ferric enterobactin and deletion of the N-domain. The results describe two conformational states *in vivo*: an unbound open receptor in which the surface loops are within close proximity of other outer membrane proteins, and a bound form with closed loops that do not cross-link with other proteins. The changes observed by cross-linking suggest the receptors possess a minimum of two conformational states when binding ferric siderophores. We addressed the possibilities that binding of ferric enterobactin blocks the reactive cross-linking reside and/or that it is located within the N-domain. The determination of lysine 483 as the reactive residue in the cross-linking reaction silences these objections, and unequivocally confirms loop dynamics despite the static picture surmised from the crystal structure. Due to the location of lysine 483 in the crystal structure and the spacer length of the cross linker used, one can only conclude that the *in vivo* conformation of cell surface loops are appreciably different from that depicted in the crystal structure. The crystal structure of FhuA

and FepA most likely imitate the conformation of the bound or "closed" receptor. Equilibrium binding studies with the purified receptors had previously raised the possibility that the conformation was altered upon solubilization from its native environment in the outer membrane. The one hundred fold increase in binding affinity for ferric enterobactin of the purified receptor is most assuredly due to an alteration in the conformational state of cell surface loops.

The importance of attaining the open state for functionality is realized upon activity measurements of the open cross-linked receptor. Restriction of FepA to the open conformation prevented it from binding ferric enterobactin or transporting colicin B. Thus, the receptor must obtain the open conformation by insertion of the N-domain and coalesce or close around the incoming ligand to promote transport. Closing of the loops is independent of the presence of TonB, indicating that this step of the transport process is not energy dependent. Experiments designed to investigate the cross-linking profile in the presence of energy inhibitors indicate that the energetic state of the cell may have some impact on the conformational state of the receptor. The precise details of the conformational state that FepA attains when cells are energy depleted is speculative at this time, nonetheless the results demonstrate for the first time that the TonB and energy dependence may be separated.

REFERENCES:

Abdella, R. M, Smith, P. K., and Royer, G.P. (1979). A new cleavable reagent for crosslinking and reversible immobilization of proteins. *Biochem. Biophys. Res. Commun.* **87**,734-742.

Ahmer, B. M., Thomas, M. G., Larsen, R. A., and Postle, K. (1995) Characterization of the exbBD operon of Escherichia coli and the role of ExbB and ExbD in TonB function and stability. *J. Bacteriol.* **177**(16):4742-4747.

Ames, G. F., and Spurich, E. N. (1976) Protein-protein interaction in transport: periplasmic histidine-binding protein J interacts with P protein. *Proc. Natl. Acad. Sci.* **76**(6):1877-1881.

Andersen, C., Bachmeyer, C., Tauber, H., Benz, R., Wang, J., Michel, V., Newton, S. M., Hofnung, M., and Charbit, A. (1999) In vivo and in vitro studies of major surface loop deletion mutants of the Escherichia coli K-12 maltoporin: contribution to maltose and maltooligosaccharide transport and binding. *Mol. Microbiol.* **32**(4):851-867.

Anton, M., and Heller, K. J. (1991) Functional analysis of a C-terminally altered TonB protein of Escherichia coli. *Gene* **105**(1):23-29.

Armstrong, S. K., Francis, C. L., and McIntosh, M. A. (1990) Molecular analysis of the Escherichia coli ferric enterobactin receptor FepA. *J. Biol. Chem.* **265**:14536-14543.

Armstrong, S. K., and McIntosh, M. A. (1995) Epitope insertions define functional and topological features of the Escherichia coli ferric enterobactin receptor. *J. Biol. Chem.* **270**(6):2483-2488.

Barnard, T. J., Watson, M. E., and McIntosh, M. A. (2001) Mutations in the Escherichia coli receptor FepA reveal residues involved in ligand binding and transport. *Mol. Micro.*. **41**(3):527-536.

Baumler, A. J., Norris, T. L., Lasco, T., Voight, W., Reissbrodt, R., Rabsch, W., and Heffron, F. (1998) IroN, a novel outer membrane siderophore receptor characteristic of Salmonella enterica. *J. Bacteriol.* **180**(6):1446-1453.

Beall, B., and Sanden, G. N. (1995) A Bordetella pertussis fepA homologue required for utilization of exogenous ferric enterobactin. *Microbiology* **141**(12):3193-3205.

Bearden, S. W., Staggs, T. M., and Perry, R. D. (1999) An ABC transporter system of Yersinia pestis allows utilization of chelated iron by Escherichia coli SAB11. *J. Bacteriol.* **180**(5):1135-1147.

Bell, P. E., Nau, C. D., Brown, J. T., Konisky, J. and Kadner, R. J. (1990) Genetic Suppression Demonstrates Interaction of TonB Protein with Outer Membrane Transport Proteins in Escherichia coli. *J. Bacteriol.* **172**(7):3826-3829.

Bejar, S., and Bouche, J. P. (1985) A new dispensable genetic locus of the terminus region involved in control of cell division in Escherichia coli. *Mol. Gen. Genet.* **201**(2):146-150.

Benz, R., Francis, G., Nakae, T., and Ferenci, T. (1992) Investigation of the selectivity of maltoporin channels using mutant LamB proteins: mutations changing the maltodextrin binding site. *Biochim. Biophys. Acta.* **1104**(2):299-307.

Bos C, Lorenzen D, Braun V. (1998). Specific in vivo labeling of cell surface-exposed protein loops: reactive cysteines in the predicted gating loop mark a ferrichrome binding site and a ligand-induced conformational change of the Escherichia coli FhuA protein. *J Bacteriol* **180**(3):605-13.

Bradbeer, C. (1991) Cobalamin transport in Escherichia coli. *Biofactors* **3**(1):11-19.

Bradbeer, C. (1993) The Proton Motive Force Drives the Outer Membrane Transport of Cobalamin in Escherichia coli. *J. Bacteriol* **175**(10) 3146-3150.

Braun, V., Gunter, K., and Hantke, K. (1991) Transport of iron across the outer membrane. *Biol. Met.* **4**(1):14-22.

Braun, V., and Herrmann, C. (1993) Evolutionary relationship of uptake systems for biopolymers in Escherichia coli: cross-complementation between the TonB-ExbB-ExbD and the TolA-TolQ-TolR proteins. *Mol. Micor.* **8**(2):261-268.

Braun, V., Gaisser, S., Hermann, C., Kampfenkel, K., Killmann, H., and Traub, I. (1996) Energy-coupled transport across the outer membrane of Escherichia coli: ExbB binds ExbD and TonB in virto, and leucine 132 in the periplasmic

region and aspartate 25 in the transmembrane region are important for ExbD activity. *J. Bacteriol.* **178**(10):2836-2845.

Braun, M., Killmann, H. and Braun, V. (1999) The β-barrel domain of FhuAΔ5-16- is sufficient for TonB-dependent activities of Escherichia coli. *Mol. Micor.* **33**(5):1037-1049.

Brewer, S., Tolley, M., Trayer, I. P., Barr, G. C., Dorman, C. J., Hannavy, K., Higgins, C. F., Evans, J. S., Levine, B. A., and Wormald, M. R. (1990) Structure and function of X-Pro dipeptide repeats in the TonB protiens of Salmonalla typhimurium and Escherichia coli. *J. Mol. Biol.* **216**(4):883-895.

Brickman, T. J., and McIntosh, M. A. (1992) Overexpression and purification of ferric enterobactin esterase from Escherichia coli. Demonstration of enzymatic hydrolysis of enterobactin and its iron comples. *J. Biol. Chem.* **267**(17):12350-12355.

Buchanan, S.K., Smith, B.S., Benkatramani, L., Xia, D., Esser, L., Palnitkar, M., et al. (1998) Crystal structure of the outer membrane active transporter FepA from Escherichia coli. *Nature Struct. Biol.* **6**:56-63.

Buchanan, S. K. (1999) Beta-barrel proteins from bacterial outer membranes: structure, function and refolding. *Curr. Opin. Struct. Biol.* **9**(4):455-61.

Cadieux, N., Bradbeer, C., and Kadner, R. J. (2000) Sequence changes in the ton box region of BtuB affect its transport activities and interaction with TonB protein. *J. Bacteriol.* **182**(21):5954-61.

Cadieux, N., and Kadner, R. J. (1999) Site-directed disulfide bonding reveals an interaction site between energy-coupling protein TonB and BtuB, the outer membrane cobalamin transporter. *Proc. Natl. Acad. Sci.* **96**(19):10673-8.

Cao, Z., Qi, Z., Sprencel, C., Newton, S. M., and Klebba, P. E. (2000) Aromatic components of two ferric enterobactin binding sites in Escherichia coli FepA. *Mol. Micro.*. **37**(6):1306-17.

Carlsson, J., Drevin, H., and Axen, R. (1978). Protein thiolation and reversible proteiN-protein conjugation. N-succinimyidyl 3-(2-pyridyldithio)propionate, a new heterobifunctional reagent. *J. Biochem.* **173**,723-737.

Carniel, E. (2001) The Yersinia high-pathogenicity island: an iron-uptake island. *Microbes Infect.* **3**(7):561-569.

Carson, S. D., Klebba, P. E., Newton, S. M., and Sparling, P. F. (1999) Ferric enterobactin binding and utilization by Neisseria gonorrhoeae. *J. Bacteriol.* **181**(9):2895-2901.

Chang, C., Mooser, A., Pluckthun, A., and Wlodawer, A. (2001) Crystal structure of the dimeric C-terminal domain of TonB reveals a novel fold. *J. Biol. Chem.* **276**(29):27535-40.

Charbit, A., Wang, J., Michel, V., and Hofnung, M. (1998) A cluster of charged and aromatic residues in the C-terminal portion of maltoporin participates in sugar binding and uptake. *Mol. Gen. Genet.* **260**(2-3):185-192.

Cope L. D., Hrkal Z., and Hansen E.J. (2000) Detection of phase variation in expression of proteins involved in hemoglobin and hemoglobin-haptoglobin binding by nontypeable Haemophilus influenzae. *Infect. Immun.* **68**(7):4092-101.

Cornelissen, C. N., Kelley, M., Hobbs, M. M., Anderson, J. E., Cannon, J. G., Cohen, M. S., and Sparling, P. F. (1998) The transferrin receptor expressed by gonococcal strain FA1090 is required for the experimental infection of human male volunteers *Mol Microbiol* **27**(3):611-616.

Cornelissen, C. N., and Sparling, P. F. (1994) Iron piracy: acquisition of transferrin-bound iron by bacterial pathogens. *Mol. Micor.* **14**(5):843-850.

Coulton, J. W., Mason, P., and DuBow, M. S. (1983) Molecular cloning of the ferrichrome-iron receptor of Escherichia coli K-12. *J. Bacteriol.* **156**(3):1315-1321.

Cowan, S.W., Schirmer, T., Rummel, G., Steiert, M., Gosh, R., Pauptit, R.A. et al. (1992) Crystal structures explain functional properties of two E. coli porins. *Nature* **358**:727-733.

Cox, G. B., Gibson, F., Luke, R. K., Newton, N. A., O'Brien, I. G., and Rosenberg, H. (1970) Mutations affecting iron transport in Escherichia coli. *J. Bacteriol.* **104**:219-226.

Dean, C. R., and Poole, K. (1993) Cloning and characterization of the ferric enterobactin receptor gene (pfeA) of Pseudomonas aeruginosa. *J. Bacteriol.* **175**:317-324.

Deisenhofer, J., Epp, O., Miki, K., Huber, R., and and Michel, H. (1984) X-ray structure analysis of a membrane protein complex. Electron density map at 3 A resolution and a model of the chromophores of the photosynthetic reaction center from *Rhodopseudomonas viridis. J. Mol. Biol.* **180**(2):385-398.

Dolence, E. K., Minnick, A. A., and Miller, M. J. (1990) N5-acetyl-N5-hydroxy-L-ornithine-derived siderophore-carbacephalosporin beta-lactam conjugates: iron transport mediated drug delivery. *J. Med. Chem.* **33**(2):461-464.

Diarra, M. S., Lavoie, M. C., Jacques, M., Darwish, I., Dolence, E. K., Ghosh, A., Ghosh, M., Miller, M. J., and Malouin, F. (1996) Species Selectivity of New Siderophore-Drug Conjugates That Use Specific Iron Uptake for Entry into Bacteria. *Anitmicrob. Agent. Chemo.* **40**(11):2610-2617.

Ecker, D. J., Matzanke, B. F., and Raymond, K. N. (1986) Recognition and transport of ferric enterobactin in Escherichia coli. *J. Bacteriol.* **167**(2):666-673.

Evans, L. J., Cooper, A., and Lakey, J. H. (1996) Direct measurement of the association of a protein with a family of membrane receptors. *J. Mol. Biol.* **255**(4):559-63.

Feldman, M. F., Marolda, C. L., Monterio, M. A., Perry, B. M., Parodi, A. J. and Valvano, M. A. (1999) The Activity of a putative polyisoprenol-linked sugar

translocase (Wzx) involved in Escherichia coli O antigen assembly is independent of the chemical structure of the O repeat. J. Biol. Chem. 274(49):35129-35138.

Ferguson, A.D., Hofmann, E., Coulton, J.W., Diederichs, K., and Welte, W. (1998) Siderophore-mediated iron transport: crystal structure of FhuA with bound lipopolysaccharide. *Science* **282**:2215-2220.

Fernandez-Beros, M. E., Gonzalez, C., McIntosh, M. A., Cabello, F. C. (1989) Immune response to the iron-deprivation-induced proteins of Salmonella typhi in typhoid fever. *Infect Immun* **57**(4):1271-5.

Forst, D., Welte, W., Wacker, T. and Diederichs, K. (1998) Structure of the sucrose-specific porin ScrY from Salmonella typhimurium and its complex with sucrose. *Nature Struct. Biol.* **5**:37-46.

Frye, L. D., and Edidin, M. (1970) The rapid intermixing of cell surface antigens after formation of mouse-human heterokaryons. *J. Cell Sci.* 7(2):319-335.

Fung-Tomc, J., Bush, K., Minassian, B., Kolek, B., Flamm, R., Gradelski, E., and Bonner, D. (1997) Antibacterial activity of BMS-180680, a new catechol-containing monobactam. *Antimicrob. Agents. Chemother.* **41**(5):1010-1016.

Furman, M., Fica, A., Saxena, M., Di Fabio, J. L., and Cabello, F. C. (1994) Salmonella typhi iron uptake mutants are attenuated in mice. *Infect. Immun.* **62**(9):4091-4.

Galanos, C. luderitz, O., Rietschel, E. T., and Westphal, O. (1977) Newer aspects of the chemistry and biology of bacterial lipopolysaccharides with special reference to their lipid A component, pp.239-335. In T. W. Goodwin (ed.), *International review of Biochemistry*, vol. **14**. *Biochemistry* of lipids II. University Park Press, Baltimore.

Gibson, F., Cox, G. B., Downie, A., and Radik, J. (1977) Partial Diploids of Escherichia coli Carrying Normal and Mutant Alleles Affecting Oxidative Phosphorylation. *Biochem. J.* **162**:665-670.

Gouaux, E. (1997) The long and short of colicin action: the molecular basis for the biological activity of channel-forming colicins. *Structure* **5**(3):313-317.

Gray-Owen, S. D., and Schryvers, A. B. (1996) Bacterial transferrin and lactoferrin receptors. *Trends Microbiol.* **4**(5):185-191.

Griffiths, E. and Williams, P. (1999) The iron-uptake systems of pathogenic bacteria, fungi, and protoza. In *Iron and Infection: Molecular, Physilogical, and and Clinical Aspects* (2nd ed.) (Bullen, J. J. and Griffiths, E., eds.) 87-212, John Wiley and Sons.

Guan, C., Li, P., Riggs, P. D., and Inouye, H. (1987) Vectors that facilitate the expression and purification of foreign peptides in Escherichia coli by fusion to maltose-binding protein. *Gene* **6**:23-30.

Gudmundsdottir, A., Bell, P. E., Lundrigan, M. D., Bradbeer, C., and Kadner, R. J. (1989) Point mutations in a conserved region (TonB box) of Escherichia coli

outer membrane protein BtuB affect vitamin B12 transport. *J. Bacteriol.* **171**(12):6526-6533.

Guerinot, M. L. (1994). Microbial Iron Transport. *Annu. Rev. Microbiol.* **48**:743-752.

Hantke, K. (1984) Cloning of the repressor protein gene or iron-regulated systems in Escherichia coli K12. *Mol. Gen. Genet.* **197**(2):337-341.

Hantke, K. (1990) Dihydrozybenzoylserine-a siderophore for E. coli. *FEMS Microbiol. Lett.* **55**(1-2):5-8.

Hashimoto-Gotoh, T., Franklin, F. C., Nordheim, A., and Timmis, K. N. (1981) Specific-purpose plasmid cloning vectors. I. Low copy number, temperature-sensitive, mobilization-defective pSC101-derived containment vectors. *Gene* **16**(1-3):227-235.

Heesemann, J., Hantke, K., Vocke, T., Saken, E., Rakin, A., Stojiljkovic, I., and Berner, R. (1993) Virulence of Yersinia enterocolitica is closely associated with siderophore production, expression of an iron-repressible outer membrane polypeptide of 65,000 Da and pesticin sensitivity. *Mol. Micor.* **8**(2):397-408.

Heidinger, S., Braun, V., Pecoraro, V. L., and Raymond, K. N. (1983) Iron supply to Escherichia coli by synthetic analogs of enterochelin. *J. Bacteriol.* **153**(1):109-115.

Helgerson, S. L., and Cramer, W. A. (1976) Changes in E. coli cell envelope structure caused by uncouplers of active transport and colicin E1. *J. Supramol. Struct.* **5**(3):291-308.

Heller, K. J., Kadner, R. J., and Gunther, K. (1988) Suppression of the butB451 mutation by mutations in the tonB gene suggests a direct interaction between TonB and TonB-dependent receptor proteins in the outer membrane of Escherichia coli. *Gene* **64**(1):147-153.

Higgs, P. I., Myers, P. S. and Postle, K. (1998) Interactions in the TonB-Dependent Energy Transduction Complex: ExbB and ExbD From Homomultimers. *J. Bacteriol.* **180**(22):6031-6038.

Howard, S. P., Herrmann, C., Stratilo, C. W., and Braun, V. (2001) In vivo synthesis of the periplasmic domain of TonB inhibits transport through the FecA and FhuA iron siderophore transporters of Escherichia coli. *J. Bacteriol.* **183**(20):5885-5895.

Hufton, S. E., Ward, R. J., Bunce, N. A., Armstrong, J. T., Fletcher, A. J., and Glass, R. E. (1995) Structure-function analysis of the vitamin B12 receptor of Escherichia coli by means of informational suppression. *Mol. Micor.* **15**(2):381-393.

Hunt, M. D., Pettis, G. S., and McIntosh, M. A. (1994) Promoter and operator determinants for fur-mediated iron regulation in the bidirectional fepA-fes control region of the Escherichia coli enterobactin gene system. *J. Bacteriol.* **176**(13):3944-3955.

Jarosik, G. P., Maciver, I., and Hansen, E. J. (1995) Utilization of transferrin-bound iron by Haemophilus influenzae requires an intact TonB gene. *Infect. Immun.* **63**(2):710-713.

Jarosik, G. P., Sanders, J. D., Cope, L. D., Muller-Eberhard, U., and Hansen, E. J. (1994) A functional tonB gene is required for both utilization of heme and virulence expression by Haemophilus influenzae type b. *Infect. Immun.* **62**(6):2470-2477.

Jaskula, J. C., Letain, T. E., Roof, S. K., Skare, J. T. and Postle, K. (1994) Role of the TonB Amino Terminus in Energy Transduction between membranes. *J. Bacteriol.* **176**(8):2326-2338.

Jelokhani-Niaraki, M., Nakashima, K., Kodama, H., and Kondo, M. (1998) Interaction and orientation of an alpha-aminoisobutyric acid and tryptophan containing short helical peptide pore-former in phospholipid vesicles, as revealed by fluorescence spectroscopy. *J. Biochem.* **123**(5):790-797.

Jiang, X., Payne, M. A., Cao, Z., Foster, S. B., Feix, J. B., Newton, S. M., and Klebba, P. E. (1997) Ligand-specific opening of a gated-porin channel in the outer membrane of living bacteria. *Science* **276**(5316):1261-1264.

Kadner, R. J. (1990). Vitamin B_{12} transport in Escherichia coli: energy coupling between membranes. *Mol. Micor.* **4**(12):2027-2033.

Kampfenkel, K., and Braun, V. (1993) Topology of the ExbB protein in the cytoplasmic membrane of Escherichia coli. *J. Biol. Chem.* **268**(8):6050-6057.

Karlsson, m., Hannavy, K., and Higgins, C. F. (1993a) A sequence-specific function for the N-terminal signal-like sequence of the TonB protein. *Mol. Micor.* **8**(2):379-388.

Karlsson, M., Hannavy, K., and Higgins, C. F. (1993B) ExbB acts as a chaperone-like protein to stabalize TonB in the cytoplasm. *Mol. Micor.* **8**(2):389-396.

Kellerman, O. K., and Ferenci, T. (1982) Malotse binding protein for E. coli. *Methods in Enzymology* **90**:459-463.

Killmann H, Benz R, Braun V. (1993). Conversion of the FhuA transport protein into a diffusion channel through the outer membrane of Escherichia coli. *EMBO J.* **12**(8):3007-16.

Killmann H, Benz R, Braun V. (1996) Properties of the FhuA channel in the Escherichia coli outer membrane after deletion of FhuA portions within and outside the predicted gating loop. *J. Bacteriol.* **178**(23):6913-20.

Killmann H, and Braun V. (1998). Conversion of the coprogen transport protein FhuE and the ferrioxamine B transport protein FoxA into ferrichrome transport proteins. FEMS Microbiol Lett **161**(1):59-67.

Killmann, H., Braun, M., Herrmann, C., and Braun, V. (2001) FhuA barrel-cork hybrids are active transporters and receptros. *J. Bacteriol.* **183**(11):3476-3487.

Klebba, P. E., McIntosh, M. A., and Neilands, J. B. (1982) Kinetics of biosynthesis of iron-regulated membrane proteins in Escherichia coli. *J. Bacteriol.* **149**:880-888.

Klebba, P. E., Rutz, J. M., Liu, J., and Murphy, C. K. (1993). Mechanisms of TonB-Catalyzed Iron Transport through the Enteric Bacterial Cell Envelope. *J. Bioeng. Biomemb.* **25**(6):603-611.

Klebba, P.E., Newton, S. M., Charbit, A., Michel, V., Perrin, D., and Hofnung, M. (1997) Further genetic analysis of the C-terminal external loop region in Escherichia coli maltoporin. *Res. Microbiol.* **148**:375-387.

Klebba, P. E. and Newton, S. M. (1998) Mechanisms of solute transport through outer membrane porins: burning down the house. *Curr. Opin. Microbiol.* **1**(2):238-247.

Kline, T., Fromhold, M., McKennon, T. E., Cai, S., Treiberg, J., Ihle, N., Sherman, D., Schwan, W., Hickey, M. J., Warrener, P., Witte, P. R., Brody, L. L., Goltry, L., Barker, L. M., Anderson, S.U., Tanaka, S. K., Shawar, R. M., Nguyen, L. Y., Langhorne, M., Bigelow, A., Embuscado, L., and Naeemi, E. (2000) Antimicrobial effects of novel siderophores linked to beta-lactam antibiotics. *Bioorg. Med. Chem.* **8**(1):73-93.

Klug, C. S., and Feix, J. B. (1998a) Guanidine hydrochloride unfolding of a transmembrane beta-strand in FepA using site-directed spin labeling. *Protein Sci.* **7**(6):1469-76.

Klug, C. S., Eaton, S. S., Eaton, G. R., and Feix, J. B. (1998b) Ligand-induced conformational change in the ferric enterobactin receptor FepA as studied by site-directed spin labeling and time-domain ESR. *Biochemistry* **37**(25):9016-23.

Klug, C. S., Su, W., and Feix, J. B. (1997) Mapping of the residues involved in a proposed beta-strand located in the ferric enterobactin receptor FepA using site-directed spin-labeling. *Biochemistry* **36**(42):13027-33.

Kock, J., Olschlager, T., Kamp, R. M., and Braun, V. (1987) Primary structure of colicin M, an inhibitor or murein biosynthesis. *J. Bacteriol.* **169**(7):3358-3361.

Koebnik, R., Baumler, A. J., Heesemann, J., Braun, V., and Hantke, K. (1993) The TonB protein of Yersinia enterocolitica and its interactions with TonB-box proteins. *Mol. Gen. Genet.* **237**(1-2):152-160.

Koebnik, R., Locher, K. P. and Gelder, P. V. (2000) Structure and function of bacterial outer membrane proteins: barrels in a nutshell. *Mol. Micor.* **37**(2)239-253.

Koronakis, V., Sharff, A., Koronakis, E., Luisi, B., and Hughes, C. (2000) Crystal structure of the bacterial membrane protein TolC central to multidrug efflux and protein export. *Nature* **405**:914-919.

Koster, W. and Braun, V. (1990a) Iron (III) Hydroxamate Transport into Escherichia coli: Substrate binding to the periplasmic FhuD protein. *J. Biol. Chem.* **265**(35):21407-21410.

Koster, W. and Braun, V. (1990b) Iron (III) Hydroxamate Transport of Escherichia coli: Restoration of iron supply by coexpression of the N- and C-terminal halves of the cytoplasmic membrane protein FhuB cloned on separate plasmids. *Mol. Gen. Genet.* **223**:379-384.

Larsen, R. A., Wood, G. E. and Postle, K. (1993) The conserved proline-rich motif is not essential for energy transduction by Escherichia coli TonB protein. *Mol. Micor.* **10**(5):943-953.

Larsen, R. A., Thomas, M. G., Wood, G. E. and Postle, K. (1994) Partial suppression of an Escherichia coli TonB transmembrane domain mutation (delta V17) by a missense mutation in ExbB. *Mol. Micor.* **13**(4):627-640.

Larsen, R. A., Foster-Hartnett, D., McIntosh, M. A. and Postle, K. (1997) Regions of Escherichia coli TonB and FepA Proteins Essential for In Vivo Physical Interactions. *J. Bacteriol.* **179**(10):3213-3221.

Larsen, R. A., Thomas, M. G. and Postle, K. (1999). Protonmotive force, ExbB and ligand-bound FepA drive conformational changes in TonB. *Mol. Micor.* **31** (6) 1809-1824.

Larsen, R. A., and Postle, K. (2001) Conserved residues Ser(16) and His(20) and their relative positioning are essential for TonB activity, cross-linking of TonB with ExbB, and the ability of TonB to respond to proton motive force. *J. Biol. Chem.* **276**(11):8111-8117.

Lazdunski, C. J., Bouveret, E., Rigal, A., Journet, L., Lloubes, R., and Benedetti, H. (1998) Colicin import into Escherichia coli cells. *J. Bacteriol.* **180**(19):4993-5002.

Letain, T. E and Postle, K. (1997) TonB protein appears to transduce energy by shuttling between the cytoplasmic membrane and the outer membrane in Escherichia coli. *Mol. Micor.* **21**(2):271-283.

Lewis, L. A., Gray, E., Wang, Y. P., Roe, B.A, and Dyer, D. W. (1997) Molecular characterization of hpuAB, the haemoglobin-haptoglobin-utilazation operon of Neisseria meningitidis. *Mol. Micor.* **23**(4):737-749.

Liu, J., Rutz, J. M., Klebba, P. E., and Feix, J. B. (1994) A site-directed spin-labeling study of ligand-induced conformational change in the ferric enterobactin receptor, FepA. *Biochemistry* **33**(45)13274-13283.

Liu, J., Rutz, J. M., Feix, J. B., and Klebba, P. E. (1993) Permeability properties of a large gated channel within the ferric enterobactin receptor, FepA. *Proc. Natl. Acad. Sci.* **90**(22):10653-10657.

Lo, R. Y. (2001) Genetic analysis of virulence factors in Mannheimia (Pasteurella) haemolytica. *Al. Vet. Micro.* **83**(1):23-35.

Locher KP, Rosenbusch JP. (1997) Oligomeric states and siderophore binding of the ligand-gated FhuA protein that forms channels across Escherichia coli outer membranes. *Eur. J. Biochem.* **247**(3):770-5.

Locher, K.P., Rees, B., Koebnik, R., Mitschler, A., Mouliner, L., Rosenbusch, J.P, et al. (1998) Transmembrane signaling across the ligand-gated FhuA receptor: crystal structurs of free and ferrichrome-bound states reveal allosteric changes. *Cell* **95**:771-778.

Ludertiz, O., Freudenberg, M. A., Galanos, C., Lehmann, V., Rietschel, E. T., and Shaw, D. M. (1982) Lipopolysaccharides of Gram-negative bacteria. *Curr. Top. Membr. Transp.* **17**:79-151.

Lundrigan, M. D., and Kadner, R. J. (1986) Nucleotide sequence of the gene for the ferricenterochelin receptor FepA in Escherichia coli. Homology among outer membrane receptors that interact with TonB. *J. Biol. Chem.* **261**(23):10797-10801.

Maina, C. V., Riggs, P.D., Grandea, A. G. III, Slatko, B. E., Moran, L. S., Tagliamonte, J. A., McReynolds, L. A., and Guan, C. (1988) A vector to express and purify foreign proteins in Escherichia coli by fusion to, and separation from, maltose binding protein. *Gene* **74**:365-373.

Makela, P. H., and Stocker, B.A.D., Genetics of the bacteial surface, p.219-264. In S.W. Glover and D.A. Hopwood (ed.), *Genetics as a tool in microbiology. Society for General Microbiology*. Symp. 31. Cambridge University Pressk, Cambridge.

McIntosh, M. A., Chenault, S. S., and Earhart, C. F. (1979) Genetic and physiological studies on the relationship between colicin B and ferricenterochelin uptake in Escherichia coli. *J. Bacteriol.* **4**:1523-1533.

Mckee, J. A., Sharma, S. K., and Miller, M. J. (1991) Iron transport mediated drug delivery systems: synthesis and antibacterial activity of spermidine and lysine-based siderophore-beta-lactam conjugates. *Bioconjug. Chem.* **2**(4):281-291.

Merianos, H. J., Cadieux, N., Lin, C. H., Kadner, R. J., and Cafiso, D. S. (2000) Substrate-induced exposure of an energy-coupling motif of a membrane transporter. *Nat. Struct. Biol.* **7**(3):205-209.

Middaugh, R., Vanin, E. F., and Ji, T. H. (1983) Chemical crosslinking of cell membranes. *Mol. Cell. Biochem.* **50**:115-141.

Mikkelsen, R. B., and Wallach, D. F. (1976) Photoactivated cross-linking of proteins within the eryghrocyte membrane core. *J. Biol. Chem.* **251**(23):7413-7416.

Miller, J. H. (1972) Experminents in molecular genetics. Cold Spring Harbor Laboratory, Cold Spring Harbor, NY.

Miller, M. J., McKee, J. A., Minnick, A. A., and Dolence, E. K. (1991) The design, synthesis and study of siderophore-antibiotic conjugates. Siderophore mediated drug transport. *Biol. Met.* **4**(1)::62-69.

Minnick, A. A., McKee, J. A., Dolence, E. K., and Miller, M. J. (1992) Iron-transport-mediated antibacterial activity of and development of resistance to hydroxamate and catechol siderophore-carbacephalosporin conjugates. *Antimicrob. Agents Chemother.* **36**(4):840-580.

Moeck, G. S., Tawa, P., Xiang, H., Ismail, A. A., Turnbull, J. L., and Coulton, J. W. (1996) Ligand-induced conformational change in the ferrichrome-iron receptor of Escherichia coli K-12. *Mol. Micor.* **22**(3):459-471.

Moeck, G. S., Coulton, J. W. and Postle, K. (1997) Cell Envelope Signaling in Escherichia coli : Ligand Binding to the Ferrichrome-Iron Receptor FhuA promotes interaction with the energy-transducing protein TonB. *J. Biol. Chem.* **272**(45):28391-28397.

Moeck, G. S., and Coulton, J. W. (1998) TonB-dependent iron acquisition: mechanisms of siderophore-mediated active transport. *Mol. Microbiol.* **28**(4):675-681.

Murphy C. K., and Klebba P. E. (1989) Export of FepA::PhoA fusion proteins to the outer membrane of Escherichia coli K-12. *J. Bacteriol.* **171**(11):5894-900.

Murphy, C. K., Kalve, V. I. and Klebba, P. E. (1990) Surface Topology of the Escherichia coli K-12 Ferric Enterobactin Receptor. *J. Bacteriol.* **172**(5):2736-2746.

Nakamura, K., and Mizushima, S. (1976) Effects of heating in dodecyl sulfate solution on the conformation and electrophoretic mobility of isolated outer membrane proteins from Escherichia coli K-12. *J. Biochem.* **80**:1411-1422.

Neidhardt, F. C., Bloch, P. L., and Smith, D. F. (1974) Culture medium for enterobacteria. *J. Bacteriol.* **119**:736-747.

Neilands, J. B., Erickson, T. J., and Rastetter, W. H. (1981) Sterospecificity of the ferric enterobactin receptor of Escherichia coli K-12. *J. Biol. Chem.* **256**(8):3831-3832.

Neilands, J. B. (1982) Microbial envelope proteins related to iron. *Annu. Rev. Microbiol.* **36**:285-309.

Neilands, J. B., Konopka, K., Schwyn, B., Coy, M., Francis, R. T., Paw, B. H., and Bagg, A. (1987) in *Iron Transport in Microbes, Plants and Animals* (Winkelmann, G., van der Helm, D., and Neilands, J. B., eds) pp.3-33, VCH Press, Weinheim.

Neilands, J. B (1995) Siderophores: Structure and Function of Microbial Iron Transport Compounds. *J. Biol. Chem.* **270**(45):26723-26726.

Newton, S. M., Allen, J. S., Cao, Z., Qi, Z., Jiang, X., Sprencel, C., Igo, J. D., Foster, S. B., Payne, M. A., and Klebba, P.E. (1997) Double mutagenesis of a postive charge cluster in the ligand-binding site of the ferric enterobactin receptor, FepA. *Proc. Natl. Acad. Sci.* **94**(9):4560-4565.

Newton, S. M., Igo, J. D., Scott, D. C., and Klebba, P. E. (1999) Effect of loop deletions on the binding and transport of ferric enterobactin by FepA. *Mol. Micro.* **32**(6):1153-65.

Nicolson, G. L., and Singer, S. J. (1971) Ferritin-conjugated plant agglutinins as specific saccharide stains for electron microscopy: application to saccharides bound to cell membranes. *Proc. Natl. Acad. Sci.* **68**(5):942-945.

Nieva-Gomez, D, and Gennis, R. B. (1977) Affinity of intact Escherichia coli for hydrophobic membrane probes is a function of the physiological state of the cells. *Proc. Natl. Acad. Sci.* **74**(5):1811-1815.

Nikaido, H. (1973) Biosynthesis and assembly of lipopolysaccraride and the outer membrane layer of gran-negative cell wall, p.131-208. In L. leive (ed.), *Bacterial membranes and walls*. Marcel Dekker, New York.

Nikaido, H, and Nakae, T. (1979) The outer membrane of gram-negative bacteria. *Adv. Microb. Physiol.* **20**:163-250.

Nikaido H, and Varra, M. (1985) Molecular Basis of Bacterial Outer Membrane Permeability *Micro. Rev.* **49**:1-32.

Occhino, D. A., Wyckoff, E. E., Henderson, D. P., Wrona, T. J., and Payne, S. M. (1998) Vibrio cholerae iron transport: haem transport genes are linked to one of two sets of tonB, exbB, exbD genes *Mol. Micro.*. **29**(6):1493-1507.

Palva, E. T., and Randall, L. L. (1976) Nearest-neighbor analysis of Escherichia coli outer membrane proteins using cleavable cross-links. J. Bacteriol. 127(3):1558-15560

Partis, M. D., Griffiths, D. G, Roberts, G. C, and Beechey, R. B.(1983). Cross-linking of protein by maleimido alkonyl N-hydroxysuccinimido esters. *J. Prot. Chem.* **2**(3),263-277.

Pautsch, A. and Schulz, G. (1998) Structure of the outer membrane porin A transmembrane domain. *Nat. Stru. Biol.* **5**(11):1013-1017.

Payne, M. A., Igo, J. D., Cao, Z., Foster, S. B., Newton, S. M., and Klebba, P. E. (1997) Biphasic binding kinetics between FepA and its ligands. *J. Biol. Chem.* **272**(35):21950-21955.

Petronilli, V., and Ames, G. F. (1991) Binding protein-independent histidine permease mutants. Uncoupling of ATP hydrolysis from transmembrane signaling. *J. Biol. Chem.* **266**(25):16293-16296

Pettis, G. S., Brickman, T. J., and McIntosh, M. A. (1988) Transcriptional mapping and nucleotide sequence of the Escherichia coli fepA-fes enterobactin region. Identification of a unique iron-regulated bidirectional promoter. *J. Biol. Chem.* **263**(35):18857-18863.

Pollack, J. R., and Neilands, J. B. (1970) Enterobactin, an iron transport compound from Salmonella typhimurium. *Biochem. Biophys. Res. Commun.* **38**(5):989-992.

Postle, K., and Skare, J. T. (1988) Escherichia coli TonB protein is exported from the cytoplasm without proteolytic cleavage of its amino terminus. *J. Biol. Chem.* **263**(22):11000-11007.

Postle, K. (1990) TonB and the gram-negative dilemma. *Mol. Micor.* **4**(12):2019-2025.

Postle, K. (1993) TonB protein and energy transduction between membranes. *J. Bioenerg. Biomembr.* **25**(6):591-601.

Postle, K. and Good, R. F. (1983) DNA sequence of the Escherichia coli tonB gene. *Proc. Natl. Acad. Sci.* **80**:5235-5239.

Pugsley, A. and Reeves, P. (1977) Uptake of Ferricenterochelin by Escherichia coli: Energy dependent stage of Uptake. *J. Bacteriol.* **130**(1) 26-36.

Reeves, S. A., Torres, A. G., and Payne, S. M. (2000) TonB is required for intracellular grwoth and virulence of Shigella dysenteriae. *Infect. Immun.* **68**(11):6329-6336.

Reissbrodt, R., Ramiandrasoa, F., Bricard, L., and Kunesch, G. (1997) Siderophore activity of chemically synthesized dihydroxybenzoyl derivatives of spermidines and cystamide. *Biometals* **10**(2):95-103.

Richardson, P. T., and Park, S. F. (1995) Enterochelin acquisition in Campylobacter coli: characterization of components of a binding-protein dependent transport system. *Microbiology* **141**(12):3181-3191.

Rohrbach, M. R., Paul, S. and Koster, W. (1995a) In vivo reconstitution of an active siderophore transport system by a binding protein derivative lacking a signal sequence. *Mol. Gen. Genet.* **248**:33-42.

Rohrbach, M.R., Braun, V., and Koster, W. (1995b) Ferrichrome transport in Escherichia coli K-12: altered substrate specificity of mutated periplasmic

FhuD and interaction of FhuD with the integral membrane protein FhuB. *J. Bacteriol.* **177**:7186-7193.

Roof, S. K., Allard, J. D., Bertrand, K. P., and Postle, K. (1991) Analysis of Escherichia coli TonB membrane topology by use of PhoA fusions. *J. Bacteriol.* **173**(17):5554-5557.

Roosenberg, J. M., Lin, Y. M., Lu, Y., and Miller, M. J. (2000) Studies and syntheses of siderophores, microbial iron chelators, and analogs as potential drug delivery agnets. *Curr. Med. Chem.* 7(2):159-197.

Rutz, J. M., Abdullah, T., Singh, S. P., Kalve, V. I., and Klebba, P.E. (1991) Evolution of the Ferric Enterobactin Receptor in Gram-Negative Bacteria. *J. Bacteriol.* **173**(19):5964-5974.

Rutz, J., Liu, J., Lyons, J. A., Goranson, J., Armstrong, S. K., McIntosh, M. A., Feix, J. B., and Klebba, P. E. (1992). Formation of a Gated Channel by a Ligand-Specific Transport Protein in the Bacterial Outer Membrane. *Science* **258**:471-475.

Sauer, M., Hantke, K., and Braun, M. (1990) Sequence of the fhuE outer-membrane receptor gene of Escherichia coli K12 and properties of mutants. *Mol. Micor.* **4**(3):427-437.

Schenkman, S., Tsugita, A., Schwartz, M. and Rosenbusch, J. P. (1984) Topology of the Phage λ Receptor Protein: Mapping Targets of Proteolytic Clevage in Relation to Binding Sites for Phage or Monoclonal Antibodies. *J. Biol. Chem.* **259**(12)7570-7576.

Schirmer, T., keller, T.A., Wanh, Y.F., and Rosenbusch, J.P. (1995) Structural basis for sugar translocation through maltoporin channels at 3.1 A resolution. *Science* **267**:512-514.

Schoffler, H. and Braun, H. (1989) Transport across the outer membrane of Escherichia coli K12 via the FhuA receptor is regulated by the TonB protein of the cytoplasmic membrane. *Mol. Gen. Genet.* **217**:378-383.

Schramm, E., Mende, J., Bruan, V., and Kamp, R. M. (1987) Nucleotide sequence of the colicin B activity gene cba: consensus pentapeptide among TonB-dependent colicins and receptors. *J. Bacteriol.* **169**(7):3350-3357.

Schryvers, A. B., Bonnah, R., Yu, R. H., Wong, H., and Retzer, M. (1998) Bacterial lactoferrin receptors. *Adv. Exp. Med. Biol.* **443**:123-133.

Schryvers, A. B., and Stojiljkovic, I. (1999) Iron acquisition systems in the pathogenic Neisseria. *Mol. Micro.* **32**(6):1117-1123.

Scott, D. C., Cao, Z., Qi, Z., Bauler, M., Igo, J. D., Newton, S. M. C., and Klebba, P. E. (2001) Exchangeability of N Termini in the Ligand-gated Porins of Escherichia coli. *J. Biol. Chem.* **276**(16):13025-13033.

Shepard, L.A., Heuck, A. P., Hannam, B. D., Rossjohn, J., Parker, M. W., Ryan, K. R., Johnson, A. E., and Tweten, R. K. (1998) Identification of a membrane-spanning domain of the thiol-activated pore-forming toxin Clostridium perfringens perfringolysin O: an alpha-helical to beta-sheet transition identified by fluorescence spectroscopy. Biochemistry 37(41):14563-14574.

Skare, J. T., and Postle, K. (1991) Evidence for a TonB-dependent energy transduction complex in Escherichia coli. *Mol. Micor.* **5**(12):2883-2890.

Skare, J. T., Ahmer, B. M. M., Seachord, C. L., Darveau, R. P. and Postle, K. (1993) Energy Transduction between Membranes: TonB, a cytoplasmic membrane protein, can be chemically cross-linked in vivo to the outer membrane receptor FepA. *J. Biol. Chem.* **268**(22):16302-16308.

Smit, J., Kamio, Y., and Nikaido, H. (1975) Outer membrane of Salmonella typhimurium: chemical analysis and freeze-fracture studies with lipopolysaccharide mutants. *J. Bacteriol.* **124**(2):942-958.

Sonntag, L. Schwarz, H. Hirota Y. and Henning, U. (1978) Cell Enveolpe and shape of E. coli.:multiple mutants missing the outer membrane lipoportein and other major outer membrane proteins. *J. Bacteriol.* **136**:280-285.

Speiser, D. M., and Ames, G. F. (1991) *Salmonella typhimurium* histidine periplasmic permease mutations that allow transport in the absence of histidine-binding proteins. *J. Bacteriol.* **173**(4):1444-1451.

Sprencel, C., Cao, Z., Qi, Z., Scott, D. C., Montague, M. A., Ivanoff, N., Xu, J., Raymond, K. M., Newton, S. C. and Klebba, P. E. (2000) Binding of Ferric Enterobactin by the Escherichia coli Periplasmic Protein FepB. *J. Bacteriol.* **182**(19):5359-5364.

Szmelcman, S., and Hofnung, M. (1975) Maltose transport in Escherichia coli K-12: involvement of the bacteriophage lambda receptor. *J. Bacteriol.* **124**:112-118.

Szmelcman, S., Schwartz, M., Silhavy, T. J., and Boos, W. (1976) Maltose transport in Escherichia coli K-12: A comparison of transport kinetics in wild-type and lambda-resistant mutants as measured by fluorescence quenching. *Eur. J. Biochem.* **65**:13-19.

Takase, H., Nitanai, H., Hoshino, K., and Otani, T. (2000) Requirement of the Pseudomonas aeruginosa TonB gene for high-affinity iron acquisition and infection. *Infect. Immun.* **68**(8):4498-4504.

Torres, A. G., and Payne, S. M. (1997) Haem-iron transport system in enterohaemorrhagic Escherichia coli O157:H7. *Mol. Micor.* **23**(4)825-833.

Thulasiraman, P., Newton, S. M., Xu, J., Raymond, K. N., Mai, C., Hall, A., Montague, M. A., and Klebba, P. E. (1998) Selectivity of ferric enterobactin binding and cooperativity of transport in gram-negative bacteria. *J. Bacteriol.* **180**(24):6689-6696.

Torres, A.G., Redford, P., Welch, R. A., and Payne, S. M. (2001) TonB-Dependent Systems of Uropathogenic Escherichia coli: Aerobactin and Heme Transport and TonB are Required for Virulence in the Mouse. *Infect. Immun.* **69**(10):6179-6185.

Traub, I., Gaisser, S., and Braun, V. (1993) Activity domains of the TonB protein. *Mol. Micor.* **8**(2):409-423.

Trommer, W. E, Kolkenbrock, H., Pfleiderer, G. (1975) Synthesis and properties of a new selective bifunctional cross-linking reagnet. Hoppe. Seylers Z. *Physiol. Chem.* **356**(9):1455-1458.

Tuckman, M. and Osburne, M. S. (1992) In Vivo Inhibition of TonB-Dependent Processes by a TonB Box Consensus Pentapeptide. *J. Bacteriol.* **174**(1):320-323.

Vandeputte-Rutten, L., Kramer, R. A., Kroon, J., Dekker, N., Egmond, M.R., and Gros, P. (2001) Crystal structure of the outer membrane protease OmpT from *Escherichia coli* suggests a novel catalytic site. *EMBO J.* **20**(18):5033-5039.

Wang, J., Kim, H. H., Yuan, X., and Herrin, D. L. (1997) Purification, biochemical characterization and protien-DNA interactions of the I-CreI endonuclease produced in Escherichia coli. *Nucl. Acids Res.* **25**(19):3767-3776.

Wayne, R. R., Frick, K. and Neilands, J. B. (1976) Siderophore protection against colicins M, B, V, and I_a in Escherichia coli. *J. Bacteriol.* **126**:7-12.

Weiss, M.S., Abele, U., Weckesser, J., Welte, W., Schiltz, E., and Schulz, G.E (1991) Molecular architecture and electrostatic properties of a bacterial porin. *Science* **254**:1627-1630.

Wen-ping, C., and Tsong, K. (1993) A simple and rapid method for the preparation of gram-negative bacterial genomic DNA. *Nucl. Acids Res.* **21**(9):2260.

Wiener, M., Freymann, D., Ghosh, P., and Stroud, R. M. (1997) Crystal structure of colicin Ia. *Nature* **385**(6615):461-464.

Williamson, M. P. (1994) The structure and function of proline-rich regions in proteins. *Biochem. J.* **297**(2):249-260.

Wooldridge, K. G., and Williams, P. H. (1993) Iron uptate mechanisms of pathogenic bacteria. *FEMS Microbiol. Rev.* **12**(4):325-348.

Zhou XH, Van der Helm D., Adjimani J. (1993) Purification of outer membrane iron transport receptors from Escherichia coli by fast protein liquid chromatography: FepA and FecA. *Biometals* **6**(1):25-35.

Zhou XH, van der Helm D, Venkatramani L. (1995) Binding characterization of the iron transport receptor from the outer membrane of Escherichia coli (FepA): differentiation between FepA and FecA. *Biometals* **8**(2):129-36.

Zhu, W., Hunt, D. J., Richardson, A. R., and Stojiljkovic, I. (2000) Use of heme compounds as iron sources by pathogenic neisseriae requires the product of the hemO gene. *J. Bacteriol.* **182**(2):439-437.